Fall 12-3-2021

# Biostratigraphy of Paleogene Diatom Assemblages in the Southern Ocean

Angela Kaup
*University of Nebraska-Lincoln*, angela.kaup@huskers.unl.edu

# BIOSTRATIGRAPHY OF PALEOGENE DIATOM ASSEMBLAGES IN THE SOUTHERN OCEAN

by

Angela Kaup

A THESIS

Presented to the Faculty of

The Graduate College at the University of Nebraska

In Partial Fulfillment of Requirements

For the Degree of Master of Science

Major: Earth and Atmospheric Sciences

Under the Supervision of Professor David Harwood

Lincoln, Nebraska

December, 2021

# BIOSTRATIGRAPHY OF PALEOGENE DIATOM ASSEMBLAGES IN THE SOUTHERN OCEAN

Angela Kaup, M.S.

University of Nebraska, 2021

Advisor: David Harwood

The record of siliceous microfossil sedimentation in the high latitude South Atlantic Ocean has great potential for dating seismic and stratigraphic units. Over the last several decades, scientists have documented diatom biostratigraphic record from sediment cores and drill cores in the Falkland Plateau and Maurice Ewing Bank region, as well as other areas of the Southern Ocean, and a robust chronostratigraphic framework is available for Neogene sequences. Given the complicated nature of ocean bathymetry, tectonic plate motion (vertical and lateral), and ocean current flow, the sedimentological evolution of this oceanic region is not well understood. Sampling sediment cores at high resolution intervals has the potential to offer additional understanding of sedimentation, erosion, and diatom occurrences in this region. This thesis adds new information from diatom records in the South Atlantic Ocean, specifically around the Falkland Plateau and Maurice Ewing Bank. Chapter 1 identifies the structure of this thesis and presents an overview of the project, including a summary of the present state of diatom biostratigraphy in the Southern Ocean. Chapter 2 presents new information on the diatom-based age of sediment cores recovered during a site survey cruise by *The Royal Research Ship (RRS) Discovery* during Cruise DY087, as well as existing cores from the same region. The goal of dating these cores is to assess the age of seismic units in this region in order to identify future drilling targets. Chapter 3 presents details of the age and diatom assemblages of two Paleogene piston cores the cores from *ARA Islas Orcadas* Cruise 1678. These cores are correlated to existing Antarctic and Southern Ocean drill core records.

# ACKNOWLEDGEMENTS

This experience has been nothing short of incredible. The pursuit of education has been something I have been passionate about but could not have achieved on my own. I would like to start with thanking my advisor Dr. David Harwood for his continued support, guidance, and endless knowledge throughout this journey. It has truly been a privilege working on this project with you. I would also like to acknowledge the support and efforts of my committee and thank Dr. Sherilyn Fritz and Dr. Mindi Searls. Thank you to the University of Nebraska-Lincoln and the Department of Earth and Atmospheric Sciences for supporting me with a teaching assistantship, funding, and access to facilities. A special thanks to Dr. Steve Bohaty at the National Oceanography Centre Southampton at the University of Southampton for providing sediment samples from Cruise DY087, in addition to his expertise and knowledge. Thank you to the Oregon State University Marine and Geology Repository for providing additional sediment samples. I would also like to acknowledge the entire crew and science team aboard the *RRS Discovery*, DY087 and the British Antarctic Survey (BAS) for their support abroad and with sample collection. Thank you to my father, Ned Kaup, for instilling a love of nature and education in his children, I am proud to be a second-generation science graduate. Thank you to my mother, Renee Fisher, for the continued support and help along the way. Thank you to my in-laws, Jerry, and Lynne Easterday, without your support and love I would have never made it to thispoint. Thank you to my sisters and close friends for always being there to listen and encourage me on thispath. Finally, thank you to my husband, Michael Easterday, and our daughter, Teva Easterday, you both have sacrificed the most to support my journey and we have finally made it, this is an accomplishment forall of us. I love you both endlessly!

TABLE OF CONTENTS

# CHAPTER 1: SCOPE AND PURPOSE OF THIS STUDY

## INTRODUCTION

The biostratigraphic record of diatoms in the South Atlantic Ocean is well developed for the Neogene but has only limited age resolution for the Paleogene. A large part of this is due to the need for more specific taxonomic documentation and clear correlation of diatom-bearing sections. Application of biostratigraphic zonations and correlation of diatom assemblages to those in regional sediment and drill cores allows for the dating of poorly studied sediment cores from the southern South Atlantic Ocean. These cores provide important constraint on the geological record of the region, specifically in dating seismic sequences that serve as the framework for identifying and proposing new drilling targets. The rapid evolutionary rates of diatoms and their wide distribution in the ocean allow the biostratigrapher to resolve significant events in Earth's history and correlate stratigraphic intervals in cores. The distribution and abundance of diatoms and other silicious organisms is often isolated with patchy distribution in time and space (Baldauf & Barron, 1990) during the Cretaceous through the Eocene (Fenner, 1984; Barron et al., 2015) but diatoms have more widespread occurrences and sustained presence in Southern Ocean sediments following the Eocene-Oligocene Transition (EOT). Thus, the Oligocene to Recent record is better understood (Scherer et al., 2007).

The southern South Atlantic region to the east of the Drake Passage is an area of current interest by the palaeoceanographic and paleoclimate community due to the tectonic, oceanographic, and climatic history and the development of the Antarctic Circumpolar Current (ACC), one of the dominant features in the modern and Cenozoic Ocean circulation. The history and timing of the Drake Passage opening, and the related deep-water flow of this region contsrains the development of the Maurice Ewing Bank and Falkland Plateau, two key features in this

region. New drilling projects are under development to target specific geological and palaeoceanographic events in this area. One developing project, for which this research project is aligned and provides supporting information, is International Ocean Drilling Discovery Program (IODP) Proposal (862-Pre-Proposal), which carried out site-survey seismic and coring activities in 2018 via *the Royal Research Ship RRS Discovery* cruise DY087 to identify potential drilling sequences. In addition, existing sediment cores are available to help constrain the age of the seismic sequences. The research on diatoms presented herein is in support of the IODP proposal and determines the age of the regional stratigraphic sequences for the Paleogene, specifically the Eocene-Oligocene Transition (EOT) when continental-scale ice sheets first formed in Antarctica, the ACC was developing, and the Southern Ocean and global climate was cooling. In support of this project, a survey of cores in the region was conducted to apply ages based on current diatom biostratigraphic zonal schemes primarily of the Neogene time interval, the age of most of the cores. However, several key sediment cores recovered Paleocene, Eocene, and Oligocene sediments, which are useful in guiding selection of drilling targets.

The Drake Passage has a complicated tectonic and oceanographic history, influenced by many small plates and ocean connections which has made dating the opening of the passageway challenging and a subject of debate. Prior to the opening of the Drake Passageway, a cluster of islands between Australia and Antarctica, including Tasmania, began to tectonically rift apart, allowing ocean currents to flow through. This opening is known as the Tasman Seaway and it's timing has been well constrained with sedimentological, geochemical, micropaleontological, and paleomagnetic data. The first evidence of a surface water connection between the east and west sides of the Tasman Seaway are documented at ~34.5 Ma (Gaina et al., 1998; Stickley et al., 2004b). Following the opening of the Tasman Seaway, the Drake Passage opened fully to

marine deep-water flow. This allowed the Antarctic Circumpolar Current (ACC) to form around Antarctica and, in conjunction with a drop in atmospheric $CO_2$ levels to below 750 ppm, led to initiation of the Antarctic Ice Sheet and the onset of the modern "Icehouse: state that continues today. Stickley et al. (2004a, b) recovered an almost continuous sediment record across the Eocene Oligocene transition during ODP Leg 189. Based on paleomagnetic and micropaleontological data, models have predicted deep seawater flow through the Tasman Seaway at ~33 Ma (Stickley et al., 2004a, b; Brinkhuis et al., 2003; Zachos et al., 2001).

It is postulated that the Drake Passage, the other dominant gateway in evolution of the Southern Ocean ACC, opened to deep water flow around 35-28 million years ago (Dalziel, 2014), but more precision for this date is of great interest to the palaeoceanographic community, as Southern Ocean circulation influences global oceanographic connections. Better constraint will aid in understanding the ACC's contribution to the EOT shift into an icehouse climate (Bohaty & Zachos, 2003) The history of Cenozoic deep-water flow and related sedimentary processes in this region of the South Atlantic Ocean represents a main objective of the IODP 862

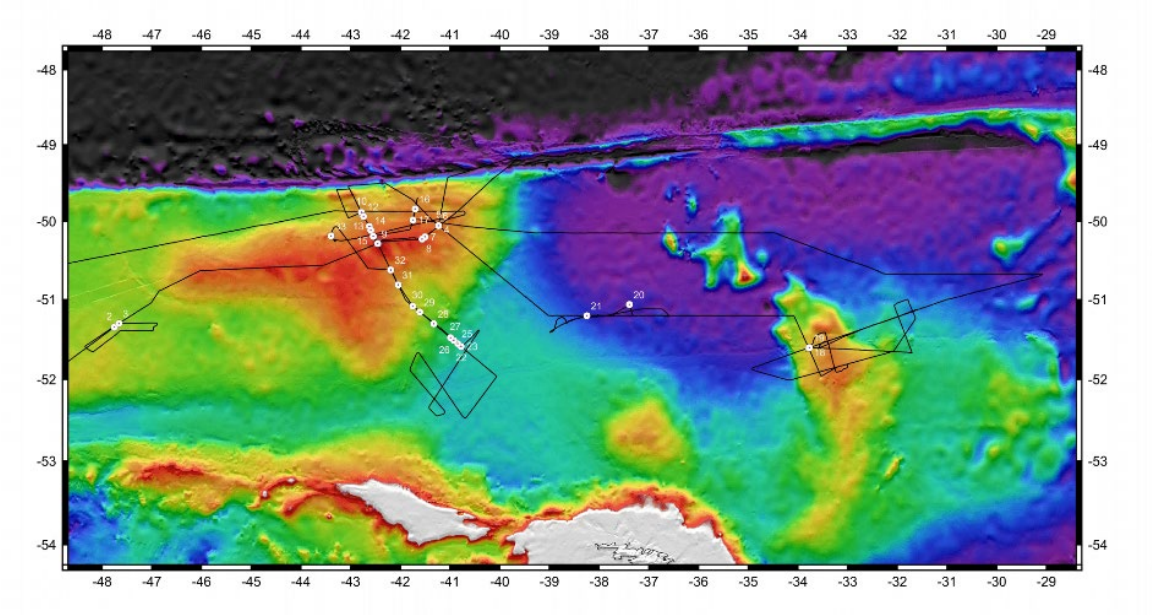


*Figure 1. DY087 Cruise Track & Station Locations for Coring, Sound Velocity Probe, & SeaCAT CTD*

pre-proposal. The patterns and timing of sediment deposition and erosion will help reveal ocean circulation changes as this region evolved. The objective of this thesis is to contribute to the dating of these sedimentary sequences.

## APPROACH

The first phase of this research project on diatom biostratigraphy (Chapter 2) focuses on dating the new suite of piston cores collected during the DY087 cruise. The DY087 cruise successfully recovered 33 piston cores and seismic data across an east-west transect from the Falkland Plateau to the West Georgia Basin (Figure 1). Most of these cores recovered only Neogene sediment. However, three cores were determined to be Late Eocene to Early Oligocene in age, and are a focus of this study.

In addition, several pre-existing sediment cores from this region were also examined and assessed biostratigraphically to provide diatom-based age information. Presentation of diatoms-based ages on the suite of Paleogene cores, and correlation to longer drill core sequences and correlative samples, is the focus of Chapter 3 of this thesis. These cores were collected over several decades from *ARA Islas Orcadas* Cruises 1678, 1176, and 0775, *VEMA* Cruises 14, 17, 18, 22, and 31, *Eltanin* Cruise 22, and *Robert Conrad* Cruises 15 and 16.

From a survey of basal sediments, several specific cores were identified for further study. Preference was given to cores that correlated with the DY087 cores and provided key information regarding the age of seismic sequences. *ARA Islas Orcadas* Cruise 1678 core 20 is of particular interest because it lacks stratigraphic constraint and is tied to seismic line RC2106-142 from the DY087 seismic survey.

New information developed from this study is organized into two chapters.

Chapter 2 presents the results of the survey of all cores examined during this project, with a focus on presenting the diatom-based ages assigned to the cores, chiefly to establish the maximum age recovered, to help date seismic sequences. Chapter 3 will focus on specific Paleogene cores of interest, chiefly those containing Eocene diatom assemblages. The basis for the age of each core, description and illustration of the taxa, and correlation of the core's intervals to previous DSDP, ODP, and IODP drill cores and other samples from the Southern Ocean and Antarctic region are discussed. Whereas Chapter 2 applies an advanced biostratigraphic framework for Neogene intervals, Chapter 3 identifies the developing nature of Paleogene diatom and other siliceous microfossil biostratigraphy. In the latter case, the siliceous microfossil assemblages include several new and poorly known species, and it is hoped that this study will guide future diatom studies on these interesting diatoms. The focus of this study in not on detailed descriptions of the diverse and multiple-age diatom floras, but to identify discrete stratigraphic intervals identified in the cores.

## SOUTHERN OCEAN DIATOM BIOSTRATIGRAPHY

### Oligocene to Recent

Diatoms of Oligocene age and younger in Southern Ocean sediments have been well studied and have extensive biostratigraphic documentation. Siliceous microfossils obtained from these sediments are often better preserved than those in deeper and older strata. Diatom biostratigraphy after the Eocene-Oligocene transition is better understood, because siliceous microfossils have a more sustained presence in the fossil record, which allows for higher resolution data and the possibility of using modern proxies for age dating. Previous work by McCollum (1975) during DSDP Leg 28 in the Ross Sea created the initial diatom zones for the Miocene. McCollum's work has since been expanded on by multiple studies including Weaver and Gombos (1981) who compared existing diatom data from the Southern Ocean to make a more concise and complete diatom zonation for the region. During DSDP Leg 71 Ciesielski

(1983) created new zones and revised those from Weaver and Gombos (1981). His work provided higher resolution detail for the biostratigraphic record and created absolute dates for the zones. Baldauf & Barron (1991) continued to improve the diatom zonation for the Oligocene to Quaternary, incorporating previous work from the region and cores collected during ODP Leg 119 on the Kerguelen Plateau and the Prydz Bay region. Harwood and Maruyama (1992) expanded on prior works, adding new information from ODP Leg 120 and created high resolution diatom zones and subzones spanning the Oligocene to Pleistocene. Barron & Mahood (1993) documented well preserved early Oligocene diatoms from ODP site 739 in Prydz Bay. The diatoms found in Core 739c had a close resemblance to Assemblage Zone B of Harwood (1989) recovered by the CIROS-1 drill core. Zielinski & Gersonde (2002) refined previously created zonations with the use of paleomagnetic data and cores collected during ODP Leg 177. Censarek & Gersonde (2002) expanded on previous work and created diatom zonations for the northern and southern South Atlantic by incorporation magnetostratigraphic interpretations, and diatom biostratigraphy and taxonomy with cores collected during ODP Leg 177 . Winter & Iwai (2002) used diatom occurrence data and well established diatom events to document stratigraphic occurences with cores from ODP Leg 178 located off the Pacific margin of the Antarctic Peninsula. Whitehead & Bohaty (2003) documented the distribution and abundance of diatoms using biostratigraphy and magnetostratigraphic data collected during ODP Leg 188 together with previous zonations to refine the record during the Quaternary-Pliocene. All these prior studies have been used in this paper to identify diatoms and provide a context for their ages.

Table 1 presents a summary of important diatom records from drill cores, sediment cores and other deposits in the Antarctic and Southern Ocean regions. A recent review of the current state of Southern Ocean and Antarctic diatom biostratigraphy is presented in the Methods chapter for IODP Expedition 374 (McKay et al., 2019).

**Eocene**

Previous biostratigraphic work in the Southern Atlantic Ocean has generated insight into the history of the region and aids in the species identification and relative age dating discussed in this paper. Gombos (1976) documented Paleogene and Neogene diatom assemblages from the Falkland Plateau and Malvinas Outer Basin from ODP Leg 36 and created a diatom zonation. Hajós (1976) documented the distribution of siliceous microfossils, with emphasis on diatoms, from locations south of Australia and New Zealand and in the Tasman Sea during DSDP Leg 29. Gombos Jr. (1983) documented the relative abundance of nearly 60 diatom species from hole 512, on the Falkland Plateau, during DSDP Leg 71. This was the longest continuous record of Eocene sediment cored to date. He identified eleven appearance and extinction datums for nine species. Gombos and Ciesielski (1983) documented diatom abundances and distribution during the late Eocene to early Miocene across the Southwest Atlantic from ODP Leg 71 at Holes 511 and 513a and further refined the zonation. Fenner (1984) emphasized the stratigraphic value of Southern Ocean diatoms, using multiple DSDP low and high southern latitude cores to enhance previous work, and they developed a zonation for Eocene to Oligocene diatom assemblages. Harwood (1989) documented the abundance and distribution of siliceous microfossils, with emphasis on diatoms, from the CIROS-1 drillhole, located in McMurdo Sound, Antarctica, and organized them stratigraphically into three assemblage zones spanning the early Oligocene to early Miocene. The lowest portion of the core was poorly preserved but did have taxa suggesting a late Eocene age. Harwood and Maruyama (1992) documented middle Eocene to Pleistocene diatoms assemblages in the Kerguelen Plateau from OPD Leg 120 and created high-resolution diatom zones spanning the last 36 million years. Harwood & Bohaty (2000) and Bohaty & Harwood (2000) documented Eocene diatom and other siliceous microfossil assemblages from erratics in glacial moraines recovered in McMurdo Sound. Six of the diatom assemblages were of Eocene age. Witkowski et al. (2012) documented microfossil assemblages and performed geochemical analysis on samples from sites 748 and 749 from ODP

Leg 120. Their evidence showed a pronounced change in environment during the Middle Eocene Climate Optimum (MECO). Barron et al. (2014) documented a complete Eocene sequence with ODP Hole 1090B, located in the southern Agulhas Ridge. They correlated the core assemblages with paleomagnetic stratigraphy and proposed a new diatom zonation for the middle Eocene to early Oligocene using the succession of *Cestodiscus* species. Based on these prior studies, I will apply a biostratigraphic framework to several cores in the southern South Atlantic.

# ANTARCTIC BIOSTRATIGRAPHIC AGE TABLE

| | | | ANTARCTIC BIOSTRATIGRAPHIC REFERENCES | Pleist. | Pliocene | Miocene | Oligocene | Eocene | Paleocene |
|---|---|---|---|---|---|---|---|---|---|
| | Leg/Locations | Sites/Formations | Publications - Author year | Ages | | | | | |
| erratics | McMurdo area | erratics | Harwood & Bohaty, 2000; Bohaty & Harwood, 2000; | | | x | | x x x | |
| Deep Sea Drilling Project (DSDP) | Leg 28 | 265 | McCollum, 1975; | x | x | x | | | |
| | | 266 | McCollum, 1975; Weaver & Gombos, 1981; | x | x x | x x x | | | |
| | | 269 | McCollum, 1975; | x | x | x x | | | |
| | | 272 | McCollum, 1975; | | x | x x | | | |
| | | 273 | McCollum, 1975; | | | x x | | | |
| | | 274 | McCollum, 1975; Fenner, 274; | x | x x | x x x | x x | | |
| | Leg 29 | 278 | Schrader, 1976; Weaver & Gombos, 1981; Fenner, 1984; | x | x | x x x | | | |
| | | 280A | Hajos, 1976; | | | | x x | x | |
| | | 281 | Hajos, 1976; | | | | | x | |
| | Leg 35 | 283 | Hajos, 1976; | | | | | x | |
| | | 323 | Schrader, 1976; | | x | x x | | | |
| | Leg 36 | 327A | Gombos, 1976; | | | | | | xx |
| | | 328 | Gombos, 1976; | x | x | x x x | x x x | x | |
| | | 329 | Gombos, 1976; | x | x | x | | | |
| | Leg 71 | 511 | Ciesielski, 1983; | | x | x | | | |
| | | 511 | Gombos & Ciesielski; 1983; Fenner, 1984; | | | | x x x | x | |
| | | 512 | Ciesielski, 1983; | | | x x | | | |
| | | 512/ 512A | Gombos, 1983; | | | | | x | |
| | | 513/ 513A | Ciesielski, 1983; | x | x x | x x | | | |
| | | 513A | Gombos & Ciesielski; 1983; | | | x | x x x | | |
| | | 514 | Ciesielski, 1983; | x | x x | | | | |
| MSSTS and CIROS (NZ & US) | McM Sound | CIROS-1 | Harwood, 1989; Harwood et al., 1989; Roberts et al., 2003; | | | | x x x | x | |
| Ocean Drilling Program (ODP) | Leg 113 | 689B, 690B | Gersonde 1990; Gersonde & Burckle, 1990; | x x | x x | x x x | x | | |
| | | 689 | Censarek & Gersonde, 2002 | | | x x x | | | |
| | | 690 | Censarek & Gersonde, 2002 | | | x x x | | | |
| | | 693A, 693B | Gersonde & Burckle, 1990; | x | x x | x | | | |
| | | 694 | Gersonde & Burckle, 1990; | x | x | x x | | | |
| | | 695 | Gersonde & Burckle, 1990; Srivastav, PhD | | x x | | | | |
| | | 696A, 696B | Gersonde & Burckle, 1990 | x | x x | x x | | | |
| | | 697A, 697B | Gersonde & Barcena, 1998 | x | x | x | | | |
| | Leg 114 | 699A | Ciesielski, 1991, data report; Fenner, 1991; | x | x | x x | | | |
| | | 701C | Fenner, 1991; | x | x | | | | |
| | | 704 | Ciesielski, 1991, data report; Fenner, 1991; | x x | x x | x x | | | |
| | Leg 119 | 736A / 736C | Baldauf & Barron, 1991; | x x | x | | | | |
| | | 737A/737B | Baldauf & Barron, 1991; | | x x | x x | | | |
| | | 739A/ 739C | Baldauf & Barron, 1991; Barron & Mahood, 1993; | x | x | x | x | | |
| | | 742 | Mahood & Barron, 1996; | | x | | | | |
| | | 744A/ 744B | Baldauf & Barron, 1991;Roberts et al., 2003; Farmer, unpub.; Florindo, et al., 2013; Tolotti, in prep.; | x x | x x | x x x | x x | | |
| | | 745B | Baldauf & Barron, 1991; | x x | x x | | | | |
| | | 746A | Baldauf & Barron, 1991; | | | x x | | | |
| | Leg 120 | 747 | Harwood & Maruyama, 1992; Harwood et al., 1992 | | | x | x x x | x | |
| | | 748 | Harwood & Maruyama, 1992; | x x | x x | x x x | x x x | | |
| | | 748 | Roberts et al., 2003; Witkowski et al., 2012 | | | | | x | |
| | | 749 | Harwood & Maruyama, 1992; Witkowski et al., 2012; | | | | | x | |
| | | 751 | Harwood & Maruyama, 1992; | x x | x x | x x x x | | | |
| | | 1088 | Censarek & Gersonde, 2002; | | | x x x x | | | |
| | | 1089 | Cortese & Gersonde, '08; Zielinski & Gersonde, '03; | x | x x | | | | |

| | | | ANTARCTIC BIOSTRATIGRAPHIC REFERENCES | Pleist. | Pliocene | Miocene | Oligocene | Eocene | Paleocene |
|---|---|---|---|---|---|---|---|---|---|
| | Leg/Locations | Sites/Formations | Publications - Author year | Ages | | | | | |
| | Leg 177 | 1090 | Cortese & Gersonde, '08; Zielinski & Gersonde, '03; | x | x x | | | | |
| | | 1090 | Barron et al., 2014; | | | | | xx | |
| | | 1091 | Cortese & Gersonde, 2008; Zielinski & Gersonde, '03; | x | x x | | | | |
| | | 1092 | Cortese & Gersonde, 2008; | x | x x | | | | |
| | | 1092 | Cortese & Gersonde, 2008; Zielinski & Gersonde, '03; | | | x x x | | | |
| | | 1093 | Cortese & Gersonde, '08; Zielinski & Gersonde, '03; | x | x x | | | | |
| | | 1094 | Cortese & Gersonde, 2008; Zielinski & Gersonde, 2003; Zielinski & Gersonde, 2002 | x | x x | | | | |
| | Leg 178 | 1095A, 1095B | Winter & Iwai, 2002; | x | x | x | | | |
| | | 1096 | Winter & Iwai, 2002; | x | x x | | | | |
| | | 1097 | Iwai & Winter, 2002; Winter & Iwai, 2002; | x | x | x x | | | |
| | | 1098 | Leventer et al., 2002 - Palmer Deep | x | | | | | |
| | | 1100 | Iwai & Winter, 2002; Winter & Iwai, 2002; | x | x | x x | | | |
| | | 1101 | Winter & Iwai, 2002; | x | x | | | | |
| | | 1103 | Iwai & Winter, 2002; Winter & Iwai, 2002; | x | x | x x | | | |
| | Leg 183 | 1138A | Bohaty et al., 2003 | x | x x | x x x x | | | |
| | | 1140 | Arney et al., 2003 | | | x x | x x x | | |
| | Leg 188 | 1165B | Whitehead & Bohaty, 2003; | x x | x x | | | | |
| | | 1166A | Whitehead & Bohaty, 2003; | x x | x x | | | | |
| | Leg 189 | 1168, 1170, 1171, 1172 | Exon et al., 2001; Stickley et al., 2004; Sluijs et al., 2002 | | | | | | |
| Cape Roberts Project (CRP) | CRP-3 | | Harwood & Bohaty 2001; Hannah et al., 2001; Olney et al., 2005, 2007; | | | | x x | x | |
| Integrated Ocean Drilling Program (IODP) | EXP 318 | U1358 | Kobayashi & Iwai, 2012;(EGU); Iwai et al., 2014 (EGU); | | | | | | |
| | | U1359 | Iwai et al., 2012 (AGU); | | | | | | |
| | | U1361A | Iwai et al., 2012 (AGU); Armbrecht et al., 2018; Taylor-Silva, | | | | | | |
| | | general | Escutia et al., 2011; Iwai et al., 2011 (AGU); Riesselman & Taylor-Silva, 2015 (AGU); Tauxe et al., 2011; | | | | | | |
| | * joint science program | | | | | | | | |
| | | | **General Southern Ocean diatom biostrat compilations and references** | | | | | | |
| | | | Fenner, 1985 - Plankton Stratigraphy | | | | x x x | x x x x x | x x |
| | | | Barron, 1985 - Plankton Stratigraphy | x x | x x | x x x x | | | |
| | | | Barron et al., 1995, Paleo Society | x | x | x x x | x x | x x x | |
| | | | Barron, J.A., 2003. Diatom Research 18:2, 203-224. | | | | | | |
| | | | Crampton et al., 2016 PNAS | x x | x x | x x | | | |
| | | | Cody et al., 2008; 2012; CONOP | x x | x x | x x | | | |
| | | | Harwood & Nikolaev, 1995; Harwood et al., 2007 | | | | | | |
| | | | Barron 1996, Marine Micropal., 27:195-213. | | x | | | | |
| | | | Scherer et al., 2007 | x | x | x x x | x x | x x x | |
| | | | | | | | | | |
| | | | | | | | | ver. 1.1 (8-2018) | |
| | | | Modified unpublished table from Dr. David Harwood | | | | | | |

*Table 1. Summary of previous Antarctic siliceous microfossil biostratigraphy and associated ages of drill cores. Summary was compiled by Dr. David Harwood (previously unpublished) and modified for this paper.*

# References


Baldauf, J. G., & Barron, J. A. (1990). Evolution of biosiliceous sedimentation patterns—Eocene through Quaternary: paleoceanographic response to polar cooling. *Geological History of the Polar Oceans: Arctic Versus Antarctic. Springer, Dordrecht*, 575-607.

Baldauf, J. G., & Barron, J. A. (1991). Diatom Biostratigraphy: Kerguelen Plateau and Prydz Bay Regions of the Southern Ocean. *In*: *Proceedings of the Ocean Drilling Program, Scientific Results*, *119*, 547-598.

Barron, J. A., & Mahood, A. D. (1993). Exceptionally well-preserved early Oligocene diatoms from glacial sediments of Prydz Bay, East Antarctica. *Micropaleontology, 39(1)*, 29-45.

Barron, J. A., Bukry, D., & Gersonde, R. (2014). Diatom and silicoflagellate biostratigraphy for the late Eocene: ODP 1090 (sub-Antarctic Atlantic). *Nova Hedwigia, Beiheft, 143*, 1-32.

Barron, J. A., Stickley, C. E., & Bukry, D. (2015). Paleoceanographic, and paleoclimatic constraints on the global Eocene diatom and silicoflagellate record. *Palaeogeography, Palaeoclimatology, Palaeoecology, 422*, 85-100.

Bohaty, S. M., & Harwood, D. M. (2000). Ebridian and silicoflagellate biostratigraphy from Eocene McMurdo erratics and the Southern Ocean. *In: Stillwell, J.; Feldman, R. (eds.), Antarctic Research Series, Paleobiology and Paleoenvironments of Eocene Rocks: McMurdo Sound, East Antarctica, 76*, 99-159.

Bohaty, S. M., & Zachos, J. C. (2003). Significant Southern Ocean warming event in the late middle Eocene. *Geology 31, no. 11*, 1017-1020.

Brinkhuis, H., Sengers, S., Sluijs, A., Warnaar, J., & Williams, G. L. (2003). Latest Cretaceous to earliest Oligocene, and Quaternary dinoflagellate cysts from ODP Site 1172, East Tasman Plateau. *In: Proceedings of the Ocean Drilling Program. Scientific results, 189,* 1-36.

Censarek, B., & Gersonde, R. (2002). Miocene diatom biostratigraphy at ODP Sites 689, 690, 1088, 1092 (Atlantic sector of the Southern Ocean). *Marine Micropaleontology, 45(3-4)*, 309-356.

Ciesielski, P. F. (1983). The Neogene and Quaternary diatom datum biostratigraphy of subantarctic sediments. Deep Sea Drilling Project Leg 71. *Initial Reports of the Deep Sea Drilling Project, 71*, 635-665.

Dalziel, I. W. (2014). Drake Passage and the Scotia arc: A tortuous space-time gateway for the Antarctic Circumpolar Current. *Geology, 42(4)*, 367-268.

Fenner, J. (1984). Eocene-Oligocene planktic diatom stratigraphy in the low latitudes and the high southern latitudes. *Micropaleontology 30.4*, 319-342.

Gaina, C., Müller, D. R., Royer, J. Y., Stock, J., Hardebeck, J., & Symonds, P. (1998). The tectonic history of the Tasman Sea: a puzzle with 13 pieces. *Journal of Geophysical Research: Solid Earth, 103(B6)*, 12413-12433.

Gombos Jr, A. M. (1983). Late Eocene to Early Miocene diatoms from the Southwest Atlantic. *Initial Reports of the Deep Sea Drilling Project, 71*, 538-634.

Gombos Jr, A. M. (1977). *Paleogene and Neogene diatoms from the Falkland Plateau and Malvinas Outer Basin: Leg 36, Deep Sea Drilling Project, 36*, 575-688.

Gombos Jr, A. M., & Ciesielski, P. F. (1983). Late Eocene to Early Miocene Diatoms From the Southwest Atlantic. *Initial Reports of the Deep Sea Drilling Project*, *71,* 538-634.

Hajós, M. (1976). Upper Eocene and lower Oligocene Diatomaceae, Archaeomonadaceae, and Silicoflagellatae in Southwestern Pacific sediments, DSDP Leg 29. *Initial Reports of the Deep Sea Drilling Project*, *35*, 817-883.

Harwood, D. M. (1989). Siliceous microfossils. *In: Barrett, P. (ed.), Antarctic Cenozoic history from the CIROS-1 drillhole, McMurdo Sound. DSIR Bulletin, 245*, 67-97.

Harwood, D. M., & Bohaty, S. M. (2000). Marine diatom assemblages from Eocene and younger erratics, McMurdo Sound, Antarctica. *In: Stilwel, J., Feldman, R. (eds.), Paleobiology and Paleoenvironments of Eocene Rocks: McMurdo Sound, East Antarctica, American Geophysical Union, Antarctic Research Series, 76*, 73-98.

Harwood, D. M., & Maruyama, T. (1992). Middle Eocene to Pleistocene diatom biostratigraphy of Southern Ocean sediments from the Kerguelen Plateau, LEG 120. *In: Wise, S., Schlich, R., et al. (eds.), Proceedings of the Ocean Drilling Project, Scientific Results, 120,* 683-733.

McCollum, D. W. (1975). Diatom stratigraphy of the Southern Ocean. *Initial Reports of the Deep Sea Drilling Project, 28*, 515-571.

McKay, R. M., De Santis, L., Kulhanek, D. K., Ash, J. L., Beny, F., Browne, I. M., . . . Ishino, S. (2019). Expedition 374 methods. *In: Proceedings of the International Ocean Discovery Program, 374*. https://doi.org/10.14379/iodp.proc.374.102.2019

Scherer, R. P., Gladenkov, A. Y., & Barron, J. A. (2007). Methods and applications of Cenozoic marine diatom biostratigraphy. *In: Starrat, S. (ed.), Pond Scum to Carbon Sink: Geological and Enviromental Applications of Diatoms, The Paleontological Society Papers, 13*, 61-83.

Stickley, C. E., Brinkhuis, H., McGonigal, K. L., Chaproniere, G. C., Fuller, M., Kelly, D. C., & Stant, S. A. (2004a). Late Cretaceous–Quaternary biomagnetostratigraphy of ODP Sites 1168, 1170, 1171, and 1172, Tasmanian Gateway. *In: Proceedings of the Ocean Drilling Program, Scientific Results, 189*, 1-57.

Stickley, C. E., Brinkhuis, H., Schellenberg, S. A., Sluijs, A., Röhl, U., Fuller, M., & Williams, G. L. (2004b). Timing and nature of the deepening of the Tasmanian Gateway. *Paleoceanography, 19(4)*.

Weaver, F. M., & Gombos Jr., A. M. (1981). Southern high-latitude diatom biostratigraphy. *In: Warme, J., Douglas, R., Winterer, E. (eds.), The Deep Sea Drilling Project: A Decade of Progress, SEPM Special Publication No. 32*, 445-470.

Whitehead, J. M., & Bohaty, S. M. (2003). Data report: Quaternary-Pliocene diatom biostratigraphy of ODP Sites 1165 and 1166, Cooperation Sea and Prydz Bay. *In Proceedings of the Ocean Drilling Program, Scientific Results, 188*, 1-25.

Winter, D., & Iwai, M. (2002). Data report: Neogene diatom biostratigraphy, Antarctic Peninsula Pacific margin, ODP Leg 178 rise sites. *In: Proceedings of the Ocean Drilling Program, Scientific Results, 178*, 1-25.

Witkowski, J., Bohaty, S. M., McCartney, K., & Harwood, D. M. (2012). Enhanced siliceous plankton productivity in response to middle Eocene warming at Southern Ocean ODP Sites 748 and 749. *Palaeogeography, Palaeoclimatology, Palaeoecology, 326*, 78-94.

Zachos, J., Pagani, M., Sloan, L., Thomas, E., & Billups, K. (2001). Trends, rhythms, and aberrations in global climate 65 Ma to present. *Science, 292(5517)*, 686-693.

Ziekinski, U., & Gersonde, R. (2002). Plio–Pleistocene diatom biostratigraphy from ODP Leg 177, Atlantic sector of the Southern Ocean. *Marine Micropaleontology, 45*, 225-268.

# CHAPTER 2: AGE SURVEY OF SEDIMENT CORES FROM FALKLAND PLATEAU AND MAURICE EWING BANK

## INTRODUCTION

The intial motivation for this project was the need for a diatom-based age survey of sediment cores collected during the IODP pre-proposal (862-pre) cruise DY087 aboard the *Royal Research Ship RRS Discovery*, from January to February of 2018. The *RRS Discovery* sailed east from Punta Arenas, across the Falkland Plateau and Maurice Ewing Bank (MEB). Sediment was collected with gravity and piston cores. The locations of these cores were chosen by using previous IODP and ODP marine sediment core logs and seismic reflection data, with the goal of penetrating into Paleogene strata to date seismic units and potential drilling targets.

| Core [DY087] | Longitude | Latitude | Water Depth [EM122] | Age of Target Strata |
|---|---|---|---|---|
| 03GC | -47.661 | -51.302 | 2621 | Recent-Pleistocene |
| 04GC | -41.23 | -50.056 | 1596 | Recent-Pleistocene |
| 06PC | -41.2304 | -50.0554 | 1600 | Eocene |
| 07PC | -41.502 | -50.2 | 1414 | middle Miocene |
| 08PC | -41.561 | -50.229 | 1373 | middle Miocene |
| 09PC | -42.455 | -50.286 | 1351 | Pleistocene-lower Miocene |
| 10PC | -42.783 | -49.884 | 1831 | early Oligocene or late Eocene |
| 12PC | -42.74 | -49.937 | 1758 | Eocene |
| 14PC | -42.594 | -50.115 | 1526 | Recent-Pleistocene |
| 15PC | -42.545 | -50.193 | 1430 | late Oligocene |
| 16PC | -41.702 | -49.839 | 1702 | Recent-Pleistocene |
| 22PC | -40.775 | -51.592 | 3798 | Recent-Pleistocene |
| 23PC | -40.775 | -51.592 | 3798 | Recent-Pleistocene |
| 25PC | -40.845 | -51.555 | 3736 | Recent-Pleistocene |
| 26PC | -40.924 | -51.515 | 3591 | Pliocene |
| 27PC | -40.989 | -51.481 | 3469 | Pliocene |
| 28PC | -41.326 | -51.306 | 2980 | late Miocene |
| 29PC | -41.607 | -51.158 | 2548 | Pliocene |
| 30PC | -41.748 | -51.084 | 2374 | Pleistocene |
| 31PC | -42.043 | -50.814 | 1911 | Pleistocene-middle Miocene |
| 32PC | -42.193 | -50.623 | 1579 | Pleistocene-late Miocene |
| 33PC | -43.393 | -50.189 | 1760 | early Pleistocene-late Pliocene |

*Table 1. DY087 Core Locations and Age of Bottom Sediment*

From the DY087 cruise, two gravity cores and twenty piston cores were assessed at various depths for diatoms of biostratigraphic significance to determine the age of the oldest sediment recovered. Seven of the cores were Pleistocene to Recent in age.

Three of the cores contained sediments of Oligocene age or older. The remaining cores spanned ages in between (See Table 1). The basis for these ages will be presented later in this chapter. The seismic data and sub-bottom profiler data collected during the DY087 cruise have also been reviewed and referenced to the piston and gravity sediment cores from the same cruise.

The sediment record before the Eocene is not well documented in this region. By collecting sediment cores at targeted locations, the science team can identify potential drill sites with the greatest potential to yield Eocene or older sediments. High resolution seismic reflection data were also gathered across various transects of the Falkland Plateau and MEB during the DY087 cruise.

The primary aim of the DY087 cruise was to collect data in order to develop a better understanding of the history of the Drake Passageway and the surrounding region. Previous drilling of marine sediments of Paleogene age yielded important information about past glacial cycles and the climate history of Antarctica. The diatom record in the South Atlantic during the Paleogene is not continuous and needs to be improved to create a more concise history for siliceous microfossil production and deposition during this time period (Bohaty & Zachos, 2003).

In addition to the examination of the DY087 sediment samples for diatom content, existing sediment cores collected during earlier expeditions in the 1960's and 1970's, during *ARA Islas Orcadas* Cruises 1678, 1176, and 0775, *VEMA* Cruises 14, 17, 18, 22, and 31, *Eltanin* Cruise 22, and *Robert Conrad* Cruises 15 and 16, were also examined to further characterize the ages of Falkland Plateau and MEB sediments. This was done to apply modern biostratigraphic data and update initial age assessments. Cores yielding Eocene ages were selected for further investigation, which will be presented in Chapter 3.

## MATERIALS AND METHODS

Sediment cores collected during cruise DY087 were transported to Southampton, UK and the British Ocean Sediment Core Research Facility (BOSCORF). Upon their arrival at BOSCORF the piston cores were split, described, and sampled for geochemical and micropaleontological analyses. The cores were also analyzed using the multi-sensor core logger (MSCL) and XRF scanner. Diatom microfossil analyses took place at the University of Nebraska-Lincoln (UNL). The MSCL, XRF, geochemical and nannofossil data related to these sediment cores were compiled by Dr. Steve Bohaty, Dr. Robert Larter, and Dr. Claus-Dieter Hillenbrand in support of a proposal for a future IODP expedition to drill in this region.

At the University of Nebraska-Lincoln, sediment samples from various depths in the DY087 cores were prepared for microscopic analysis. Samples were weighed in increments of approximate 0.75 to 1.0 grams and dried in a desiccation chamber overnight. The samples were then reweighed and place in centrifuge tubes. The samples were then cleaned with 20 ml of concentrated HCl and 20 ml of 30% $H_2O_2$. They were then rinsed with ROPure water to neutralize the chemical additives. Next, approximately 15 ml of a diluted solution of sodium-hexametaphosphate and approximately 35 ml of ROPure water were added to the tubes, and they were left to react overnight and then rinsed with ROPure water to remove any chemicals remaining. A sample volume of 1 ml of the cleaned sediment suspension was then extracted and mixed with 40 ml of ROPure water and immediately transferred to a petri dish with 20 x 20 mm cover slips. Suspended sediment in the petri dishes were allowed to settle overnight and dry. Once dried, the cover slips were removed and affixed to glass slides with Norland Optical Adhesive #61 and cured under UV light.

Additionally, core sediment samples from *ARA Islas Orcadas* Cruises 1678, 1176, and 0775, *VEMA* Cruises 14, 17, 18, 22, and 31, *Eltanin* Cruise 22, *Robert Conrad* Cruises 15 and 16 were

requested from their corresponding repositories. These cores were selected due to their proximity to DY087 cruise sub-bottom profiler lines or seismic lines and based on initial age estimates. Slides prepared in the same manner as the DY087 samples. The cores of greatest interest to the DY087 research goals, those that reached target ages of Eocene or older (e.g., IO-1678-20PC and IO-1678-48PC), were sampled at higher resolution, and results from these two cores are presented in Chapter 3.

Slides were examined using a Leica DMRX Light Microscopy (LM) and 40x and 100x objectives. The relative abundance and stratigraphic distribution of diatom and silicoflagellate taxa were documented and described. Diatoms with the greatest utility in biostratigraphic age assessment were selected, and ages associated with first and last occurrences were used to assign ages to the sediment cores. The diatom biostratigraphic scheme employed in this study followed that of Harwood and Maruyama (1992) with supporting information from Gombos (1977), Gombos & Ciesielski (1983), Ciesielski (1983), Fenner (1984), and Scherer et al. (2000), among other papers cited in Chapter 1. Relative age assignments to specific samples are presented in Tables 3 and 4, in relation to the diatom biostratigraphic framework presented in the Methods chapter for IODP Expedition 374
(McKay et al., 2019). The systematic paleontology for all diatoms is presented in Chapter 3, where key information of the taxa is present, and the literature used in identification and age determinations is provided.

## RESULTS

### Cruise DY087 Cores

Two gravity cores and twenty piston cores were analyzed from the DY087 expedition. The samples were assessed biostratigraphically based upon the siliceous microfossil assemblages presented in Table 5 and Figures 1 and 2. Key taxa and biostratigraphic events used in determining ages for these cores are identified in Table 5, with an underline below the

occurrence information for First Appearance Datum (FAD) events, or with a line above the occurrence information for Last Appearance Datum (LAD) events.

**DY087-03GC** was sampled at 3 cm and 55 cm core depths. *Fragilariopsis kerguelensis* and *Fragilariopsis barronii* are present at 3 cm, which suggests the age of the sample to be 2.3 to 1.3 Ma. *F. kerguelensis* is present at 55 cm, suggesting the age to be 2.3 Ma or younger, within the transition of morphologies between *F. kerguelensis* and *F. barronii*.

**DY087-04GC** was sampled at 3 cm, 10 cm, and 55 cm core depths. *F. kerguelensis* is present in the sample at 3 cm, suggesting the age to be 2.3 Ma or younger. *F. kerguelensis* and *F. barronii* are present in the samples at 10 cm and 55 cm, which suggests the age to be 2.3 to 1.3 Ma. The samples at 10 cm and 55 cm have taxa of *F. kerguelensis* and *F. barronii* with a morphology that is transitional between the two species, and *Fragilariopsis curta* and *Actinocyclus actinochilus* are also present.

**DY087-06PC** was sampled at the 220 cm core depth. *Distephanosira architecturalis, Pyxilla reticulata,* and the silicoflagellate *Naviculopsis constricta* suggest a middle to late Eocene age. Calcareous nannofossils suggest a middle Eocene age (pers. comm., S. Bohaty). The age of this sample is older than ~33.6 Ma.

**DY087-07PC** was sampled at 260 cm core depth. The co-occurrence of diatoms *Crucidenticula nicobarica, Denticulopsis maccollumii, Denticulopsis lauta*, and *Actinocyclus ingens* var. *nodus* suggests a late Miocene age between 14.5 and 13.0 Ma.

**DY087-08PC** was sampled at the 84 cm core depth. The overlapping ranges of diatoms *Denticulopsis dimorpha, Denticulopsis praedimorpha*, and *Denticulopsis simonsenii* suggest a late Miocene age between 12.8 to 10.7 Ma.

**DY087-09PC** was sampled at 8 cm and 220 cm core depth. A disconformity is present within this core, as the sample at 8 cm is late Pliocene to early Pleistocene, based on transitional forms of *Fragilariopsis kerguelensis* and *F. barronii*, and the sample at 220 cm contains *Thalassiosira praefraga* from the early Miocene with an age range between 19.2 to 17.7 Ma.

**DY087-10PC** was sampled at the 129 cm core depth. An assemblage of diatoms and silicoflagellates and ebridians, including *Pyxilla reticulata, Rocella praenitida, Porotheca danica, Distephanosira architecturalis, Kisseleviella fabelliforma* (Olney et al., 2005), *Cavitatus jouseanus*, and *Naviculopsis constricta* suggest an early Oligocene to late Eocene age.

**DY087-12PC** was sampled at the 195.5 cm core depth. Diatoms in this sample include *Distephanosira architecturalis, Asterolampra schmidtii, Sceptroneis caducea* (in Gombos, 1977), and *Pyxilla reticulata*, which collectively suggest an Eocene age, in agreement with the middle Eocene age suggested by foraminifera (S. Bohaty, pers. comm.).

**DY087-15PC** was sampled at 27, 52, 64, 113, and 122 cm core depths, with a disconformity noted between samples 64 and 52 cm, separating distinct Pliocene and late Oligocene intervals. *Thalassiosira vulnifica* occurs in the sample at 52 cm, and *Rocella gelida, Cavitatus jouseanus, Naviculopsis biapiculata, Triceratium groningensis*, and rare *Rocella vigilans* are in the lower interval.

**DY087-16PC** was sampled at 21 cm, 55 cm, and 176 cm core depth. *F. kerguelensis* is present in the sample at 21 cm, suggesting the age to be younger than 2.3 Ma, and the interval at 55 cm is also Pliocene in age. A disconformity separates this upper interval from the sample at 176 cm, as it contains *Corbisema hastata*, which suggests a Paleocene age.

**DY087-22PC** was sampled at 80 cm and 179 cm core depths. Both depths had the diatom taxon *Fragilariopsis kerguelensis*, which has a first occurrence at approximately 2.3 Ma. *Actinocylcus ingens* is absent in both samples, suggesting an age younger than 0.6 Ma.

**DY087-23PC** was sampled at 74 cm, 383 cm, 674 cm, and 870 cm core depths. *F. kerguelensis* and *F. barronii* are both present in the samples from 74 cm, 383 cm, and 674 cm. Their documented ranges suggest these samples are 2.3 to 1.3 Ma. The sample at 74 cm has diatoms transitional between *F. kerguelensis* and *F. barronii*. The sample from 870 cm lacks *F. barronii*, but still contains *F. kerguelensis*, suggesting it is 2.3 Ma or younger.

**DY087-25PC** was sampled at 140 cm, 346 cm, 555 cm, and 763 cm core depths. *Fragilariopsis barronii* is absent from samples at 140 cm, 346 cm, and 555 cm, which contain *F. kerguelensis*, suggesting they are 2.3 Ma or younger. The sample from 763 cm does not contain *F. kerguelensis*, suggesting an age older than 2.3 Ma. This, combined with the presence of *Thalassiosira elliptipora* and *Shionodiscus oestrupii,* supports an older age between 3.3 to 2.3 Ma.

**DY087-26PC** was sampled at the 867-870 cm core depth. The diatoms *Thalassiosira insigna*, *Thalassiosira lentiginosa*, *Thalassiosira vulnifica, Thalassiosira inura, Rouxia diploneidies, Fragilariopsis barronii,* and *Fragilariopsis praecurta* are present, suggesting an age between 3.4 to 2.6 Ma.

**DY087-27PC** was sampled at 1075-1080 cm core depth. *Fragilariopsis barronii* is present, with a documented first occurrence at approximately 4.4 Ma. *Fragilariopsis praeinterfrigidaria* is also present, with a last occurrence at approximately 3.5 Ma, and an age for this sample between 4.4 to 3.5 Ma.

**DY087-28PC** was sampled at 50-55 cm and 174-179 cm core depths. *F. kerguelensis* and *F. barronii* are both present at 50-55 cm, suggesting the age of the sample to be approximately 2.3-1.3 Ma. The late Miocene diatom taxon *Actinocylcus ingens* var. *ovalis* also occurs in this sample and is likely reworked. *Fragilariopsis reinholdii* and *Denticulopsis crassa* occur at 174-179 cm, suggesting the age of this sample to be approximately 8.5 to 8.1 Ma. The diatom taxon *Nitzschia denticuloides* is alsoin this sample and is likely reworked.

**DY087-29PC** was sampled at the 80-85 cm core depth. The diatom *Thalassiosira vulnifica* is present, with a first known occurrence of approximately 3.2 Ma. *Thalassiosira insigna* is also present, with a last known occurrence at approximately 2.6 Ma. Together, these suggest an age between 3.2 to 2.6 Ma. *Denticulopsis maccollumii* is also present in this sample and is likely reworked.

**DY087-30PC** was sampled at the 196.5-199.5 cm core depth. *F. kerguelensis* and *F. barronii* suggests the age of the sample to be approximately 2.3 to 1.3 Ma. The morphology of *F. kerguelensis* and *F. barronii* indicates a transitional range between the two species.

**DY087-31PC** was sampled at 8 cm, 62 cm, and 269.5 cm core depths. *Fragilariopsis rhombica, F. kerguelensis,* and *Eucampia antarctica* are present at 8 cm, suggesting the sample is 1.4 Ma or

younger. *Nitzschia denticuloides*, *Denticulopsis praedimorpha, Denticulopsis delicata,* and *Denticulopsis dimorpha* are present in samples at 62 cm and 269.5 cm, suggesting an age for this lower interval of the core to be 12.8 to 11.75 Ma.

**DY087-32PC** was sampled at 17 cm, 59.5 cm, 156 cm, 420 cm, and 573 cm core depths. The presence of *F. kerguelensis* and *Thalassiosira lentiginosa* at 17 cm suggests the age of the sample to be 2.3 Ma or younger. *Actinocyclus actinochilus, Thalassiosira vulnifica, Fragilariopsis barronii,* and *Fragilariopsis weaveri* are present at 59.5 cm, suggesting the age of the sample to be 2.7 Ma. There is a gap in time between the samples at 59.5 cm and 156 cm, from the late Pliocene to late Miocene. *Thalassiosira oliverana* var. *sparsa* and *Actinocyclus ingens ovalis* are present in the three underlying samples, suggesting a late Miocene age of the sediment below the disconformity, where these 4 samples are interpreted to be 8.6 to 6.5 Ma.

**DY087-33PC** was sampled at 31.5 cm and 60 cm core depths. *F. kerguelensis* and *Actinocyclus karstenii* are present in the sample at 31.5 cm, suggesting the age to be 2.3 to 2.1 Ma. *Actinocyclus maccollumii* and *Thalassiosira insigna* were present at 60 cm, suggesting the age to be 3.4 to 2.6 Ma.

**Islas Orcadas Cores**

Of the twenty-one core catchers assessed from *ARA Islas Orcadas* Cruise 1678, core catchers 20, 37, 43, 48, and 49 were all determined to be Eocene to Oligocene in age. The core catchers of the target ages were then compared to the seismic sequences of interest, identified by the DY087 expedition. Two cores with ties to the DY087 seismic lines and that met the target ages of the DY087 Cruise research goals were then selected for further study that will be detailed in Chapter 3.

In addition to the age assessment determined for DY087 cores, core catcher samples from piston cores from prior cruises in this region, were examined for their stratigraphic potential, and ages were determined where possible. Cores with no diatoms present or of Neogene to Quaternary age will not be presented here but some information is presented in Tables 3 and 4.

Twenty-one samples from core catchers were examined from *Ara Islas Orcadas* Cruise 1678 and nine of those were determined to be of Oligocene age or older: 19CC, 20CC, 37CC, 38CC, 43CC, 44CC, 47CC, 48CC, and 49CC. Fifteen core catcher samples were examined from *Ara Islas Orcadas* Cruise 0775, and two of those were determined to be Oligocene age or older: 45CC and 46CC. Two core catcher samples were assessed from *ARA Islas Orcadas* Cruise 1176 and one of those was determined to be Oligocene age or older, 12CC.

**IO-1678-19CC** The presence of *Rocella gelida* and *Rocella vigilans*, *Cestodiscus antarcticus, Pyxilla reticulata, Cavitatus jouseanus, Cavitatus miocenicus, Fragilariopsis truncata*, and *Raphidodiscus marylandicus*, and the silicoflagellate *Naviculopsis biapiculata* suggest this sample is 26.4 to 25.4 Ma, based on the overlapping ranges of *Rocella* taxa. Taxa in this sample are similar to those documented by Gombos & Ciesielski (1983), Leg 71 Hole 513 Cores 12-2 through 12-4.

**IO-1678-20CC** contains *Hemiaulus dissimilis* and *Porotheca danica*, suggesting this sample is 34.5 Ma or older. This sample is near DY087 sub-bottom profiler lines and is correlative to DSDP Leg 36 Site 328B Core 5 and Site 328 Core 4, as documented by Gombos (1977).

**IO-1678-30CC** contains Actinocyclus ingens, Actinocyclus ingens var. nodus, Denticulopsis

*delicata,* and *Denticulopsis simonsenii*, which collectively suggest a late Miocene age between 14.6 to 12.6 Ma.

**IO-1678-32CC** Diatoms present in this sample include *Rocella praenitida, Pyxilla reticulata, Hyalopoda hajosae,* and *Thalassiosira bukryii* of Harwood & Maruyama (1991), which suggest an early Oligocene age.

**IO-1678-33CC** Diatoms from this core include *Denticulopsis dimorpha* and *Denticulopsis ovata*; the concurrent range of these two species indicates an age of 11.1 to 10.7 Ma.

**IO-1678-34CC** The age of this core is indicated by *Fragilariopsis weaverii,* which ranges from 3.5 to 2.5 Ma.

**IO-1678-35CC** Diatoms in this sample include *Fragilariopsis weaverii, Hemidiscus karstenii, Thalassiosira inura, Thalassiosira vulnifica,* and *Thalassiosira insigna*, which collectively suggest a Pliocene age between 3.5 to 2.7 Ma.

**IO-1678-37CC** Silicoflagellate *Corbisema hastada*, and diatoms *Hemiaulus subacutus*, and *Hemiaulus incurvus* are present; the latter indicates a late Paleocene age. This core has taxa similar to those documented in DSDP Leg 36 Hole 327A, Cores 5 through 8, as reported in Gombos (1977).

**IO-1678-38CC** *Hemiaulus altus, Hemiaulus incurvus, Hemiaulus inaequilaterus*, and *Fenneria* spp. are present, which collectively indicate a late Paleocene age. The core has taxa similar to those documented in DSDP Hole 327A, Cores 5 through 8, as reported in Gombos (1977).

**IO-1678-43CC** has *Distephanosira architecturalis*, which suggests the age of the sample to be middle to late Eocene in age. This core is located near DY087 sub-bottom profiler lines.

**IO-1678-44CC** The presence of *Azpeitia oligocenica*, *Rocella praenitida, Pyxilla reticulata, Pseudotriceratium monile, Distephanosira architecturalis*, and the silicoflagellate taxon *Naviculopsis constricta* suggest a late Eocene age for this sample.

**IO-1678-47CC** The presence of *Rocella gelida, Rossiella symmetrica, Azpeitia oligocenica, Hemiaulus taurus, Asterolampra tela*, and silicoflagellate *Naviculopsis biapiculata* suggest this sample is 26.4 to 22.7 Ma, based chiefly on the overlapping ranges of *R. gelida* and *H. taurus*, and correlative to the interval in DSDP Hole 513A, Cores 13 to 15.

**IO-1678-48CC** The presence of *Rocella praenitida*, *Cavitatus jouseanus,* and *Pyxilla reticulata*, suggests the sample is Oligocene in age. This sample is near DY087 sub-bottom profiler lines.

**IO-1678-49CC** The presence of *Hemiaulus subacutus* and *Hemiaulus polymorphus*, and silicoflagellates *Corbisema hastada*, *Naviculopsis biapiculata*, and *Naviculopsis constricta* suggest a Late Paleocene age. This sample is near DY087 sub-bottom profiler lines.

**IO-0775-45CC** The silicoflagellates *Corbisema hastada* and *Naviculopsis constricta* suggest the this sample islate Paleocene. This sample also contains Cretaceous diatoms and silicoflagellates that are assumed to be reworked – *Costopyxis, Gladiopsis*, and *Lyramula*.

**IO-0775-46CC** Diatoms *Distephanosira architecturalis, Sceptroneis spp*., and silicoflagellates *Corbisema hastada* and *Naviculopsis biapiculata*, in the absence of *Naviculopsis trispinosa*, suggest an earliest Oligocene to late Eocene age.

**IO-1176-12CC** *Trinacria simulacrum* (Shown in appendix, Pl. 3, fig. 12)*, Pseudotriceratium radiosoreticulatum*, Genus and species uncertain #1 of Gombos (1983) (Shown in appendix, Pl. 6, figs. 1-3, 8-9), *Pyxilla reticulata, Azpeitia oligocenica, Rocella praenitida, Triceratium unguiculatum*, *Triceratium quadrangulare* (Pl. 4, fig. 6), *Distephanosira architecturalis, Asterolampra acutiloba, Asterolampra uraster* (Pl. 1, fig. 6), *Asterolampra affinis* (Pl. 1, figs. 10-13), *Hemiaulus reflexispinosis* (Pl. 7, figs 2-4), *Hemiaulus* sp. A (Pl. 2, fig. 3), which was illustrated in Harwood (1989) (pl. 4, fig. 15, *Biddulphia* sp. B), *Tubaformis unicornis* (Pl. 8, figs. 1-8), and silicoflagellates *Dictyocha haxacantha*, and *Naviculopsis* sp. collectively suggest an age of middle Eocene for this sample, and a correlation to the middle Eocene interval in DSDP Site 512 reported by Gombos (1983), and likely also correlative with the assemblage documented by Fenner (1979) from Site 358, Cores 2-4, 30-31 cm. suggesting the age of this sample to be ~40 to ~22 Ma.

**Robert Conrad Cores**

Samples from seven piston cores were examined from *Robert Conrad* Cruises 15 and 16. The following three cores from RC-15 were determined to be Oligocene or older, and the two cores from RC-16 were determined to be late Miocene.

**RC-15-81PC** was sampled at the 511-516 cm core depth. Diatoms *Asteromphalus oligocenicus, Araniscus lewisianus,* and silicoflagellates *Dictyocha crux* and *Mesocena apiculata* were present in this sample, which suggest a late Oligocene age.

**RC-15-84PC** was sampled at the 550-555 cm core depth. Diatoms *Hemiaulus altus*, *Hemiaulus incurvus, Hemiaulus subacutus,* and silicoflagellates *Corbisema hastada* and *Naviculopsis constricta* were present, indicating a late Paleocene age.

**RC-15-121PC** was sampled at the 165-170 cm core depth. Diatoms *Distephanosira architecturalis, Hemiaulus subacutus, Sceptroneis grunowii,* and *Trinacria simulacrum,* and silicoflagellate *Naviculopsis constricta* were present in this sample, which suggests an early Eocene to late Paleocene age.

**RC-16-108PC** was sampled at the 483-488 cm core depth. Diatoms *Asterolampra kennettii, and Denticulopsis simonsenii*, and the silicoflagellate genus *Octactis* collectively suggest a late Miocene age for this sample.

**RC-16-111PC** was sampled at the 430-435 cm core depth. Diatoms include *Actinocyclus ingens, Azpeitia tabularis, and Denticulopsis ovata*, and the latter suggests a late Miocene age between 11.1 and 8.4 Ma.

**Vema Cores**

Twenty-three piston core samples were examined from *Vema* Cruises 14, 17, 18, 22, and 31. The following seven were determined to be late Miocene to Oligocene age or older.

**VM-17-107PC** was sampled at the 195-200 cm core depth. This sample contained a well-preserved assemblage of diatoms, with many specimens observed as complete frustules and often in chains. Kisseleviella spp., Cymatosira sp., and *Hemiaulus caracteristicus* are present in this sample. This interval is likely correlative to the intervals in DSDP Holes 513A and 511, Cores 31 through 33, due to the abundant *Sceptroneis* spp. here and within the DSDP Leg 71 cores (Gombos & Ciesielski, 1983), an early Oligocene age is likely.

**VM-18-104PC** was sampled at the 328-333 cm core depth. Diatoms include *Azpeitia oligocenica, Pyxilla reticulata, Pyxilla johnsonianus, Pyrgupyxix eocenica, Eurossia irregularis, Hemiaulus dissimilis, and Distephanosira archetecturalis,* which collectively suggest a middle Eocene age. This assemblage is similar to erratic D-1 of Harwood & Bohaty (2000), Cores 6 through 19 in DSDP Leg 71, Hole 512, Cores 6 to 19 Gombos (1983), and ODP site 748B, Cores 16 to 20 of Harwood & Maruyama (1992), which were determined to be Eocene in age. It also is similar to the middle Eocene silicoflagellate and ebridian assemblages documented in ODP Hole 748B by Bohaty & Harwood (2000), and DSDP Leg 29, Hole 281, Cores 14 to 16, and Hole 283, Cores 2 to 8 of Hajós (1976), determined to be middle Eocene in age.

**VM-18-106PC** was sampled at the 195-200 cm core depth. Diatoms include *Eucampia antarctica, Denticulopsis simonsenii, Denticulopsis dimorpha, Actinocyclus ingens, Neobrunia mirabilis, Thalassiosira oliverana* var. *sparsa*, and *Thalassiosira torokina*, which collectively suggest an age between 10.7 to 8.6 Ma.

**VM-18-109PC** was sampled at the 284-289 cm core depth. The co-occurrence of *Denticulopsis simonsenii, Denticulopsis ovata, Denticulopsis dimorpha, Rouxia naviculoides, Asterolampra kennettii*, and *Nitzschia denticuloides* collectively suggest an age between 12.5 to 11.7 Ma.

**VM-18-112PC** was sampled at the 255-260 cm core depth. The following diatoms were observed: *Pyxilla reticulata, Triceratium unguiculatum, Purgupyxis eocena, Rocella praenitida*, and *Rouxia granda*, along with silicoflagellate *Naviculopsis biapiculata*. Collectively this assemblage suggests the age is older than 30.9 Ma, and likely early Oligocene to late Eocene.

**VM-31-60PC** was sampled at the 550-559 cm core depth. Diatoms *Eurossia irregularis, Bicornis incisus, Pyxilla reticulata, Eurossia irregularis* var. *incurvata,* a diverse assemblage of *Stephanopyxis spp*., and *Sphynctolethus pacificus* were present, suggesting the age is early Oligocene.

**VM-31-61PC** was sampled at the 330-335 cm core depth. Diatoms include *Hemiaulus taurus, Hemiaulus caracteristicus, Hyalopoda hajosae, Pyrgupyxis eocenica,* Gn et sp. indet. #3 of Harwood & Maruyama (1992), *Eurossia irregularis, Porotheca danica,* and *Kisseleviella tricoronata* suggesting an early Oligocene age. This sample is similar to the early Oligocene assemblage from ODP Leg 119, Hole 739C, Core 30 in Prydz Bay, East Antarctica as described by Barron & Mahood (1993). This site also has similarities to Assemblage Zone B, at 366 to 500 m of Harwood (1989) from the CIROS-1 drill hole in the western McMurdo Sound area.

## DISCUSSION

The diatom record from the Eocene is not well understood, but recent advances and summaries of existing knowledge in the works of Barron et al. (2015), Scherer et al. (2007), and Fenner (1985) indicate advances in our understanding.

The DY087 expedition and site survey effort was successful and helps to identify stratigraphic targets for future IODP drilling. The newly acquired piston and gravity cores from the DY087 cruise, and potential future drill cores from the eventual IODP expedition to this region, if scheduled, will benefit from an understanding of the ages of seismic units from this study of sediment cores from this region. Piston cores 20 and 48 from the *ARA Islas Orcadas*

Cruise 1678 are located near sub-bottom profiler lines collect on the DY087 cruise. IO-1678-20 is tied into DY087 seismic Line RC2106-142, both cores are discussed in greater detail in Chapter 3. IO-1678-43CC is located near DY087 seismic line L20A, IO-1678-49CC and IO-1678-50CC are located near DY087 seismic line L18B. IO-0775-49CC and IO-0775-50CC are located near DY087 seismic line L01. IO-1176-10CC is located near DY087 seismic line L18A, and VM-14-47CC is located near DY087 seismic line L20B. IO-1176-12CC is located near sub-bottom profiler lines collect on DY087. Tables 3 and 4 summarizing these results can be found at the end of this chapter.

| Core Cruise | Catcher (CC) | Age |
|---|---|---|
| IO-1678 | 20 | older than 34.5 Ma |
| IO-1678 | 37 | late Paleocene |
| IO-1678 | 43 | older than ~33.6 Ma |
| IO-1678 | 48 | Oligocene |
| IO-1678 | 49 | late Paleocene |

*Table 2. Eocene to Oligocene age core catchers from Ara Islas Orcadas Cuise 1678*

## CONCLUSIONS

The DY087 expedition successfully recovered three piston cores with samples of Oligocene age and older, DY087-10PC at 129 cm, DY087-12PC at 195.5 cm, DY087-15PC at 64 cm and 122 cm. These target age strata have the potential to aid in the understanding of the development of the Drake Passageway and ocean conditions of that time. Other DY087 cores are Miocene age or younger. Although these cores did not reach the target age, they still provide valuable information about the distribution of Miocene sediment, and they can be used to date seismic sequences of this age. The regional survey of previously collected sediment cores on the Falkland Plateau and MEB provide additional age constraint on the ages of these sequences.

# References


Barron, J. A. & Mahood, A. D. (1993). Exceptionally well-reserved early Oligocene diatoms from glacial sediments of Prydz Bay, East Antarctica. *Micropaleontology, 39(1)*, 29-45.

Barron, J. A., Stickley, C. E., & Bukry, D. (2015). Paleoceanographic, and paleoclimatic constraints on the global Eocene diatom and silicoflagellate record. *Palaeogeography, Palaeoclimatology, Palaeoecology, 422*, 85-100.

Bohaty, S. M. & Harwood, D. M. (2000). Ebridian and silicoflagellate biostratigraphy from Eocene McMurdo erratics and the Southern Ocean. *In: Stillwell, J.; Feldman, R. (eds.), Antarctic Research Series, Paleobiology and Paleoenvironments of Eocene Rocks: McMurdo Sound, East Antarctica, 76*, 99-159.

Bohaty, S. M. & Zachos, J. C. (2003). Significant Southern Ocean warming event in the late middle Eocene. *Geology 31, 11*, 1017-1020.

Cassidy, D. S., Ciesielski, P. F., Kaharoeddin, F. A., Wise, S.W. Jr, & Zemmels, I. (1978). ARA Islas Orcadas Cruise 0775 Sediment descriptions. *Antarctic Research Department of Geology, Florida State University, Tallahassee Florida*, Contribution No. 45, 82 pp.

Ciesielski, P. F. (1983). The Neogene and Quaternary diatom datum biostratigraphy of subantarctic sediments. Deep Sea Drilling Project Leg 71. *Initial Reports of the Deep Sea Drilling Project, 71*, 635-665.

Fenner, J. (1984). Eocene-Oligocene planktic diatom stratigraphy in the low latitudes and the high southern latitudes. *Micropaleontology, 30*, 319-342.

Fenner, J. (1985). Late Cretaceous to Oligocene planktic diatoms. *In: Bolli, H., Saunders, J., and Perch-Nielsen, K. (eds.), Plankton Stratigraphy*: Cambridge (Cambridge Univ. Press), 713-762.

Gombos Jr, A. M. (1983). Late Eocene to early Miocene diatoms from the Southwest Atlantic. *Initial Reports of the Deep Sea Drilling Project, 71*, 538-634.

Gombos Jr, A. M. (1977). Paleogene and Neogene diatoms from the Falkland Plateau and Malvinas Outer Basin: Leg 36. *Intital Reports of the Deep Sea Drilling Project*, *36*, 575-688.

Gombos Jr, A. M. & Ciesielski, P. F. (1983). Late Eocene to Early Miocene diatoms from the Southwest Atlantic. *Initial Reports of the Deep Sea Drilling Project*, 538-634.

Hajós, M. (1976). Upper Eocene and lower Oligocene diatomaceae, archaeomonadaceae, and silicoflagellatae in Southwestern Pacific sediments, *DSDP Leg 29*. *Initial Reports of the Deep Sea Drilling Project*, *35*, 817-883.

Harwood, D. M. & Bohaty, S. M. (2000). Marine diatom assemblages from Eocene and younger erratics, McMurdo Sound, Antarctica. *In: Stillwell, J., Feldman, R. (eds.), Paleobiology and Paleoenvironments of Eocene Rocks: McMurdo Sound, East Antarctica, American Geophysical Union, Antarctic Research Series, 76*, 73-98.

Harwood, D. M. & Maruyama, T. (1992). Middle Eocene to Pleistocene diatom biostratigraphy of Southern Ocean sediments from the Kerguelen Plateau, LEG 120. *In: Wise, S.W. Jr, Schlich, R., et al. (eds.), In Proceedings of the Ocean Drilling Program, Scientific Results, 120,* 683-733.

Kaharoeddin, F. A., Eggers, M., Graves, S., Hattner, J., Jones, S., MacKenzie, D., . . . Zemmels, I. (1978). ARA Islas Orcadas Cruise 1176 sediment descriptions. *Antarctic Research Facility, Department of Geology, Florida State University, Tallahassee Florida,* Contribution No. 6, 130 pp.

Kaharoeddin, F. A., Graves, R. S., Bergen, J. A., Eggers, M. R., Harwood, D. M., Humphreys, C. L., . . . Watkins, D. K. (1982). ARA Islas Orcadas Cruise 1678 sediment descriptions. *Antarctic Research Facility, Department of Geology, Florida State University, Tallahassee Florida,* Contribution No. 50, 178 pp.

McKay, R. M., De Santis, L., Kulhanek, D. K., Ash, J. L., Beny, F., Browne, I. M., . . . Ishino, S. (2019). Expedition 374 methods. *In: Proceedings of the International Ocean Discovery Program, 374*. https://doi.org/10.14379/iodp.proc.374.102.2019

Olney, M. P., Scherer, R. P., Bohaty, S. M., & Harwood, D. M. (2005). Eocene–Oligocene paleoecology and the diatom genus Kisseleviella Sheshukova-Poretskaya from the Victoria Land Basin, Antarctica. *Marine Micropaleontology, 58(1)*, 56-72.

Scherer, R. P., Gladenkov, A. Y., & Barron, J. A. (2007). Methods and applications of Cenozoic Scherer, R. P., Gladenkov, A. Y., & Barron, J. A. (2007). Methods and applications of Cenozoic marine diatom biostratigraphy. *In: Starrat, S. (ed.), Pond Scum to Carbon Sink: Geological and Enviromental Applications of Diatoms, The Paleontological Society Papers, 13*, 61-83.

Scherer, R., Bohaty, S. M., & Harwood, D. M. (2000). Oligocene and lower Miocene siliceous microfossil biostratigraphy of Cape Roberts Project Core CRP-2/2A, Victoria Land Basin, Antarctica. *Terra Antartida 7 (4)*, 417-442.

# TABLES AND FIGURES

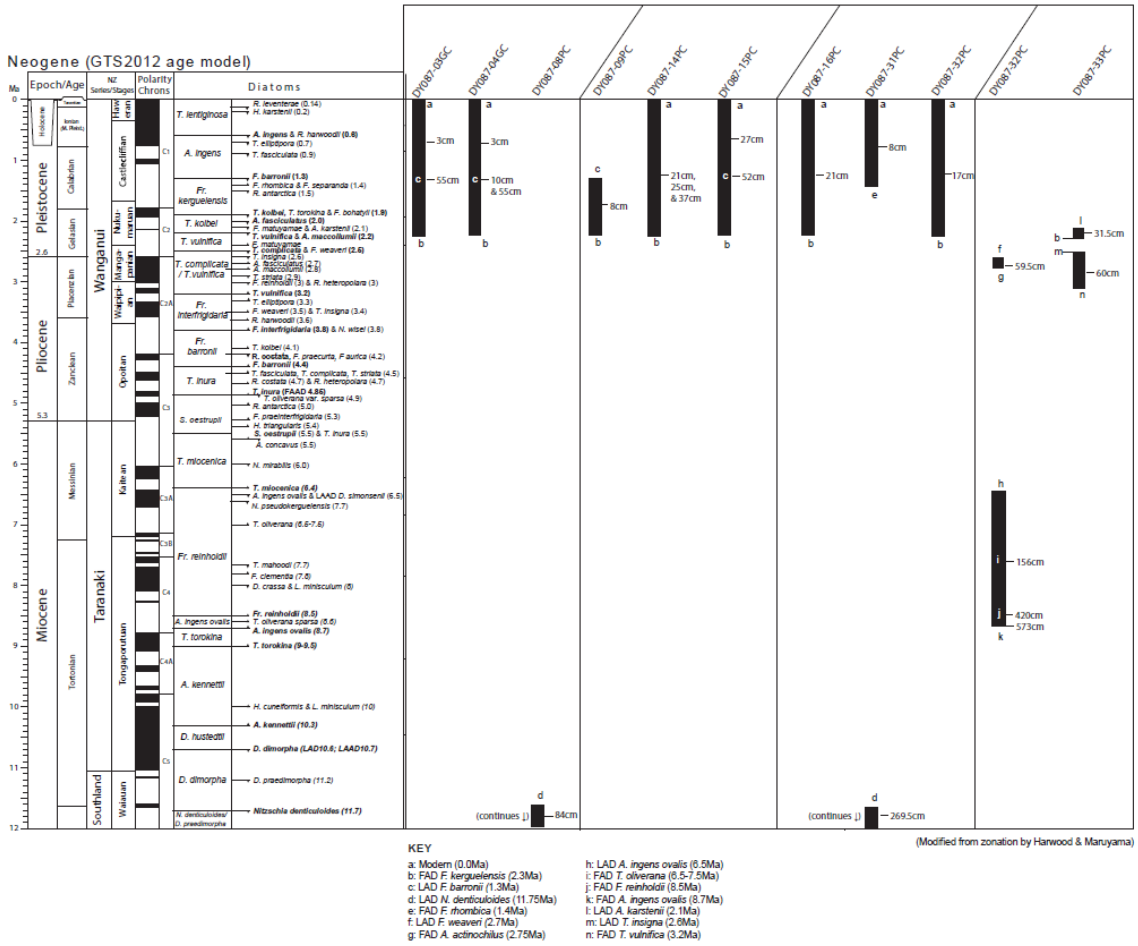


*Figure 1. Lower Miocene to Holocene summary of piston core samples from Cruise DY087. Ages are approximated using diatom first and last occurrence data. The GTS2012 Age Model was used and is modified from zonation by Harwood & Maruyama (1992).*

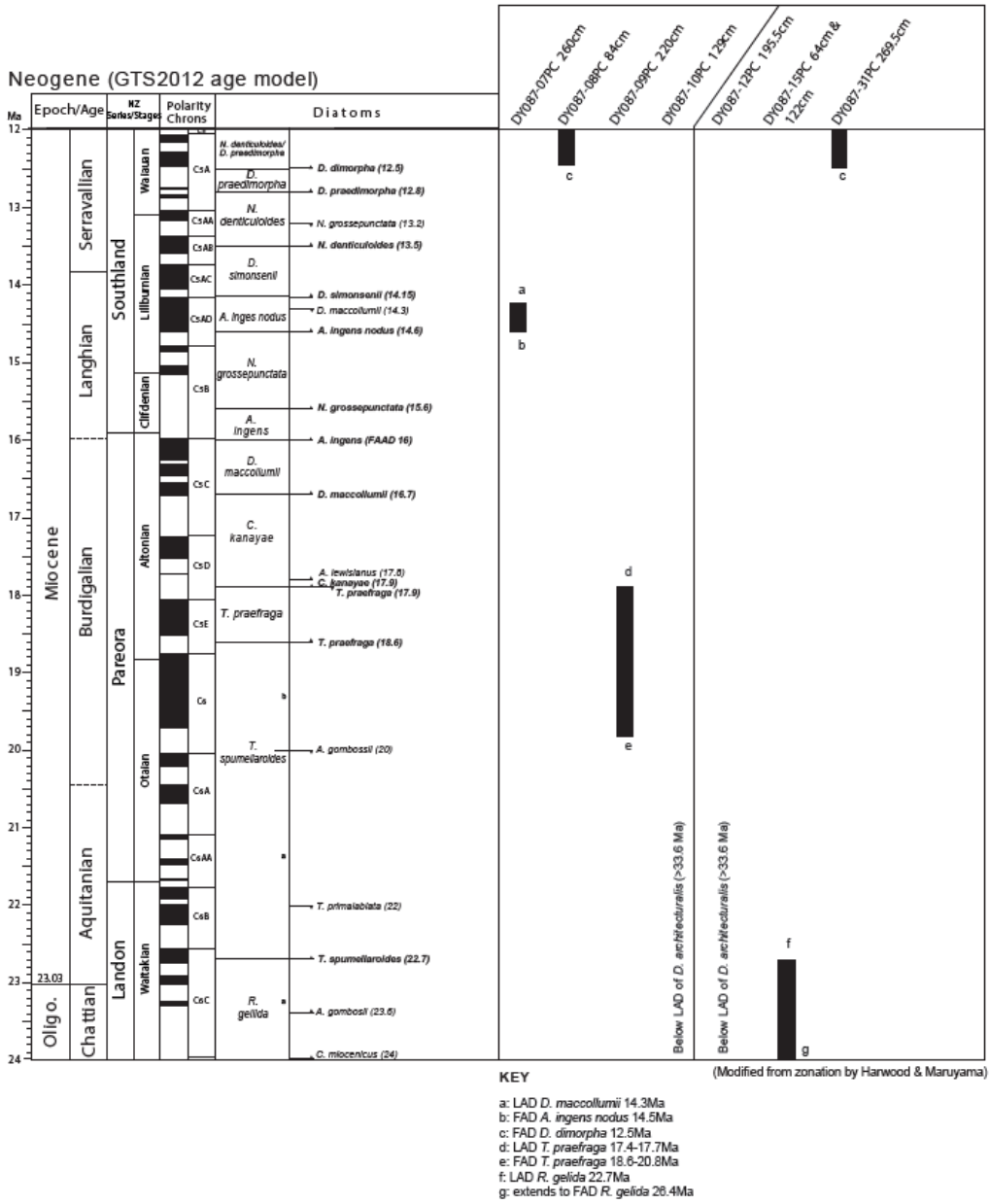


*Figure 2. Lower Oligocene to Middle Miocene summary of piston core samples from Cruise DY087. Ages are approximated using diatom first and last occurrence data. The GTS2012 Age Model was used and is modified from zonation by Harwood & Maruyama (1992).*

| Cruise | Core Catcher (CC) | Age |
|---|---|---|
| IO-1678 | 19 | 26.4 Ma to 25.4 Ma |
| IO-1678 | 20 | Older than 34.5 Ma |
| IO-1678 | 21 | 10 Ma to 4.45 Ma |
| IO-1678 | 26 | NADP |
| IO-1678 | 28 | NADP |
| IO-1678 | 30 | 14.6 Ma to 12.6 Ma |
| IO-1678 | 32 | early Oligocene |
| IO-1678 | 33 | 11.1 Ma to 10.7 Ma |
| IO-1678 | 34 | 3.5 Ma to 2.5 Ma |
| IO-1678 | 35 | 3.5 Ma to 2.7 Ma |
| IO-1678 | 37 | late Paleocene |
| IO-1678 | 38 | late Paleocene |
| IO-1678 | 39 | NADP |
| IO-1678 | 41 | NADP |
| IO-1678 | 43 | mid to late Eocene |
| IO-1678 | 44 | late Eocene |
| IO-1678 | 47 | 26.4 Ma to 22.7 Ma |
| IO-1678 | 48 | Oligocene |
| IO-1678 | 49 | late Paleocene |
| IO-1678 | 50 | ~11.3 Ma |
| IO-1678 | 104 | 3.5 Ma |
| IO-1176 | 9 | 12.8 Ma to 11.2 Ma |
| IO-1176 | 10 | 10.2 Ma to 9 Ma |
| IO-1176 | 12 | middle Eocene |
| IO-0775 | 2 | 9-7.5 Ma to 4.45 Ma |
| IO-0775 | 40 | 3.4 Ma to 3.0 Ma |
| IO-0775 | 43 | 5.3 Ma to 4.45 Ma |
| IO-0775 | 44 | NADP |
| IO-0775 | 45 | late Paleocene |
| IO-0775 | 46 | early Oligocene to late Eocene |
| IO-0775 | 47 | NADP |
| IO-0775 | 48 | ~10 Ma to 8.0 Ma |
| IO-0775 | 49 | 10.2 Ma to 8.1 Ma |
| IO-0775 | 50 | NADP |
| IO-0775 | 52 | 9-7.5 Ma to 2.2 Ma |
| IO-0775 | 53 | NADP |
| IO-0775 | 54 | 7.5-6.5 Ma or younger |
| IO-0775 | 55 | 2.3Ma to 2.2Ma |
| IO-0775 | 56 | NADP |
| EL-22 | 10 | 11.1Ma to 10.6Ma |

*Table 3. Basal ages of core catchers from Ara Islas Orcadas Cruises 1678, 1176, and 0775, and Eltanin Cruise 22. Previously published ages can be found in the initial core description volumes for the cruises (Kaharoeddin, 1982) (Kaharoeddin, et al., 1978) (Cassidy, et al., 1978). (NADP=No age date possible)*

| Cruise | Core | Top Depth in Core (cm) | Bottom Depth in Core (cm) | Age |
|---|---|---|---|---|
| RC-15 | 81PC | 511 | 516 | ~30 Ma to 17.3 Ma |
| RC-15 | 82PC | 1064 | 1069 | NADP |
| RC-15 | 84PC | 550 | 555 | Late Paleocene-Late Oligocene |
| RC-15 | 85PC | 138 | 143 | 2.3 Ma to 0.6 Ma |
| RC-15 | 121PC | 165 | 170 | Older than ~33.6 Ma |
| RC-16 | 108PC | 483 | 488 | 8.7 Ma to 8.1 Ma |
| RC-16 | 111PC | 430 | 438 | 11.1 Ma to 8.4 Ma |
| VM14 | 44PC | 239 | 244 | 12..5 Ma to 11.2 Ma |
| VM14 | 47PC | 410 | 415 | 11.1 Ma to 8.4 Ma |
| VM17 | 107PC | 195 | 200 | ~35 Ma to 33.4 Ma |
| VM18 | 104PC | 328 | 333 | 28.3 Ma to 14.5 Ma |
| VM18 | 106PC | 195 | 200 | 14.2 Ma to 6.0-6.5 Ma |
| VM18 | 107PC | 420 | 427 | 8.5 Ma to 3 Ma |
| VM18 | 109PC | 284 | 289 | 10.3 Ma to 8.4 Ma |
| VM18 | 112PC | 255 | 260 | Older than 30.9 Ma |
| VM18 | 114PC | 480 | 490 | 8.5 Ma to 3 Ma |
| VM18 | 115PC | 76 | 81 | 11.1 Ma to 8.4 Ma |
| VM18 | 116PC | 175 | 185 | NADP |
| VM18 | 117PC | 243 | 245 | 8.5 Ma to 3 Ma |
| VM18 | 118PC | 1111 | 1116 | NADP |
| VM22 | 92PC | 142 | 147 | 8.5 Ma to 3 Ma |
| VM22 | 93PC | 258 | 263 | 9.7 Ma to 9 Ma |
| VM22 | 94PC | 421 | 426 | 12.5 Ma to 10.6 Ma |
| VM22 | 99PC | 493 | 498 | 3.5 Ma to 3 Ma |
| VM31 | 60PC | 550 | 559 | ~31 Ma to 30.3 Ma |
| VM31 | 61PC | 330 | 335 | ~28 Ma to 20.4 Ma |
| VM31 | 67PC | 575 | 580 | 0.65 Ma or younger |
| VM31 | 68PC | 510 | 518 | NADP |
| VM31 | 74PC | 457.5 | 464 | NADP |
| VM31 | 75PC | 130 | 135 | NADP |

*Table 4. Age approximations of piston cores from Robert Conrad Cruises 15 and 16, and Vema Cruises 17, 18, 22, and 31 (NADP=No age date possible)*

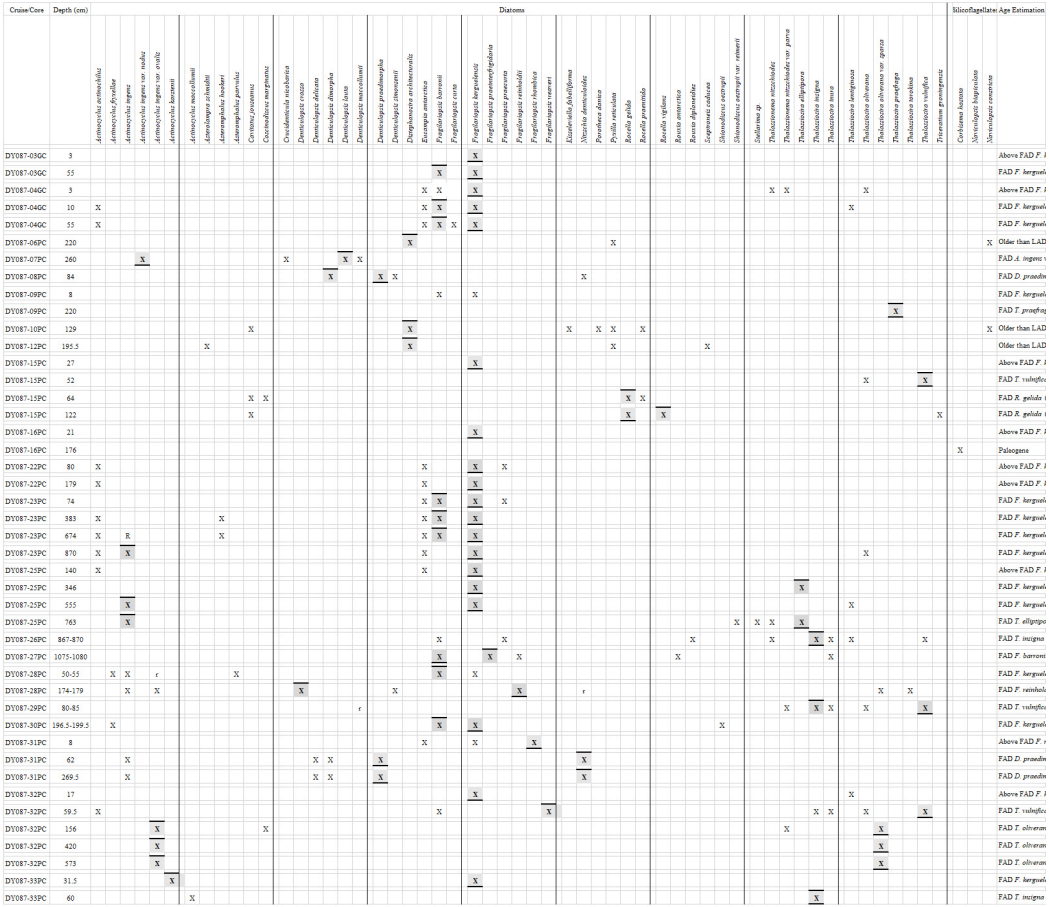


*Table 5. Summary of diatom and silicoflagellate taxa from DY087 cores. First Appearance Datum (FAD) events are indicated by a line below the occurrence, Last Appearance Datum (LAD) events are indicated by a line above occurrence. (r=rare; x=present)*

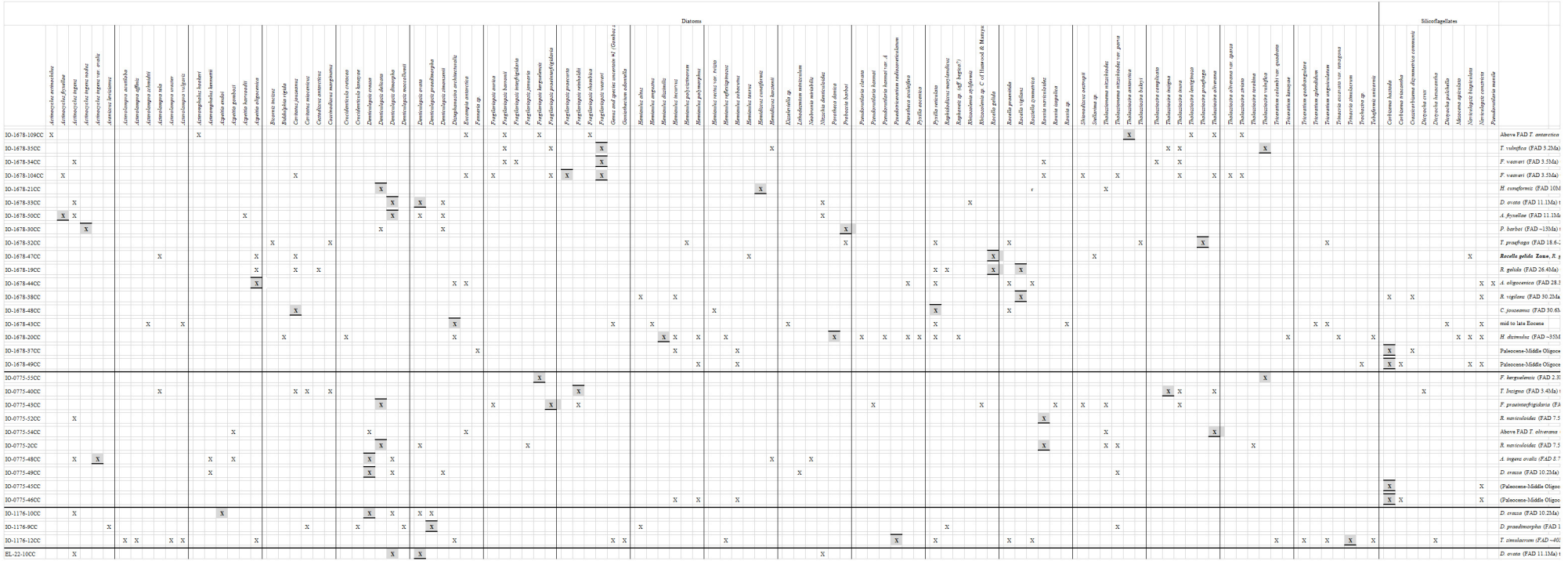


*Table 6. Summary of diatom and silicoflagellate taxa from ARA Islas Orcadas and Eltanin core catchers. First Appearance Datum (FAD) events are indicated by a line below the occurrence, Last Appearance Datum (LAD) events are indicated by a line above occurrence.*

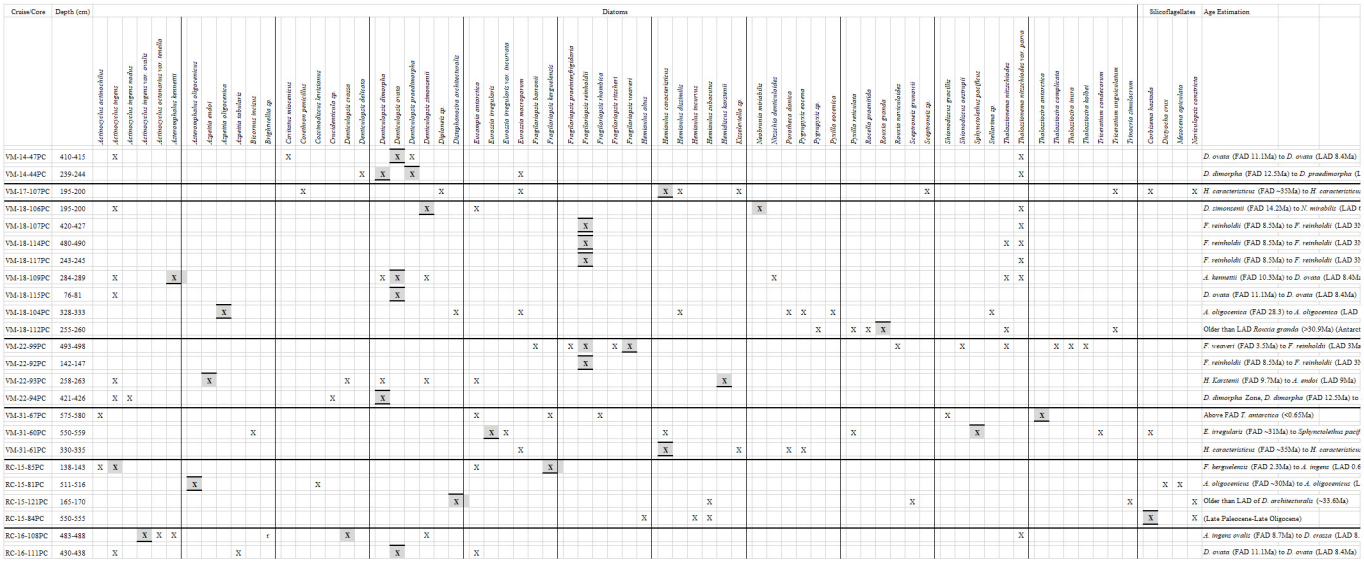


*Table 7. Summary of diatom and silicoflagellate taxa from VEMA and Robert Conrad cores. First Appearance Datum (FAD) events are indicated by a line below the occurrence, Last Appearance Datum (LAD) events are indicated by a line above occurrence.*

# CHAPTER 3: EOCENE DIATOM ASSEMBLAGES FROM SOUTHERN SOUTH ATLANTIC OCEAN SEDIMENT CORES

## INTRODUCTION

A better understanding of the age of sediment cores that constrain the age of seismic sequences on the Maurice Ewing Bank and Falkland Plateau is needed to assess the history of Cenozoic deep-water current flow in this region, an objective of IODP Pre-Proposal 862. The Drake Passageway is the location of the lithospheric boundary between the Antarctic and South American tectonic plates. When this passage opened fully to marine deep-water flow, the Antarctic Circumpolar Current (ACC) formed around Antarctica. The timing of the initiation of this major element of Cenozoic ocean circulation has been debated and occurred somewhere between 35-28 million years ago. Better constraints on this age are of interest to the paleoceanographic community (Daziel, 2014).

Diatoms are useful for biostratigraphic analyses because they evolve rapidly and are highly sensitive to environmental changes, making them capable of resolving the age of significant events in the history of the Southern Ocean. Improving key biostratigraphic tools, such as diatoms, is an important step in advancing paleoceanographic and paleoclimate models, as well as in increasing our understanding of glacial cycles, the ACC, and their climatic effects (Basov et al., 1983; Fenner, 1984; Bohaty & Zachos, 2003; Livermore et al., 2007; Daziel, 2014).

Marine oxygen isotope records developed and interpreted by Bohaty and Zachos (2003) indicated a pronounced warming event during the Middle Eocene (~41.5Ma) at Ocean Drilling Program (ODP) sites 689, 690, 738, 744, and 748 in the Southern Ocean. They interpreted their results as a regional warming event in the South Atlantic and Indian oceans and distinguished it

as the Middle Eocene Climate Optimum (MECO) (Bohaty & Zachos, 2003). A more in-depth survey of marine sediment cores from other regions of the Southern Ocean has the potential to provide additional constraint on the timing, character, and extent of the MECO.

The biostratigraphic occurrence of diatoms of Oligocene and younger age have been fairly well documented in the South Atlantic Ocean. However, diatom assemblages of Eocene and older age have fewer biostratigraphic constraint, and further investigation will lead to an improved understanding of the sedimentology and diatom record of the region.

Sediment cores collected during *ARA Islas Orcadas* Cruises 1678, 1176, and 0775; *VEMA* Cruises 14, 17, 18, 22, and 31; *Eltanin* Cruise 22; and *Robert Conrad* Cruises 15 and 16 were selected here for study of the diatoms in these cores (Figure 1). Diatoms and silicoflagellates in core samples were examined biostratigraphically in order to assign approximate ages (Figure 2). After a general survey of the cores in the region of the Maurice Ewing Bank and Falkland Plateau (Chapter 2), three cores were selected for detailed study and examination of a suite of samples. Cores IO-1678-20PC, IO-1678-48PC, and IO-1176-12PC contained taxa of Eocene age. Two of these (IO-1678-20PC, IO-1678-48PC) were analyzed at high resolution with a sample spacing of ~5-10 cm. Sediment core IO-1176-12PC was lost in the move of the Antarctic Core Repository from Florida State University to Oregon State University, so only the Core Catcher sample is available for study. Documenting the diatom assemblage composition and assessing the biostratigraphic age of distinct stratigraphic intervals from a sequence of samples from cores IO-1678-20PC and IO-1678-48PC is the primary focus of this chapter. The objectives are to define the age of distinct stratigraphic intervals that are bounded by disconformities that reflect missing intervals of time. These disconformities reflect times of higher ocean current strength that either eroded previously deposited sediment and/or prevented deposition. The timing of these events yield important clues in resolving the history of  Southern Ocean currents in the region of

the Drake Passage, their strength, and perhaps episodic intervals of intensification.

## REVIEW OF PALEOGENE AND EOCENE DIATOM SCIENCE

Diatom biostratigraphy provides the ability to date stratigraphic sections in different locations and reveal past climate history. Paleocene and Eocene diatom records are understudied, with gaps in the stratigraphic record. the slow pace of advances in the study of Eocene diatoms is in part due to (1) the limited number of diatom paleontologists, (2) limitations in deep-sea drilling of this time interval, and (3) poor core recovery over thick diatom-bearing intervals. High latitude diatoms are especially useful for stratigraphic control due to their high diversity and abundance (Fenner, 1984). Building a more complete diatom record for the Southern Ocean will enable a better understanding and dating of ocean circulation strength and the extent to which it facilitated or prevented sediment accumulation during the Paleocene and Eocene.

The study of siliceous microfossils underwent major expansion with the initiation of the Deep Sea Drilling Project (DSDP) in 1968. One of the first Paleocene diatom zonations was constructed during DSDP Leg 36 using Hole 327A (Gombos, 1977) on the Falkland Plateau. The zonation included three zones for the mid to Late Paleocene. During DSDP Leg 44, Hole 390a was used by Gombos (1982) who proposed a discontinuous zonal framework for the Early Eocene. During DSDP Leg 74, Hole 208 was used to construct zones for the Early to mid Paleocene (DePrado & Ling, 1981) from Lord Howe Rise. Although these initial zonations contributed valuable stratigraphic information, it has been suggested that their use is limited to the Southern Ocean (Witkowski et al., 2020), as many taxa are endemic to this region.

During DSDP Leg 71, diatoms from Sites 511, 512, and 513 were assessed biostratigraphically; Site 511 is located on the Falkland Plateau, Site 512 on the Maurice Ewing Bank, and Site 513 on the lower flank of the Mid-Atlantic Ridge. The diatoms in Hole 512 did not enable construction of a zonation but were described and determined to be Eocene age and described by Gombos (1983). Holes 511 and 513A were used to construct a continuous diatom zonation comprising 12 biostratigraphic zones, uninterrupted by disconformities, from the Late Eocene to Early Micoene by Gombos & Ciesielski (1983).

Most Eocene to Oligocene age diatoms had a broad geographical distribution, which allowed the integration of diatom sequences from multiple sites and oceans to be used in zonations. Fenner (1984) built upon previously proposed zones and integrated diatom records from DSDP Leg 15, Hole 149 and 94 and from DSDP Leg 41, Hole 366, 369A, and 390A. The sites span most ocean basins, with the exception of the Arctic. Fenner (1984) combined data from these sites to make a low-latitude zonation scheme that spans from the Middle Eocene to Oligocene.

In 2007, Fenner's (1984) zonations were modified by Scherer et al. (2007). In 2014, Barron et al. (2014) again updated the zonation scheme for the Late Eocene using ODP site 1090 on the southern flank of the Agulhas Ridge, with the development of four alternative zones (Barron et al., 2014). The following year a multisite zonation was published, including diatom zones, diatom ranges, and silicoflagellate zones, that spanned from the Late Paleocene to Early Oligocene (Barron et al., 2015).

Scherer et al. (2007) incorporated previously proposed zonations to create a global low-latitude, North Pacific diatom zonal scheme for the Paleocene to mid Eocene using first and last occurrences of diatoms compared with the Geomagnetic Polarity Time Scale (Cande & Kent,

1992; 1995). Eight biostratigraphic ones were proposed in the low latitudes, from the Late mid Eocene through the Oligocene.

Renaudie et al. (2018) examined legacy DSDP sites 86, 208, 327A, 384, 524 and ODP sites 700B, 761B, 1051A and 1121B for their siliceous microfossil content. They documented species abundance and diversity from the Paleocene through Early Eocene, noting differences in deposition at different locations, and associated assemblage and diversity changes.

Witkowski et al. (2020) created a biostratigraphic diatom zonation that incorporates previous work from Fenner (1984), McLean & Barron (1988), Fourtanier (1991), and Barron et al. (2014) and includes 14 uninterrupted zones, spanning the mid Paleocene to Early Oligocene. ODP Leg 171B Holes 1050A,C and Hole 1051A were emphasized due to the excellent magnetostratigraphy, with tightly constrained reversals, and their biostratigraphic record. This study refined previous age models and provided high-resolution age control for Paleogene sites. Witkowski et al. (2020) notes both the concurrence with the suggested methods for diatom examination in Renaudie et al. (2018) and the likely high rate of survivorship across the K/Pg boundary.

## MATERIALS AND METHODS

Samples from *ARA Islas Orcadas* Cruise 1678 core 20 and *ARA Islas Orcadas* Cruise 1678 core 48 were prepared and examined with the same procedures outlined in Chapter 2 methods.

Subsequently, diatoms in the samples were documented and interpreted biostratigraphically. IO-1678-20PC became a major focus of this study, because of the complex stratigraphy and the presence of several discrete, unconformity bound, stratigraphic intervals. In addition, samples at ~5-10 cm spacing were examined from 135 to 6 cm core depths. IO-1678-48PC was also

sampled in increments of 5-10 cm throughout the length of the core between 53 and 12 cm core depth. Locations of the cores are highlighted in Figure 1.

Diatoms and silicoflagellate species were identified and assessed using abundance and occurrence data and then compared to lithologic descriptions. Distinct First Appearance Datum event levels (FAD) and Last Appearance Event Datum levels (LAD) were identified in the cores at specific depths. The depths and accepted age estimates for these events were plotted (Figures 3, 4). Age x depth lines are constrained by the array of LAD and FAD events. Coherent intervals of sediment are identified and bounded by interpreted breaks in the core that reflect disconformities. Changes in lithology are coincident in most cases with the location of inferred age breaks. The lithological change likely reflects the location of the disconformity. An initial assessment of the distribution of these biostratigraphic events from 1678-20, indicated that the samples from 96-97 cm and below reached Oligocene age or older. Additional

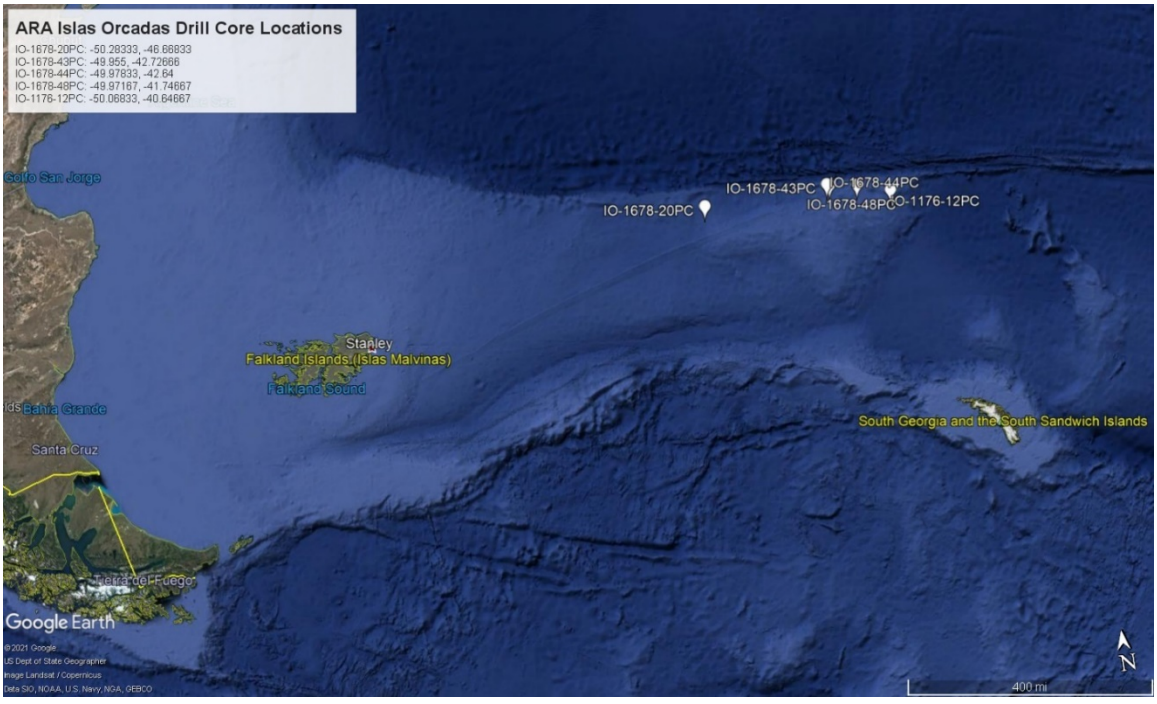


*Figure 1. Locations of coring sites from ARA Islas Orcadas cruises referred to in this study, IO-1678-20PC, IO-167-43PC, IO-1678-44PC, IO-1678-48PC, IO-1176-12PC.*

sediment samples were requested from the repository to generate a higher resolution assessment of this fraction of the core. Following the initial review, samples between 96 cm and 135 cm were sieved to concentrate identifiable diatoms. Fifty ml of the prepared sediment suspension was sieved at >20 micrometers and washed into a 15 ml centrifuge tube. Subsequently 1 ml of the suspended sediment was extracted and used to prepare slides. The slides were affixed to a cover glass using Norland Optical Adhesive #61 and cured under UV light.

Prepared slides were examined using a Leica DMRX, type 301-371.010 Light Microscope (LM) using 40X and 100X objectives. Diatoms and silicoflagellates were identified with reference to standard taxonomic literature, biostratigraphic zones, and logs from previous cruises. Diatoms with previously documented stratigraphic ages were used to date the samples using first and last occurrence data. Diatom species and range zones were identified using literature and zonations produced by Harwood and Maruyama (1992) together with other diatom literature (Gombos, 1977; Gombos & Ciesielski, 1983; Ciesielski, 1983; Fenner, 1984; Harwood & Maruyama, 1992; Scherer et al., 2000). Relative ages were assigned to the diatom flora using first and last occurrence datum and diatom zones (McKay et al., 2019)

## RESULTS

Core catchers from piston cores collected during *ARA Islas Orcadas* Cruises 1678, 1176, and 0775, *VEMA* Cruises 14, 17, 18, 22, and 31, *Eltanin* Cruise 22, and *Robert Conrad* Cruises 15 and 16 were sampled and assigned relative dates. IO-1678-20PC and IO-1678-48PC were selected as the primary cores of focus. They are significant due to their proximity to the sub-bottom profiler and seismic lines obtained by the DY087 Cruise, their location along the MEB, and due to their age, Eocene and older. IO-1678-20PC and IO-1678-48PC were sampled at 5-10 cm increments and assessed at high resolution. Siliceous microfossils, including diatoms and

silicoflagellates, were documented and described. Diatoms with well-known and documented first and last occurrences were used to assign relative ages to the samples. Dating was done using the Antarctic Diatom Biostratigraphy table produced by D. Harwood during IODP Expedition 374 (Sangiorgi, et al., 2019).

**Islas Orcadas Core 1678-20PC**

Islas Orcadas Core 1678-20PC total core length is 144 cm at a water depth of 2498 m. Samples from 0 to 44 cm are a diatomaceous ooze with a light olive color (10Y 5/4).
From 44 to 94 cm is a diatomaceous ooze with a light olive grey color (5Y 5/2) that abruptly changes to yellowish gray (5Y 8/1) at 81 cm. At 94 to 119 cm the lithology changes to a diatomaceous mud with a pale olive color (10Y 6/2), followed by a diatomaceous mud with a yellowish gray color (5Y 7/2) at 119 to 144 cm. Sediment descriptions note that the bottom topography is gently sloping near the base of the northwest flank of the Maurice Ewing Bank (Kaharoeddin et al., 1982).

Core IO-1678-20PC includes 24 samples from 6 to 135 cm core depth. The distribution of diatoms inidcates four distinct intervals of sediment deposition, separated by erosional breaks or hiatuses. Figure 3 plots the LAD and FAD events of diatoms with reasonably well-resolved age information in this core. Core IO-1678-20PC spans four distinct units of sediment separated by three disconformities.

Unit A, the oldest interval, is ~40 Ma to 34.5 Ma in age, as constrained by diatoms events FAD *Trinacria simulacrum* at 134-135 cm and LAD *Porotheca danica* at 125-126 cm. The top of this interval is bounded by an unconformity between 118 cm and 121 cm.

Unit B spans sample intervals 118 to 96 cm, dated from 26.4 Ma to 25.4 Ma as indicated by the FAD of *Rocella gelida* at 117-118 cm and the LAD of Rocella vigilans var. B at 96-97 cm. The top of this interval is bounded by an unconformity between 96 cm and 92 cm.

Unit C is present between sample intervals 92 to 26 cm, and spans from 14.2 Ma to 8.4 Ma as contrained by FAD *Denticulopsis simosensii* at 92-91 cm and LAD *Denticulopsis ovata* at 33-34 cm. The top of this interval is bounded by an unconformity between 26 cm and 13 cm.

Unit D between sample intervals 13 cm to 6 cm is the youngest interval and is 3.5 Ma to 2.2 Ma in age, as indicated by the FAD of *Fragilariopsis weaverii* at 12-13 cm and the LAD of *Thalassiosira vulnifica* at 6-7 cm.

**Islas Orcadas Core 1678-48PC**

Islas Orcadas Core 1678-48PC is 532 cm in total core length at a water depth of 1598 m. From 0 to 9 cm is a glauconitic diatomaceous sand with olive gray color (5Y 3/2), followed by a radiolarian, diatomaceous ooze with dusky yellow color (5Y 6/4) from 9 to 14 cm. From 14 to 52 cm is a nannofossil ooze with yellowish gray color (5Y 8/1), followed by a gradational change to flow-in at 53 cm. The bottom topography is gently sloping on the eastern portion of the northern flank of the Maurice Ewing Bank and near the top of the bank (Kaharoeddin et al., 1982).

Review of IO-1678-48PC includes six samples from 12-53 cm, with a hiatus/lithology change between samples at 12-13 cm and 20-21 cm, interpreted as a disconformity. At 20 cm and below, the samples are Oligocene age or older. Figure 4 plots the LAD and FAD events of

diatoms with reasonably well-resolved age information and their occurrence in this core with respect to the disconformity.

Unit A from 53 cm to 20 cm is the oldest interval and is 30.1 Ma to 25.4 Ma, as indicated by the FAD of *Rocella vigilans* at 52-53 cm and the LAD of Rouxia antarctica at 45-46 cm. The top of this interval is bounded by an unconformity between 20 cm and 13 cm.

Unit B is the youngest interval present and is 3.2 Ma to 2.2 Ma in age, as constrained by the FAD *Thalassiosira vulnifica* at 12-13 cm and LAD *Thalassiosira vulnifica* at 12-13 cm.

## DISCUSSION

The *ARA Islas Orcadas* samples show similarities to other sites in the region such as the D-1 erratic from McMurdo (Harwood & Bohaty, 2000), Site 512 from Leg 71 (Gombos, 1983), Sites 511 and 513a from Leg 71 (Gombos & Ciesielski, 1983), Site 1090B and 1090E from Leg 177 (Barron et al., 2014), and Sites 747A, 747B, 749B, and 751A from Leg 120 (Harwood & Maruyama, 1992) (Figure 2).

The D-1 Erratic from McMurdo had similar Eocene taxa to the *ARA Islas Orcadas* samples, especially *Bidduphia* sp., *Hemiaulus* sp., and *Triceratium* sp. (Appendix, Plates 2-4). Site 512 from DSDP Leg 71 was not useful in creating a diatom zonation but it did have unique taxa. IO-1678-20 had an abundance of *Hemiaulus reflexispinosis* and a taxon similar to that identified as *Hemiaulus* sp. by Gombos in Hole 511-13CC, 125-126cm (Figure 2). It is possible that these two species are related due to their similar morphology (Appendix, Plate 7) (Gombos, 1983). *Tubaformis unicornis* was also present in the lowest portions of IO-1678-20PC. It was

named by Gombos (1983) and has the potential to have stratigraphic value. *T. unicornis* was documented in a range of sizes in 1678-20PC and 1176-12CC (Appendix, Plate 8).

Holes 511 and 513A from DSDP Leg 71 were used to create a composite diatom zonation (Gombos & Ciesielski, 1983). Hole 513A has an occurrence of *R. gelida* similar to Core 1678-20PC (Figure 2). This zone is also similar to the *R. gelida* zone established by Harwood and Maruyama during ODP Leg 120 (Harwood & Maruyama, 1992). Hole 511 has taxa similar to those found in the *Hemiaulus incisus* and *Rhizosolenia oligocenica* Zones from Gombos & Ciesielski (1983) (Appendix, Plate 5). The *Cestodiscus robustus* Zone from Hole 1090B and 1090E, during ODP Leg 177, are similar to the Oligocene aged sediments from IO-1678-20PC and IO-1678-48PC (see plate 4 in appendix) (Barron et al., 2014). The *Rocella vigilans* Zone from ODP Leg 120 is also similar to the Oligocene aged sediments from IO-1678-20PC and IO-1678-48PC (Harwood & Maruyama, 1992).

Two notable species were present in this study (Appendix, Plate 6). The first is Genus and species uncertain #1, which was first identified by Gombos (1983) Site 512 during DSDP Leg 71. It was also present in samples 1176-12CC and 1678-43CC. This diatom has a unique morphology and is rare in occurrence. It also may provide stratigraphic context for the region if additional specimens are found and first and last occurrence can be established. The second unique diatom is a *Cerataulina* sp., which was present in samples 1176-12CC, 1678-43CC, and 1678-44CC. This diatom is similar to *Cerataulina cretacea* (Hajós) but has slight morphological differences (Hajós, 1976). Due to its unique form and rare occurence, it also could be stratigraphically significant if investigated further.

In Figure 2 letters “z” through “o” are used to correlate cores previously examined and with established biostratigraphic zones, to the ARA Islas Orcardas cores 20PC and 48PC. Tie points are included between all Paleogene to Early Miocene samples examined in this study and the cores examined previously.

**Paleocene:** Seven cores examined in this study recovered intervals of the Paleocene: IO-1678-37CC, IO-1678-38CC, IO-1678-49CC, IO-0775-45CC, RC-15-84PC, RC-15-121PC, and DY087-16PC. IO-1678-37CC and IO-1678-38CC correlate to Cores 5 to 8 from Leg 36 Site 327A (Gombos, 1977). The presence of silicoflagellate *Corbisema hastada*, and diatoms *Hemiaulus altus, Hemiaulus subacutus*, and *Hemiaulus incurvus* indicate a late Paleocene age.

**Middle Eocene:** Four cores sampled intervals of the Early Eocene: IO-1678-43CC, IO-1176-12CC, VM-18-104PC, and DY087-12PC. IO-1176-12 is correlated to Cores 6 to 19 from Leg 71 Site 512 (Gombos, 1983). VM-18-104PC is correlated to the D-1 Erratic (Harwood & Bohaty, 2000), Cores 6 to 19 from Leg 71 Site 512 (Gombos, 1983), Cores 16 to 20 from Leg 120 Site 748B (Harwood & Maruyama, 1992), Cores 2 to 8 from Leg 29 Site 283, and Cores 14 to 16 from Leg 29 Site 281 (Hajós, 1976). The presence of diatoms *Trinacria simulacrum* (Pl. 3, fig. 12)*, Pseudotriceratium radiosoreticulatum*, *Pyxilla reticulata, Pyxilla johnsonianus, Pyrgupyxis eocenica, Eurossia irregularis, Hemiaulus dissimilis, Azpeitia oligocenica, Rocella praenitida, Triceratium unguiculatum*, *Triceratium quadrangulare* (Pl. 4, fig. 6), *Distephanosira architecturalis, Asterolampra acutiloba, Asterolampra uraster* (Pl. 1, fig. 6), *Asterolampra affinis* (Pl. 1, figs. 10-13), *Hemiaulus reflexispinosis* (Pl. 7, figs 2-4), *Tubaformis unicornis* (Pl. 8, figs. 1-8), and silicoflagellates *Dictyocha haxacantha*, and *Naviculopsis* sp. collectively suggest a Middle Eocene age.

**Late Eocene:** Six cores sampled intervals of the Late Eocene: IO-1678-20CC, IO-1678-44CC, IO-0775-46, VM-18-121PC, DY087-06PC, DY087-10PC. IO-1678-20CC is correlative to Core 5 from Leg 36 Site 328B and Core 4 from Leg 36 Site 328 (Gombos, 1977). The presence of diatoms *Azpeitia oligocenica*, *Rocella praenitida, Pyxilla reticulata, Pseudotriceratium monile, Distephanosira architecturalis*, and silicoflagellates *Naviculopsis constricta, Corbisema hastada* and *Naviculopsis biapiculata* suggest a Late Eocene age.

**Early Oligocene:** Five cores sampled intervals of the Early Oligocene: IO-1678-32CC, IO-1678-48CC, VM-17-107PC, VM-31-60PC, and VM-31-61PC. VM-17-107PC is correlative to Cores 31 to 33 from Leg 71 Site 513A (Gombos & Ciesielski, 1983). VM-31-61PC is correlative to Core 30 from Leg 119 Site 739C (Barron & Mahood, 1993) and to 360 to 500 m of the CIROS-1 Drillhole (Harwood, 1989). The presence of diatoms such as *Rocella praenitida, Pyxilla reticulata, Hyalopoda hajosae, Thalassiosira bukryii, Hemiaulus taurus, Hemiaulus caracteristicus, Pyrgupyxis eocenica, Eurossia irregularis, Porotheca danica,* and *Kisseleviella tricoronata* suggest an Early Oligocene age.

**Late Oligocene:** Four cores sampled intervals of the Late Oligocene: IO-1678-19CC, IO-1678-47CC, RC-15-81PC, and DY087-15PC. IO-1678-19CC is correlative to Cores 12-2 and 12-4 from Leg 71 Site 513A. IO-1678-47CC is correlative to Cores 13 to 15 from Leg 71 Site 513A (Gombos & Ciesielski, 1983). Diatoms *Rocella gelida* and *Rocella vigilans*, *Cestodiscus antarcticus, Pyxilla prolongata, Cavitatus jouseanus, Cavitatus miocenicus, Fragilariopsis truncata*, *Hemiaulus taurus*, and *Raphidodiscus marylandicus*, and silicoflagellate *Naviculopsis biapiculata* suggest a Late Oligocene age.

## CONCLUSIONS

The main objective of this study was to document the age of sediment cores from the South Atlantic Ocean that might span the Paleogene and to describe their fossil diatom biostratigraphy. Elaboration of the Paleogene deep-sea diatom record has great potential to provide stratigraphic correlation during diatom rich intervals. The early Paleocene lacks a diatom zonation and further investigation of deep-sea diatoms could provide more clarity to past environmental conditions. There are also many species yet to still be identified and assessed for their stratigraphic value, making establishing a better record for the Eocene and Paleocene even more crucial.

Independent and multi-site compilations have enabled charaterization of gaps of time missing at certain locations in prior studies. Although no zones were identified in this paper, the description and documentation of the diatom flora provides additional stratigraphic context for this period. In addition, relative ages were assigned to sediment intervals from IO-1678-20PC and IO-1678-48PC with the Antarctic Diatom Biostratigraphy table produced by D. Harwood during IODP Expedition 374, adding value to the biostratigraphic record (McKay et al., 2019).

SYSTEMATIC PALEONTOLOGY

**Diatoms**

***Actinocyclus actinochilus*** (Ehrenberg) Simonsen 1982, p. 105, pl. 9, figs. QK569, D5, B125.
Basionym: *Coscinodiscus actinochilus* Ehrenberg 1844, p. 200.

***Actinocyclus ingens*** Rattray emend. M.C. Whiting & H.J. Schrader 1985, p. 74, pl. 1, figs. 1-2; pl. 2, figs. 4-10; pl. 3, fig. 13.

***Actinocyclus ingens* f. *nodus*** (Baldauf) Whiting & Schrader 1985, pl. 1, fig. 3; pl. 2, fig. 11; pl. 3, fig. 14.
Synonyms: *Actinocyclus ingens* Rattray 1971, pl. 40.6, fig. 8; *Coscinodiscus margaritaceus*, Castracane, sensu Zhuse 1977, pl. 74, fig. 20; *Actinocyclus ingens* var. *nodus* Baldauf 1980, pl. 1, figs. 5-9.

***Actinocyclus ingens* var. *ovalis*** Gersonde 1990, p. 792, pl. 1, fig. 7; pl. 3, figs. 1-3; pl. 5, figs. 4, 7; pl. 6, figs. 1, 4, 5.

***Actinocyclus karstenii*** Van Heurck 1909, p. 44. pl. 12, fig. 158; Harwood and Maruyama 1992, p. 700, pl. 13, figs. 1, 2, 6-8, 10-11, 13.

***Actinocyclus maccollumii*** Harwood & Maruyama 1992, p. 700, pl. 17, fig. 29.

***Arachnoidiscus clarus*** Brown 1933, p. 68-70, pl. 6, fig. 1-2.
(Plate 4, Fig. 10)

***Arachnoidiscus stictodiscoides*** Hanna, Hendey & Brigger 1976, pp. 2-20, pl. 3, fig. 1-4.
(Plate 4, Fig. 10)

***Araniscus lewisianus*** (Greville) Komura 1998, p. 1-23, pl. 6, figs. 20-22, 87-104.
Basionym: Coscinodiscus lewisianus, Greville 1866, p. 78, pl. 8, figs. 8-10.

***Asterolampra affinis*** Greville 1862, p. 45; pl. 7, fig. 7-9; Gombos 1983a, pl. 1, fig. 1.
(Plate 1, Figs. 10, 11, 13)

***Asterolampra affinis* var. *cellulosa*** Forti 1913, p. 1566; pl. 2, fig. 3, 11
Synonym: *Asterolampra schmidti* Hajós 1976, p. 827; pl. 21, fig. 6
(Plate 1, Figs. 1-4)

***Asterolampra gradiata*** Gombos in Gombos & Ciesielski 1983, p. 606; pl. 1, fig. 4-6.
(Plate 1, Fig. 15)

***Asterolampra punctifera*** (Grove in Schmidt et al.) Forti in Tempère & Peragallo 1914, p. 451; No. 926-929 as "*Asterolampra punctifera* (Grove) Forti";
Basionym: *Asterolampra affinis var. punctifera* Grove in Schmidt 1896.
(Plate 1, Figs. 6-8)

***Asterolampra schmidtii*** Hajós 1976, p. 827, pl. 21, fig. 6.

***Asterolampra tela*** Gombos in Gombos & Ciesielski 1983, p. 600; pl. 3, fig. 1-4 (this diatom was incorrectly referred to as *Asterolampra sp. A* on p. 600 of this paper, but *A. tela* on the plate caption.
(Plate 1, Fig. 5)

***Asterolampra uraster*** Grove & Sturt 1887, p. 143; pl. 13, fig. 42.
(Plate 1, Fig. 16)

***Asterolampra vulgaris*** Greville 1862, p. 47; pl. 7, fig. 17-25.
(Plate 1, Fig. 9)

***Asteromphalus acutiloba*** Forti 1913, p. 1564, pl. 3, figs. 1, 5, 6, 9.

***Asteromphalus kennettii*** Gersonde 1990, p. 793, pl. 2, fig. 1; pl. 6, fig. 2

***Asteromphalus oligocenicus*** Schrader & Fenner 1976, p. 965-966; pl. 21, fig. 8, 13, 14, pl. 28, fig. 1.
(Plate 1, Fig. 14)

***Azpeitia endoi*** (Kanaya) P.A. Sims & G. Fryxell in Fryxell, Sims & Watkins 1986, p. 16.
Basionym: *Coscinodiscus endoi* Kanaya 1957, p. 76, pl. 3, figs. 8-12.

***Azpeitia gombosi*** Harwood & Maruyama 1992, p. 701; pl. 3, fig. 1-2.
(Plate 4, Fig. 14, 17)

***Azpeitia oligocenica*** (Jousé) P.A. Sims in Fryxell, Sims & Watkins 1989, p. 302, pl. 2, figs. 1-3; pl. 3, figs. 8-9.
Basionym: *Coscinodiscus oligocenicus* Jousé 1973, p. 348, pl. 1, figs. 6-8.

***Azpeitia tabularis*** (Grunow) G. Fryxell & P.A. Sims in Fryxell, Sims & Watkins 1986, p. 15, pl. 57, fig. 43.
Basionym: *Coscinodiscus tabularis* Grunow 1884, p. 86.

***Bicornis incisis*** (Hajós) Fenner 1994, p. 109;
Basionym: Hemiaulus incisis Hajós 1976, p. 829, pl. 23, fig. 4-9.
(Plate 2, Figs. 15,16)

***Biddulphia fimbriata*** Greville 1865, p. 6; pl. 1, fig. 4.
(Plate 2, Fig. 17)

***Biddulphia rigida*** Schmidt in Schmidt et al. 1888, pl. 120, fig. 1, 2.
(Plate 2, Fig. 14)

***Biddulphia*** **sp. A** Harwood 1989, p. 27 pl. 4, fig. 15 and 20.
Description: Heavily silicified, fine, spare pores at valve face and extending up horns, no visible blades on horns present. Valve face is bulbus and horns angle outward from the face and are rounded at the ends of the extensions.
Comments: Very similar to *Hemiaulus* sp. A identified in Harwood & Bohaty, 2000, however the one shown in this paper appears to have a more bulbus base and more angularity to the horn structures.
Taxon noted in the early Miocene.

(Plate 2, Fig. 3)

***'Biddulphia'* sp. A**
(Plate 2, Fig. 18)
Description: The entire valve face is finely perforate, with unsymmetrical horns that extend up. The horns do not have perforations or pores. One horn has more curvature and extends higher than the other, both are rounded at the tip.
Comments: Has slight taxonomic similarities to *Biddulphia infundibuloides* of Desikachary, Gowthaman & Latha 1987, such as similar valve structure and pore size. The taxa pictured in this paper has a wider valve face and does not have apical extensions in the center.

***Biddulphia* sp. B**
(Plate 5, Fig. 9)
Description: The overall shape of the valve is triangular and it is convex, with rounded edges. Two tubular extensions can be seen in the LM photo; it is likely a third is also present and not in view. The valve face is finely perforate with many labiate processes scattered throughout.
Comments: Has slight taxonomic similarity to *Biddulphia scutum* Bones & Gosden 1967, due to triangular shape and a finely perforated valve face, the species discussed here differs due to the tubular extensions and lack of spines on valve face.

***Cavitatus jouseanus*** (Sheshukova-Poretskaya) Williams 1989, p. 360, pl. 1, figs. 1-9.
Basionym: *Synedra jouseana* Sheshukova-Poretskaya 1962, p. 208, fig. 4.

***Cavitatus miocenicus*** (Schrader) Akiba & Yanagisawa in Akiba, Hiramatsu & Yanagisawa 1993, figs. 9-1-11.
Basionym: *Synedra miocenica* Schrader 1976, p. 636, pl. 1, figs. 1, 1a-b.

***Cerataulina cretacea*** Hajós in Hajós & Stradner 1975, p. 930-931; pl. 10, fig. 3, 4.
(Plate 6, Fig. 12)

***Ceratulina* sp. A**
(Plate 6, Figs. 4-6, 10-11)

***Cestodiscus antarcticus*** Fenner 1984, p. 331, pl. 1, fig. 1.

***Cestodiscus robustus*** Jousé 1974, p. 345; pl. 1, fig. 14, 15.
(Plate 4, fig. 12)

***Coscinodiscus hajosiae*** Fenner 1984, p. 331, pl. 2, fig. 1.

***Coscinodiscus rhombicus*** Castracane 1886, pl. 1-30; p. 164, pl. 22, fig. 11.

***Coscinodiscus superbus*** (Hardman) Fenner 1978, p. 516, pl. 13, figs. 1−5; pl. 14, figs. 1−4.
(Plate 6, Fig. 14)

***Crucidenticula nicobarica*** (Grunow) Akiba & Yanagisawa 1986, p. 486, pl. 1, fig. 9; pl. 2, figs. 1-7; pl. 3, fig. 7; pl. 5, figs. 1-9.
Basionym: Denticula nicobarica Grunow 1868, p. 97, pl. 1A, figs. 5a-b.

***Dactyliosolen antarcticus*** Castracane 1886, p. 75, pl. 9, fig. 7.

***Denticulopsis crassa*** Yanagisawa & Akiba 1990, p. 248, pl. 3, figs. 21-27; pl. 12, figs. 1-8.
Synonym: *Denticula hustedtii* Simonsen and Kanaya, Schrader 1973a, pl. 2, figs. 29-30.

***Denticulopsis delicata*** Yanagisawa & Akiba 1990, pl. 7, fig. 1.

***Denticulopsis dimorpha*** (Schrader) Simonsen 1979, p. 64.
Basionym: *Denticula dimorpha* Schrader 1973, p. 704, pl. 1, figs. 37-46.

***Denticulopsis lauta*** (Bailey) Simonsen 1979.
Basionym: *Denticula lauta* Bailey 1854, p. 9, figs. 1, 2.
Synonym: Eunotia sancti antonii Ehrenberg 1854, pl. 33, figs. 9, 10.

***Denticulopsis maccollumii*** Simonsen 1979.
Synonym: *Denticula antarctica* McCollum in Hayes, Frakes, et al. 1975, p. 527, pl. 8, figs. 6-10.

***Denticulopsis ovata*** (Schrader) Yanagisawa & Akiba 1990, p. 257, pl. 6, figs. 6-14, 24-32.
Basionym: *Denticula hustedii var. ovata* Schrader 1976, p. 632, pl. 4, figs. 5-6, 12, 14-15.

***Denticulopsis praedimorpha*** (F. Akiba) J.A. Barron 1986, p. 785, figs. 13, 24-25.
Basionym: *Denticula praedimorpha* Akiba 1979, p. 158, pl. 1, figs. 11-19; pl. 2, figs. 1-5, 7-21.

***Denticulopsis simonsenii*** Yanagisawa & Akiba 1990, p. 242, pl. 3, figs. 1-3; pl. 11, figs. 1, 5.

***Distephanosira architecturalis*** (Brun) Gleser in Gleser, Makarova, Moisseeva & Nikolaev 1992, p. 68, pl. 56, figs. 1-9.
Basionym: *Melosira architecturalis* Brun 1892.

***Eucampia antarctica*** (Ehrenberg) Mann 1937.
Basionym: *Hemiaulus antarcticus* Ehrenberg, pl. 35a, group 21, fig. 15; group 22, fig. 15

***Eunotogramma* sp. A**
(Plate 5, Figs. 15, 16)

***Eurossia irregularis*** (Greville) Sims in Mahood, Barron & Sims 1993, p. 254; fig. 23-24, 31-36, 65, 74-75.
Basionym: *Triceratium irregulare* Greville
Synonym: *Triceratium polymorphus* Harwood & Maruyama 1992, p. 708-709; pl. 1, fig. 1-2, non pl. 1, fig. 3
(Plate 3, Figs. 2, 6, 8)

***Eurossia irregularis var. incurvatus*** Sims in Mahood, Barron & Sims 1993, p. 256, 258; fig. 37-42, 66-67.
Synonym: *Triceratium polymorphus* Harwood & Maruyama 1992, p. 708-709; pl. 1, fig. 3, non pl. 1, figs. 1,2.
(Plate 3, Figs. 7, 9)

***Fenneria kanayae*** (Fenner 1984a) Witkowski 2020, p. 43-45, pl. 3, fig. 1−7; pl. 4, fig. 1−24.
Basionym: *Triceratium kanayae* Fenner 1983a, p. 334, pl. 1, figs 5, 6, pl. 2, figs 3, 4.
Synonym: *Triceratium inconspicuum var. trilobata* Fenner 1977, p. 534; pl. 30, fig. 23-26; *Trinacria insipiens* Witt 1927; *Triceratium schulzii* (Jousé) Fenner 1977, p. 535, pl. 30, figs 1−11, pl. 37, fig. 3.

For a detailed synonymy refer to Witkowski 2020 p. 13-14, pl. 3-4.
(Plate 4, Fig. 3-4)

***Fragilariopsis barronii*** (Gersonde) Gersonde et Barcena 1998, p. 146-157, pl. 3, fig. 6; pl. 4, fig. 1-3; pl. 5, fig. 1-17.

***Fragilariopsis curta*** (Van Heurck) Hustedt 1958, p. 160, fig, 140-144, 159.

***Fragilariopsis januaria*** (Schrader) Bohaty 2003.
Basionym: *Nitzschia januaria* Schrader 1976, p. 634, pl. 2, fig. 25-29.

***Fragilariopsis kerguelensis*** (O'Meara) Hustedt 1952.
Basionym: *Terebraria kerguelensis* O'Meara 1877.

***Fragilariopsis praecurta*** (Gersonde) Gersonde et Barcena 1998, p. 92.
Basionym: *Nitzschia praecurta* Gersonde 1991, p. 148-149, pl. 1, fig. 7-1; pl. 2, figs. 5-6; pl. 3, figs. 3-4; pl. 10, fig. 7.

***Fragilariopsis praeinterfrigidaria*** (McCollum) Gersonde et Barcena 1998.
Basionym: *Nitzschia praeinterfrigidaria* McCollum 1975, p. 535, pl. 10, fig. 1.

***Fragilariopsis reinholdii*** (Kanaya ex Barron and Baldauf) Zielinski and Gersonde.

***Fragilariopsis rhombica*** (O'Meara) Hustedt 1952.
Basionym: *Diatoma rhomicum* O-Meara 1886.

***Fragilariopsis truncata*** H.T. Brady ex M.P. Olney in Olney et al. 2007, p. 2332, pl. 1, fig. 6-11; pl. 2, fig. 23-28.

***Fragilariopsis weaveri*** (Ciesielski) Gersonde et Barcena 1998.
Basionym: *Nitzschia weaveri* Ciesielski 1983, p. 655, pl. 1, figs. 1-10.

***Goniothecium danicum*** (Grunow) Fenner 1994, p. 111, pl. 5, figs. 6, 7-11
Basionym: *Goniothecium odontella danica* Grunow in Van Heurck 1880-1885, pl. 105, figs. 11, 12.
(Plate 5, fig. 8)

***Hemiaulus altus*** Hajós 1975, p. 931, pl. 5, fig. 17-19.
(Plate 2, Fig. 8)

***Hemiaulus angustus*** Greville 1865, p. 35, pl. 40, fig. 7-9.
(Plate 2, Fig. 5)

***Hemiaulus caracteristicus*** Hajós 1976, p. 828-829, pl. 15, fig. 10.
(Plate 6, Fig . 13)

***Hemiaulus centralitenius*** Ross & Sims 1977, p. 182-184, pl. 2, fig. 7-9.
(Plate 2, Figs. 6-7)

***Hemiaulus curvatulus*** Strelnikova 1971, p. 49, pl. 1, fig. 12, 13.
(Plate 2, Fig. 11)

***Hemiaulus dissimilis*** Grove & Sturt 1887, p. 143, pl. 13, fig. 43.
(Plate 2, Fig. 12)
***Hemiaulus incurvus*** Schibkova in Krotov & Schibkova 1959, p. 124, figs. 4,8.

***Hemiaulus inaequilateris*** Gombos 1976, p. 594, pl. 20, figs. 5-7.

***Hemiaulus polymorphus*** Grunow 1884.

***Hemiaulus prolongatus*** Ross & Sims 1977, p. 188-189, pl. 7, fig. 42-44.
(Plate 2, Fig. 4)

***Hemiaulus rectus var. twista*** Fenner 1984, p. 332; pl. 2, fig. 6.
(Plate 2, Figs. 1a,1b, 2)

***Hemiaulus reflexispinosus*** Ross & Sims 1977, p. 185-186, text fig. 2, pl. 3, fig. 17-19.
(Plate 7, Figs. 1-8)

***Hemiaulus subacutus*** Grunow 1884, p. 9, pl. 5, fig. 55.

***Hemiaulus taurus*** Gombos in Gombos & Ciesielski 1983, p. 606, pl. 19, figs. 1-8.

***Hemiaulus* sp. B**
Description: The valve face is smooth, oval shaped, and finely perforate. Long slender horns that are wider at the base and become slenderer towards the horn's blades. Horns are uneven in height.
Comments: Like *Hemiaulus altus* Hajós in size and shape of valve face but has finer pores and longer apical elevations that are not symmetrical in height. Like *Hemiaulus oonkii* Fenner in size, shape of valve face, and height of apical extensions but differs due to size of pores and non-symmetrical apical elevations.
(Plate 2, Fig. 9)

***Hemiaulus* sp. C**
Description: The valve face is elongated with medium size pores randomly distributed throughout. The horns curve inward slightly before the reach their highest elevation. Small blades are located at the top of horns, blades have a triangular shape and are short. Horn height and size are slightly asymmetrical.
Comments: Similar to *Hemiaulus altus* due to valve height and pore distribution. Differs do to horn and blade shape.
(Plate 2, Fig. 13)

***Hemiaulus* sp. D**
Description: The valve face has a concave center. The entire valve has larger pores randomly distributed, with the number of pores increase extending up the horns. The horns have a long blade the extends from the tip.
Comments: Has similarities to *Hemiaulus speciosus* Jousé 1951, such as the rounded valve face and length and shape of horns. Differs due to pore distribution and curvature of the horns.
(Plate 2, Fig. 10)

***Hemiaulus* sp.** of Gombos 1983, p. 628, pl. 20, figs. 7-9.
(Plate 7, Figs. 10-12)

***Hemidiscus cuneiformis*** Wallich 1960, p. 42, pl. 11, figs. 3-4.

***Hemidiscus karstenii*** Jousé in Jousé, Koroleva (Karaleva), & Nagaeva 1962, p. 78, pl. 2, figs. 7-9.

***Kisseleviella faballiforma*** M.P. Olney in Olney et al. 2005, p. 69, pl. IV, fig. 24-26; pl. V, fig. 33-34.

***Kisseleviella tricoronata*** M.P. Olney in Olney et al. 2005, p. 61, pl. 1, figs. 3-8; pl. V, figs. 27-30.

***Neobrunia mirabilis*** (Brun in Brun & Tempère) Kuntze 1898.
Basionym: Brightwellia mirabilis Brun in Brun & Tempère 1889, p. 27, pl. 8, fig. 1.

***Nitzschia denticuloides*** Hustedt 1942, p. 130, figs. 280-281; Simonsen 1987, p. 290-291, pl. 429, figs. 18-22.

***Peripteris trinodis*** (Hanna) Suto 2005, p. 295, figs. 5, 6.
Basionym: Dicladia trinodis Hanna 1927, p. 112, pl. 18, figs 4-5.
(Plate 5, Fig. 7)

***Porotheca danica*** (Grunow) Fenner 1994, p. 114-115, pl. 4, figs. 16-17; pl. 15, figs. 1-6.
Basionym: *Stephanogonia (Pterotheca?) danica* Grunow 1866, p. 146; Grunow 1884, p. 92-93, pl. 5, fig. 47.

***Pseudorutilaria clavata*** Ross & Sims 1987, pl. 3 & 12, fig. 90-91.
(Plate 5, Figs. 11, 12)

***Pseudorutilaria hannai*** Ross & Sims 1987, pl. 5 & 12, fig. 93.
(Plate 5, Fig. 10)

***Pseudorutilaria hannai*** **var. A** Ross & Sims 1987.
(Plate 5, Fig. 14)

***Pseudorutilaria monile*** Grove & Sturt 1886, p. 393, figs. 149-152.

***Pseudotriceratium cheneveri*** (Meister) Gleser 1974, pl. 28, fig. 12, pl. 25, fig. 6.
Basionym: Triceratium chenevieri Meister 1937
(Plate 3, Fig. 3)

***Psuedotriceratium radiosoreticulatum*** (Grunow) Jouse in Dzinoridze, Jouse & Strelnikova 1979, p. 51, fig. 151.
Basionym: *Triceratium radiosoreticulatum* Grunow in V. H. 1883, pl. 112, fig. 5.

***Pterotheca aculeifera*** (Grunow in Van Heurck) Van Heurck 1896, p. 430; fig. 151.
(Plate 5, Fig. 6)

***Pyrgupyxis eocena*** Hendey 1969, p. 3, figs. 1-4.

***Pyxilla johnsonianus*** Greville 1865.

***Pyxilla reticulata*** Grove & Sturt 1887; Witkowski, Sims, & Williams 2017, p. 393-394, figs. 145-146.
***Raphidodiscus marylandicus*** Christian 1887, p. 66-68.

***Rhaphoneis* sp. A**
Description: Valve face is unsymmetrical with one end having a longer, thinner extension. Valve ends are rounded. Pseudoraphe extends across the valve face with the striae at a slight angle to it. (Plate 5, Fig. 5)

***Rhizosolenia antarctica*** Fenner 1984, p. 333, pl. 2, fig. 5.

***Rhizosolenia oligocaenica*** Schrader 1976, p. 635; pl. 9, fig. 7.
Synonym: *Rhizosolenia gravida* Gombos & Ciesielski 1983, p. 606; pl. 11, figs. 1-7.
(Plate 5, Fig. 12)

***Rocella gelida*** (Mann) Bukry n. comb. 1978, p. 788, pl. 5, figs. 1-13.
Basionym: *Stictodiscus gelidus* Mann 1907, p. 268, pl. 50, fig. 5.

***Rocella praenitida*** (Fenner) Fenner in Kin & Barron 1986, v. 1(2): p. 177; pl. 4, fig. 3.
(Plate 4, Figs. 11, 14)

***Rocella vigilans*** Fenner 1984, p. 333, pl. 1, fig. 11.

***Rossiella symmetrica*** Fenner emend Yanagisawa 1995, v. 177: p. 5; pl. 4, figs. 1-6.
(Plate 5, Figs. 1, 2)

***Rouxia antarctica*** (Heiden & Kolbe) Hanna 1930.
Basionym: *Rouxia peragalli* var. *antarctica* Heiden & Kolbe 1928, p. 447-715, pl. 31-43; p. 632, pl. 4, fig. 90.

***Rouxia diploneides*** Schrader 1973, p. 710, pl. 3, figs. 24, 25.

***Rouxia granda*** Schrader in Schrader & Fenner 1976, p. 997, pl. 7, fig. 17.

***Rouxia naviculoides*** Schrader 1973, p. 710, pl. 3, fig. 30.

***Rouxia obesa*** Schrader in Schrader & Fenner 1976, p. 997; pl. 24, figs. 5, 6.
(Plate 5, fig. 3)

***Sceptroneis caducea*** Ehrenberg 1844.

***Sceptroneis grunowii*** Anissimova ex Proschkina-Lavrenko 1949, p. 217.

***Sheshukovia excavata*** (Heiberg) V.A. Nikolaev & D.M. Harwood in Nikolaev, V.A., Kociolek, J.P., Fourtanier, E., Barron, J.A. & Harwood, D.M. 2001, p. 21.
Basionym: *Trinacria excavata* Heiberg 1863, p. 51, pl. 4, fig. 9.
(Plate 3, Figs. 10. 11)

***Sheshukovia?* sp. A**

Description: The valve is triangular shaped with rounded tips on apical points. One of the apical points has fine perforations throughout while the other two do not. Pores are large and radiate out from the center. Labiate processes can be seen scattered throughout the valve face.
(Plate 3, Fig. 1)

***Shionodiscus oestrupii*** (Ostenfeld) A.J. Alverson, S.H. Kang & E.C. Theriot 2006, p. 251-262; p. 258.
Basionym: *Coscinosira oestrupii* Ostenfeld 1900, p. 45-93; p. 52.

***Sphynctolethus pacificus*** (Hajós) Sims 1986, p. 250, 252, figs, 29-44, 69
Basionym: *Ceratalus pacificus* Hajós 1976, p. 828, pl. 22, figs. 1-6.

***Stephanopyxis marginata*** Grunow 1884.
(Plate 4, Fig. 16)

***Synedra? sp. A***
Description: The valve face is symmetrical, with pores radiating out almost parallel from the center. The tips of the valve face are rounded.
(Plate 5, fig. 4)

***Thalassiosira elliptipora*** (Donahue) Fenner 1991, p. 201, pl. 4, figs. e, i-m.

***Thalassiosira insigna*** (Jousé) Harwood & Maruyama 1992, p. 707, pl. 14, figs. 3-5.
Basionym: *Cosmiodiscus insignis* Jousé 1959, pl. 4, fig. 9.

***Thalassiosira inura*** Gersonde 1991, p. 151, pl. 6, figs. 7-14; pl. 8, figs. 1-6.

***Thalassiosira lentiginosa*** (Janisch in Schmidt) G. Fryxell 1977, p. 103, figs. 13 (a-d), 14 (a-d).
Synonym: Coscinodiscus lentiginosus Janisch in Schmidt 1878, pl. 58, fig. 11.

***Thalassiosira oliverana*** **var.** ***sparsa*** Harwood & Maruyama 1992, p. 708, pl. 16, fig. 13.

***Thalassiosira praefraga*** Gladenkov et Barron 1995, p. 30-31, pl. 2, figs. 3-6, 9.

***Thalassiosira torokina*** Brady 1977, p. 22-123, 5 fig.

***Thalassiosira vulnifica*** (Gombos) Fenner amend Mahood & Barron 1996, p. 285, figs. 1-14, 25-26.
Basionym: *Coscinodiscus vulnificus* Gombos 1976, p. 593, pl. 4, figs. 1-3; pl. 42, figs. 1-2.

***Triceratium columbi*** **var.** ***quadrata*** Reinhold 1937, p. 125, pl. 20, fig. 8.
(Plate 4, Fig. 8)

***Triceratium groningensis*** Reinhold 1937, p.126, pl. 20, fig. 9.

***Triceratium reticulum*** **f.** ***pentagona*** *Hustedt* 1930, p. 123-124, pl. 197, fig. 3.
(Plate 4, Fig. 9)

***Triceratium (Trinacria?) splendidium*** Hustedt in Schmidt et al. 1959, p. 17-18, pl. 469, fig. 2
(Plate 3, Figs. 4-5)

***'Triceratium' quadrangulare*** Greville 1864, p. 58, pl. 70, figs. 7-8.
(Plate 4, Fig. 6)

***Triceratium unquiculatum*** Greville 1864, p. 85; pl. 11, fig. 9.
(Plate 4, Fig. 1)

***'Triceratium'* sp. B**
Description: The valve is triangular shaped with rounded corners; sides are slightly curved inward. There are large pores randomly clustered in the center, pores thin but are still randomly distributed to outer edges, pores reach margins.
Comments: Similar to *Triceratium bellum* Long, Fuge & Smith 1946 due to shape of valve, irregular distribution of pores. Differs due to shape of sides, and the species mentioned here has central pores, whereas *T. bellum* has a hyline center.
(Plate 4, Figs. 2a, 2b)

***'Triceratium'* sp. C**
Description: The valve has four extending angles that appear to round at their points. The center of the valve is perforate and has an elevated ring in the center; pores extend outward to the margins with a random distribution.
Comments: Slight similarities to Triceratium zonatulatum Greville 1865 such as four angles on the valve, similar shape, and pores on valve face. Differences in pore distribution and placement; the species pictured in this paper also has raised elevations on the valve face.
(Plate 4, Fig. 5)

***Trinacria excavata* f. *tetragona*** Schmidt in Schmidt et al. 1890, pl. 152, fig. 26-28.
(Plate 4, Fig. 7)

***'Trinacria' simulacrum*** Grove & Sturt 1887, p. 144; pl. 13, fig. 46.
(Plate 3, Fig. 12)

***Tubaformis unicornis*** Gombos 1983, p. 572; pl. 5, figs. 1-6, pl. 6, fig. 1-2.
(Plate 8, Figs. 1-8)

**Genus and species uncertain #1** of Gombos 1983, p. 580, pl. 7, figs. 1-6.
(Plate 6, Figs. 1-3, 8, 9)

**Genus et sp. uncertain #3** of Harwood and Maruyama 1992, p. 716, pl. 2, figs. 3-5.

**Silicoflagellates**

***Bachmannocena bispicata***
Basionym: *Mesocena bispicata* Shaw & Ciesiekski 1983, pl. 20, figs. 3, 6-8.
(Plate 9, Figs. 11, 12)

***Cannopilus sphaericus*** Gemenhardt 1931b, p. 104, pl. 10, figs. 3-4; Shaw & Ciesiekski 1983, pl. 18, figs. 1-5.
(Plate 10, Figs. 3, 4, 8)

***Corbisema flexuosa*** (Stradner) Perch-Nielsen 1975, p. 685, pl. 3, fig. 10; Shaw & Ciesiekski 1983 pl. 1, figs. 7, 9.

Basionym: *Corbisema triacantha var. flexuosa* Stradner 1961, p. 89, pl. 1, figs. 1-8.
(Plate 9, Fig. 8)

***Corbisema hastada*** (Lemmermann) Frenguelli 1975, p. 685, pl. 3, figs. 2-4, 8.
Basionym: *Dictyocha triacantha var. hastada* Lemmermann 1901, p. 259, pl. 10, figs. 16-17.

***Dictyocha aspera aspera*** (Lemmermann) Perch-Nielsen 1975, p. 686, pl. 4, figs. 10, 15. Shaw & Ciesiekski 1983, pl. 2, figs, 10-12; pl. 3, figs. 1-2, 4, 6, 9.
(Plate 9, Fig. 1)

***Dictyocha fibula*** Ehrenberg 1838, pl. 5, figs. 1-2; pl. 11, figs. 8-9; Shaw & Ciesiekski 1983, pl. 4, figs. 1-4.
(Plate 9, Fig. 2)

***Dictyocha hexacantha*** Schulz 1928, p. 255, fig. 43; Shaw & Ciesiekski 1983, pl. 4, figs. 8-9.
(Plate 9, Fig. 6)

***Dictyocha pentagona*** (Schulz) Ciesielski 1975, p. 659, pl. 7, figs. 6-7; Shaw & Ciesiekski 1983, pl. 4, figs. 12-13.
Basionym: *Dictyocha fibula var. pentagona* Schulz 1928, pp. 225-292.
(Plate 10, Figs. 5, 6)

***Dictyocha sp.*** specimen with apical structure broken off
(Plate 9, Fig. 3)

***Distephanus crux crux*** (Ehrenberg) Haeckel 1887, p. 1563; Shaw & Ciesiekski 1983, pl. 10, figs. 6-7; pl. 11, fig. 1.
Basionym: *Dictyocha crux* Ehrenberg 1840, p. 207.
(Plate 10, Fig. 7)

***Mesocena apiculata*** (Schulz) Hanna 1931, no. 2, pl. D, fig. 3; Shaw & Ciesiekski 1983, pl. 12, figs. 1-7.
Basionym: *Mesocena oamaruensis var. apiculata* Schulz 1928, p. 240, fig 11.
(Plate 9, Fig. 10)

***Mesocena oamaruensis*** Schulz 1928, p. 240, fig. 10a, b; Shaw & Ciesiekski 1983, pl. 12, figs. 8-10; pl. 13, figs. 1-9; pl. 14, figs. 1-2.
(Plate 9, Fig. 9)

***Mesocena occidentalis*** Hanna 1931, pl. E, fig. 1; Shaw & Ciesiekski 1983, pl. 13, figs. 3-8.
Basionym: *Mesocena oamaruensis var. quadrangula* Schulz 1928, p. 240, figs. 12-13.
(Plate 9, Figs. 4, 5)

***Mesocena sp. A***
Description: Features a triangular form with spines at apices. One of the apices has a gap where the form is not connected, both arms show a small spine extending.
Comments: Very similar to *Mesocena apiculata*; the species discussed here differs due to gap at one of the apical points.
(Plate 9, Fig. 7)

***Naviculopsis biapiculata*** (Lemmermann) Frenguelli 1940.

Basionym: *Dictyocha navicula* var. *biapiculata* Lemmermann 1901, p. 258, pl. 10, figs. 14, 15.

***Naviculopsis constricta*** (Schulz) Frenguelli 1940, figs. 11a, b; Shaw & Ciesiekski 1983, pl. 15, figs. 4-8.
Basionym: *Dictyocha navicula var. constricta* Shulz 1928, p. 246, fig. 21.

***Naviculopsis trispinosa*** (Schulz) Glezer 1966, pp. 277-278, pl. 17, fig. 7; Shaw & Ciesiekski 1983, pl. 16, fig. 8, 11.
Basionym: *Dictyocha navicula var.trispinosa* Schulz 1928, p. 246, figs. 23a, b.

***Stephanocha speculum***
Basionym: *Distephanus speculum* Ehrenberg 1839, p. 129, table, and pl. 4, fig. 10n.
(Plate 10, Fig. 1)

***Stephanocha boliviensis***
Basionym: *Dictyocha boliviensis* Frenguelli 1940, p. 44, fig. 4.
Synonym: *Distephanus boliviensis* Bukry & Foster 1973, p. 287, pl. 4, figs. 1-3; Shaw & Ciesiekski 1983, pl. 10, figs. 5, 8.
(Plate 10, fig. 2)

# References


Barron, J. A. & Mahood, A. D. (1993). Exceptionally well-preserved early Oligocene diatoms from glacial sediments of Prydz Bay, East Antarctica. *Micropaleontology, 39(1)*, 29-45.

Barron, J. A., Bukry, D., & Gersonde, R. (2014). Diatom and silicoflagellate biostratigraphy for the late Eocene: ODP 1090 (sub-Antarctic Atlantic). *Nova Hedwigia, Beiheft, 143*, 1-32.

Barron, J. A., Stickley, C. E., & Bukry, D. (2015). Paleoceanographic, and paleoclimatic constraints on the global Eocene diatom and silicoflagellate record. *Palaeogeography, Palaeoclimatology, Palaeoecology, 422*, 85-100.

Basov, I. A., Ciesielski, P. F., Krasheninnikov, V. A., Weaver, F. M., Wise, S. W., & Ludwig, W. J. (1983). Biostratigraphic and paleontologic synthesis: Deep sea drilling project Leg 71, Falkland Plateau and Argentine Basin. *Initial Reports of the Deep Sea Drilling Project, 71*, 445-460.

Bohaty, S. M. & Zachos, J. C. (2003). Significant Southern Ocean warming event in the late middle Eocene. *Geology 31, no. 11*, 1017-1020.

Cande, S. C. & Kent, D. V. (1992). A new geomagnetic polarity time scale for the Late Cretaceous and Cenozoic. *Journal of Geophysical Research: Solid Earth, 97(B10)*, 13917-13951.

Cande, S. C. & Kent, D. V. (1995). Revised calibration of the geomagnetic polarity timescale for the Late Cretaceous and Cenozoic. *Journal of Geophysical Research: Solid Earth, 100(B4)*, 6093-6095.

Ciesielski, P. F. (1983). The Neogene and Quaternary diatom datum biostratigraphy of subantarctic sediments. Deep Sea Drilling Project Leg 71. *Initial Reports of the Deep Sea Drilling Project, 71*, 635-665.

Dalziel, I. W. (2014). Drake Passage and the Scotia arc: A tortuous space-time gateway for the Antarctic Circumpolar Current. *Geology, 42(4)*, 367-268.

DePrado, C. & Ling, H. Y. (1981). Early to early-middle Paleocene diatom zonation. *Boreas, 9*, 115-137.

Fenner, J. (1984). Eocene-Oligocene Planktic Diatom Stratigraphy in the Low Latitudes and the High SouthernLatitudes. *Micropaleontology Vol. 30, No. 4*, 319-342.

Fourtanier, E. (1991). Paleocene and Eocene diatom biostratigraphy and taxonomy of eastern Indian Ocean site 752. *Proceedings of the Ocean Drilling Program, Scientific Results, Vol. 121*, 171-187.

Gombos Jr, A. M. (1982). Early and middle Eocene diatom evolutionary events. *Bacillaria, 5*, 225-242.

Gombos Jr, A. M. (1983). Middle Eocene diatoms from the South Atlantic. *Initial Reports of the Deep Sea Drilling Project, 71,* 565-581

Gombos Jr, A. M. (1977). Paleogene and Neogene diatoms from the Falkland Plateau and Malvinas Outer Basin: Leg 36. *Initial Reports of the Deep Sea Drilling Project, 36*, 575-688.

Gombos Jr, A. M., & Ciesielski, P. F. (1983). Late Eocene to Early Miocene Diatoms From the Southwest Atlantic. *Initial Reports of the Deep Sea Drilling Project*, *71,* 538-634.

Hajós, M. (1976). Upper Eocene and lower Oligocene Diatomaceae, Archaeomonadaceae, and Silicoflagellatae in Southwestern Pacific sediments, DSDP Leg 29. *Initial Reports of the Deep Sea Drilling Project*, *35*, 817-883.

Harwood, D. M. (1989). Siliceous microfossils. In: Barret P.J. (ed.) *Antarctic Cenozoic history from the CIROS-1 drillhole, McMurdo Sound. DSIR Bulletin, 245*, 67-97.

Harwood, D. M. & Bohaty, S. M. (2000). Marine diatom assemblages from Eocene and younger erratics, McMurdo Sound, Antarctica. *In: Stillwell, J., Feldman, R. (eds.), Paleobiology and Paleoenvironments of Eocene Rocks: McMurdo Sound, East Antarctica, American Geophysical Union, Antarctic Research Series, 76*, 73-98.

Harwood, D. M. & Maruyama, T. (1992). Middle Eocene to Pleistocene diatom biostratigraphy of Southern Ocean sediments from the Kerguelen Plateau, LEG 120. *In: Wise, S.W. Jr, Schlich, R., et al. (eds.), Proceedings of the Ocean Drilling Program, Scientific Results, 120,* 683-733.

Kaharoeddin, F. A., Graves, R. S., Bergen, J. A., Eggers, M. R., Harwood, D. M., Humphreys, C. L., . . . Watkins, D. K. (1982). ARA Islas Orcadas Cruise 1678 sediment descriptions. *Antarctic Research Facility, Department of Geology, Florida State University, Tallahassee Florida,* Contribution No. 50, 178 pp.

Livermore, R., Hillenbrand, C. D., Meredith, M., & Eagles, G. (2007). Drake Passage and Cenozoic climate: An open and shut case? *Geochemistry, Geophysics, Geosystems 8 (1)*, *Q01005.*

McKay, R. M., De Santis, L., Kulhanek, D. K., Ash, J. L., Beny, F., Browne, I. M., . . . Ishino, S. (2019). Expedition 374 methods. *In: Proceedings of the International Ocean Discovery Program, 374*. https://doi.org/10.14379/iodp.proc.374.102.2019

McLean, H. & Barron, J. A. (1988). A late Middle Eocene diatomite in Northwestern Baja California Sur, Mexico: implications for tectonic translation. *Filewicz, M., Squires, R.(ed.), In Paleogene Stratigraphy, West Coast of North America, 58,* 1-8.

Renaudie, J., Drews, E. L., & Böhne, S. (2018). The Paleocene record of marine diatoms in deep-sea sediments. *Fossil Record, 21(2)*, 183-205.

Sangiorgi, F., Wubben, E., Browne, I. M., Shevenell, A., Dodd, J. P., Prebble, J., . . . Harwood, D. M. (2019). Ocean properties and Antarctic cryosphere dynamics during the early and middle Miocene: results from the IODP Expedition 374 (Ross Sea). *In: AGU Fall Meeting Abstracts*, pp. PP21B-1602.

Scherer, R. P., Gladenkov, A. Y., & Barron, J. A. (2007). Methods and applications of Cenozoic marine diatom biostratigraphy. *In: Starrat, S. (ed.), Pond Scum to Carbon Sink:*

*Geological and Enviromental Applications of Diatoms, The Paleontological Society Papers, 13*, 61-83.

Scherer, R., Bohaty, S. M., & Harwood, D. M. (2000). Oligocene and lower Miocene siliceous microfossil biostratigraphy of Cape Roberts Project Core CRP-2/2A, Victoria Land Basin, Antarctica. *Terra Antartida 7 (4)*, 417-442.

Witkowski, J., Harwood, D. M., Wade, B. S., & Bryłka, K. (2020). Rethinking the chronology of early Paleogene sediments in the western North Atlantic using diatom biostratigraphy. *Marine Geology, 424*, 106-168.

*ARA Islas Orcadas* Cruise 1678-20PC,48PC with ODP and DSDP Legacy Sites

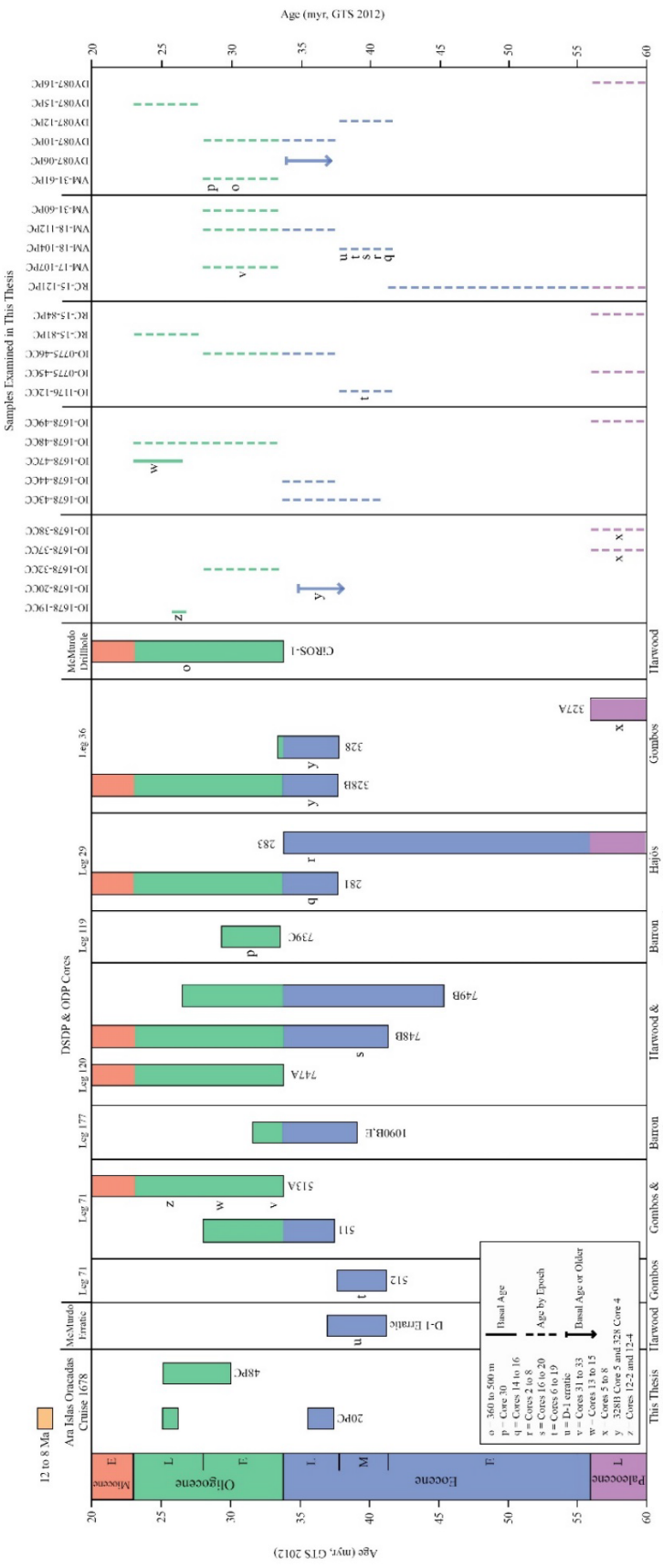


*Figure 2. Summary of existing diatom biostratigraphic sites compared with Ara Islas Orcadas 1678 samples. Letters "o" through "z" used to correlated previous cores with established biostratigraphic zones.*

*ARA Islas Orcadas* Cruise 1678-20PC

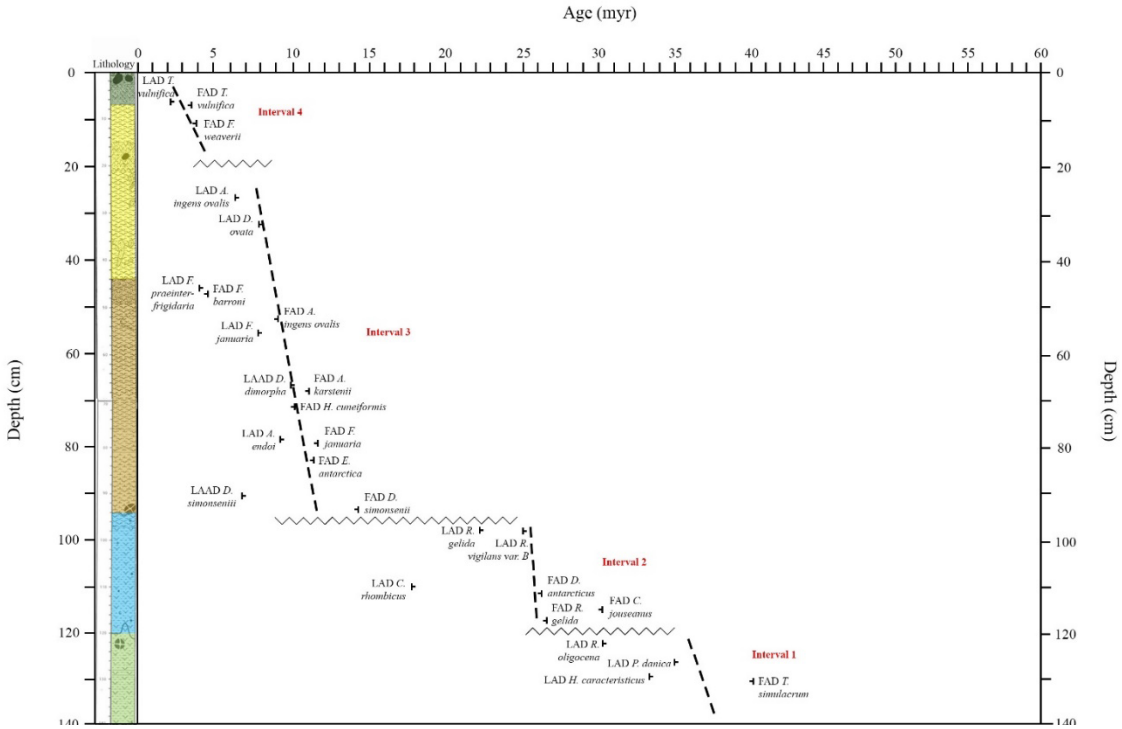


*Figure 3. Age x depth plot of sediment samples from ARA Islas Orcadas Cruise 1678-20PC with diatom and silicoflagellate FAD and LAD events used for age control*

*ARA Islas Orcadas* Cruise 1678-48PC

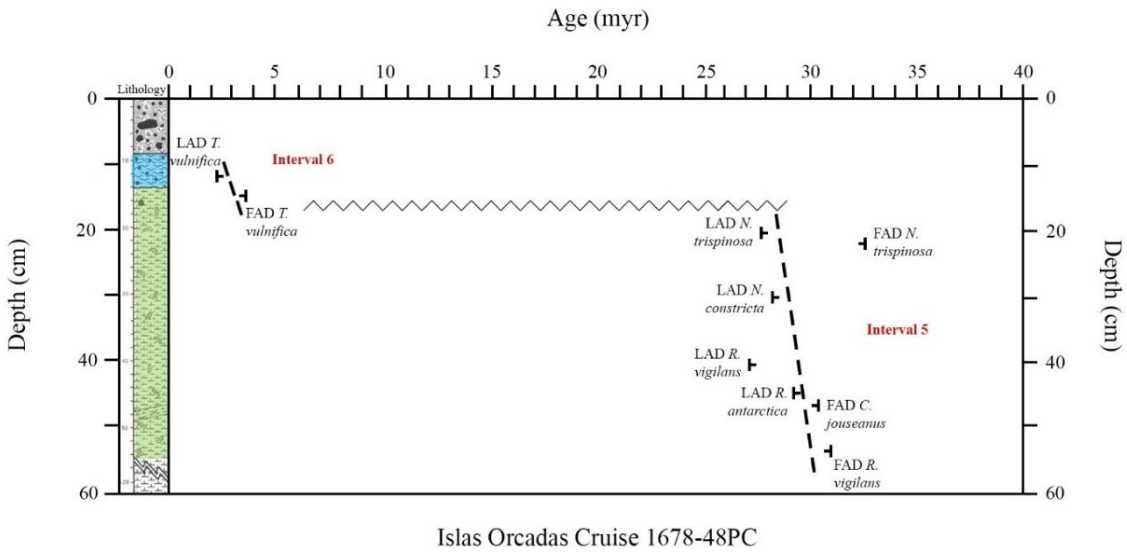


*Figure 4. Age x depth plot of sediment samples from ARA Islas Orcadas Cruise 1678-48PC with diatom and silicoflagellate FAD and LAD events used for age control*

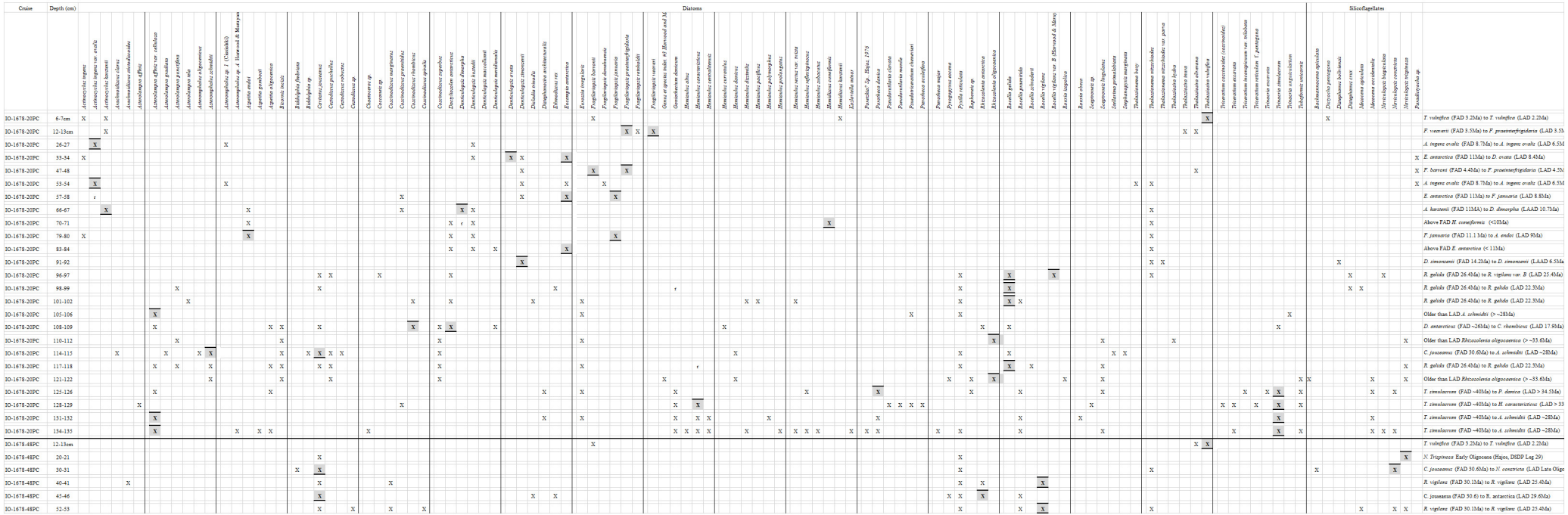


*Table 1. Summary of diatom and silicoflagellate taxa from ARA Islas Orcadas cores. First Appearance Datum (FAD) events are indicated by a line below the occurrence, Last Appearance Datum (LAD) events are indicated by a line above occurrence.*

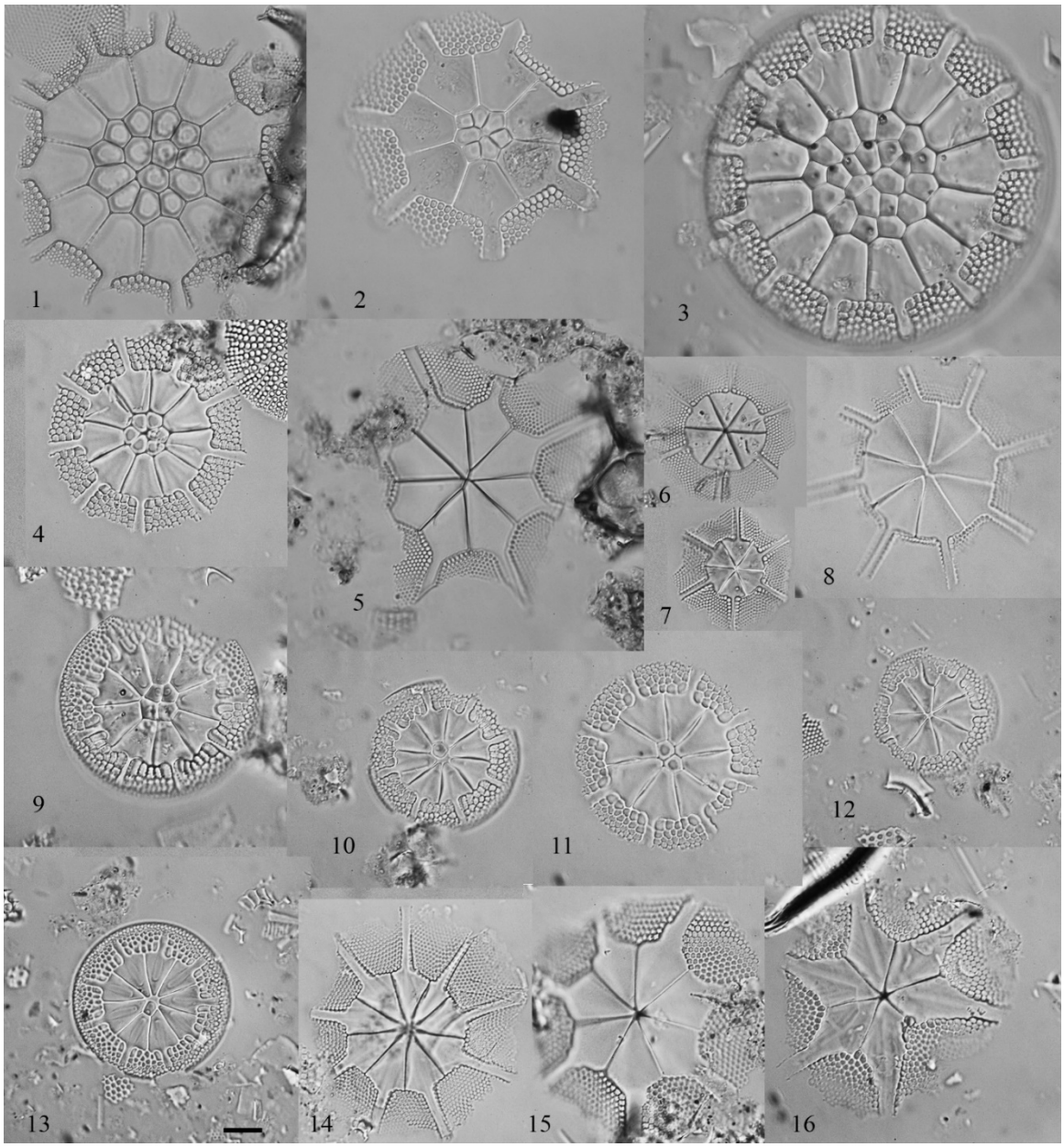


Plate 1. Scale bar equals 10 µm. **1-4.** *Asterolampra affinis var. cellulosa* Forti; (1) Sample 1678-20, 105-106 cm; (2) Sample 1678-20, 117-118 cm; (3) Sample 1678-43CC; (4) Sample 1678-20, 134-134 cm. **5.** *Asterolampra tela* Gombos; Sample 1678-20 101-102 cm. **6-8.** *Asterolampra punctifera* Grove; (6) Sample 1678-20, 98-99 cm; (7) Sample 1678-20, 110-112 cm; (8) Sample 1678-20, 117-118 cm. **9.** *Asterolampra vulgaris* Greville*;* Sample 1678-43CC. **10-13.** *Asterolampra affinis* Greville; (10, 12-13) Sample 1176-12CC; (11) Sample 1678-20, 128-129 cm. **14.** *Asteromphalus oligocenicus* Schrader & Fenner; Sample 1678-20, 114-115 cm. **15.** *Asterolampra gradiata* Gombos; Sample 1678-20, 114-115 cm. **16.** *Asterolampra uraster* Grove & Sturt; Sample 1176-12CC.

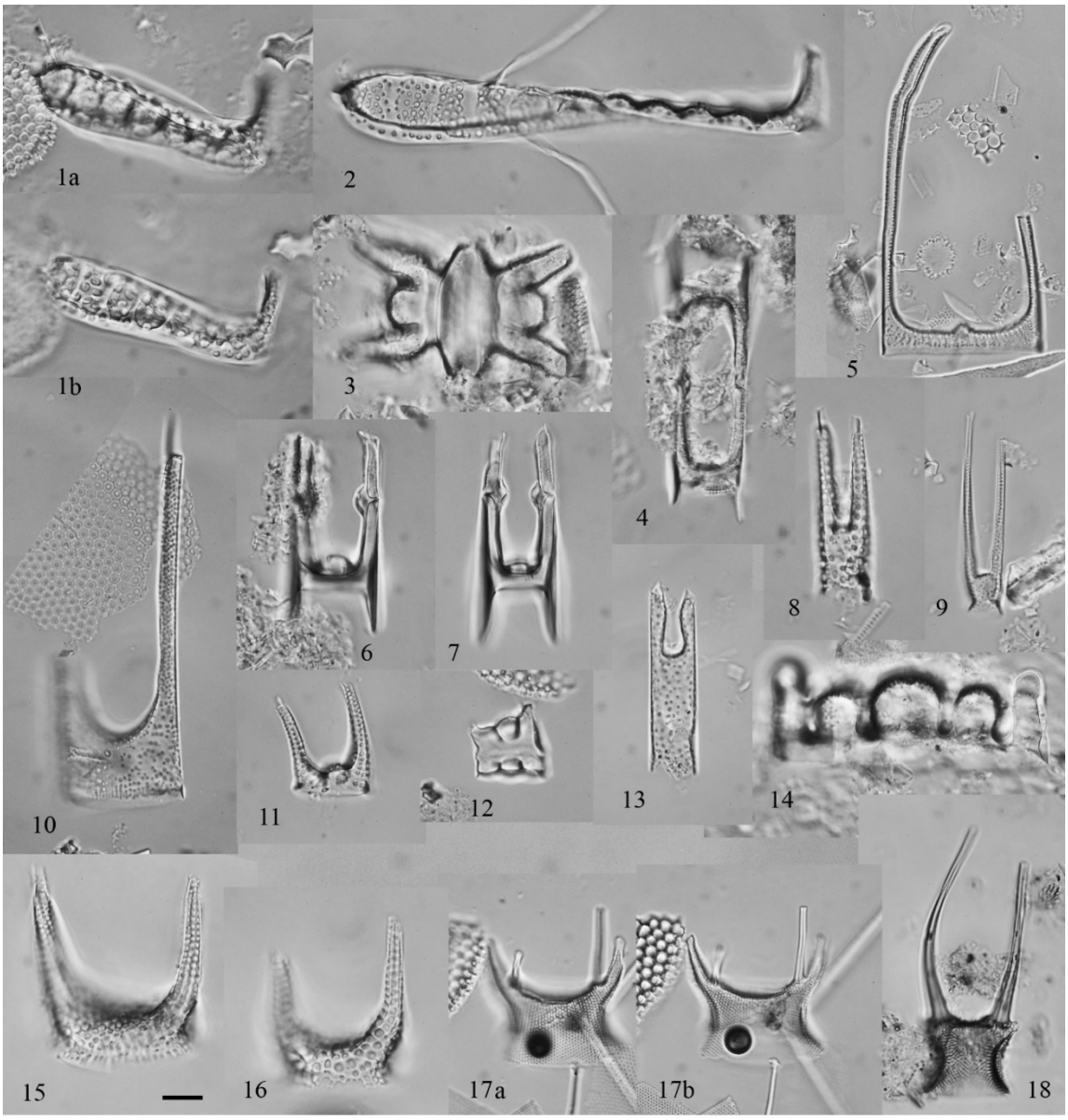


Plate 2. Scale bar equals 10µm. **1-2.** *Hemiaulus rectus var. twista* Fenner; (1) Sample 1678-48CC**;** (2) Sample 1678-20, 134-135 cm. **3.** *Hemiaulus sp. A*; Sample 1176-12CC **4.** *Hemiaulus prolongatus* Ross & Sims; Sample 1678-20, 134-135 cm. **5.** *Hemiaulus angustus* Greville; Sample 1678-43CC **6-7.** *Briggera sp.*; (6) Sample 1678-20, 134-135 cm; (7) Sample 1678-20, 131-132 cm. **8.** *Hemiaulus altus* Hajós; Sample 1678-20, 134-135 cm. **9.** *Hemiaulus sp. B*; Sample 1678-20CC. **10.** *Hemiaulus sp. D;* Sample 1678-20, 131-132 cm. **11.** *Hemiaulus curvatulus* Strelnikova; Sample 1678-20, 108-109 cm. **12.** *Hemiaulus dissimilis* Grove & Sturt; Sample 1678-20, 101-102 cm. **13.** *Hemiaulus sp. C*; Sample 1678-20, 108-109 cm. **14.** *Biddulphia rigida* Schmidt; Sample 1678-20CC. **15-16.** *Bicornis incisis* Hajós*;* (15) Sample 1678-20, 117-118 cm; (16) Sample 1678-20, 121-122 cm. **17.** *Biddulphia fimbriata* Greville*;* Sample 1678-48, 30-31 cm **18.** *Biddulphia sp. A*; Sample 1678-20, 101-102 cm.

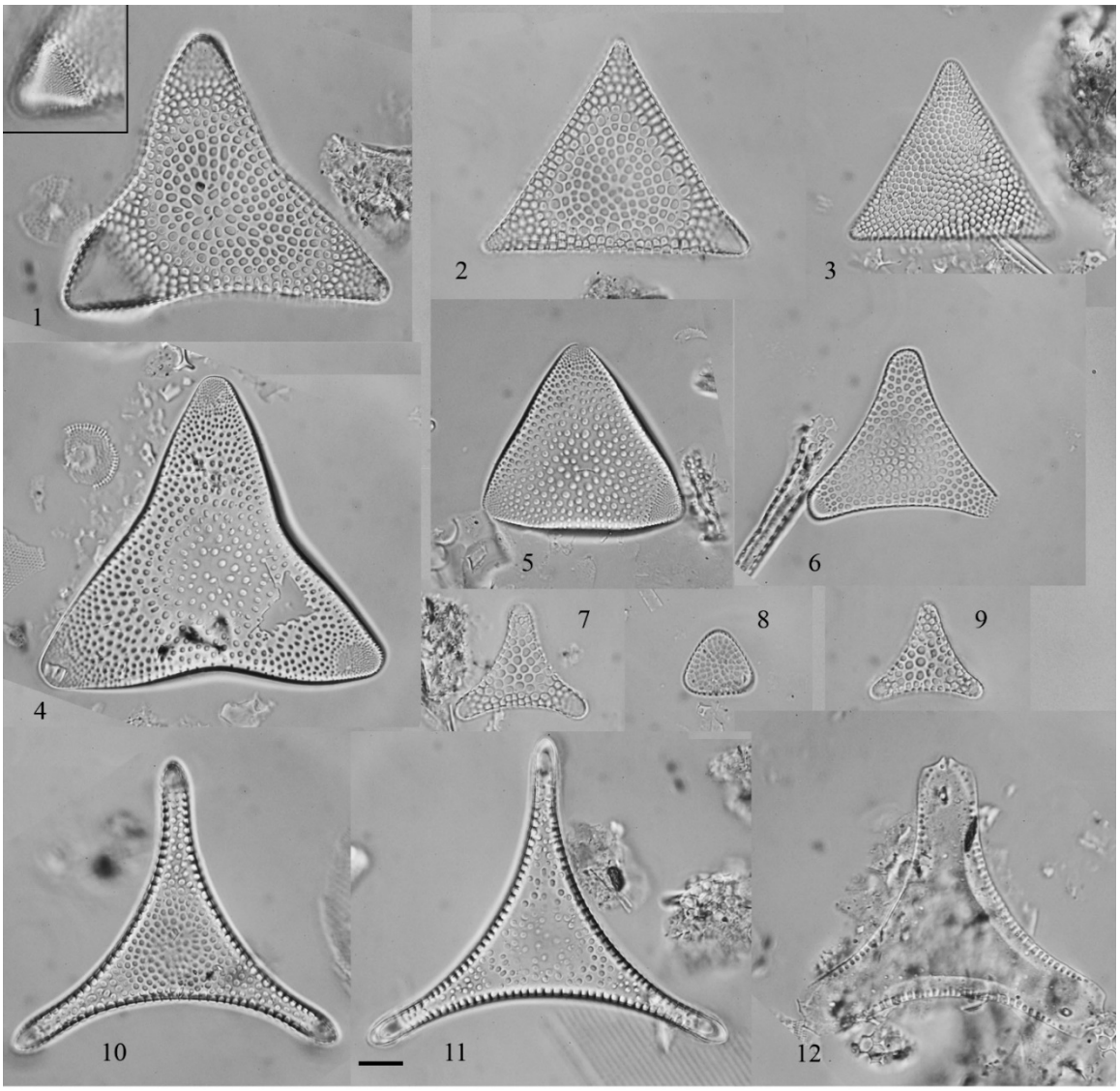


Plate 3. Scale bar equals 10µm. **1.** *Sheshukovia? sp. A*; Sample 1678-20, 134-135 cm. **2, 6-9.** *Eurossia irregularis* (Greville) Sims in Mahood, Barron & Sims; (2) Sample 1678-20, 117-118 cm; (6) Sample 1678-20, 110-112 cm; (7-8) Sample 1678-20, 125-126 cm; (9) Sample 1678-20, 131-132cm. **3.** *Pseudotriceratium cheneveri* (Meister) Gleser 1974; Sample 1678-20, 128-129 cm. **4-5.** *Triceratium splendidum* Hustedt in Schmidt et al.; Sample 1678-43CC. **10-11.** *Sheshukovia excavata* (Heiberg) Strelnikova; (10) Sample 1678-20, 128-129cm; (11) Sample 1678-20, 134-135 cm. **12.** *Trinacria simulacrum* Grove & Sturt; Sample 1176-12CC.

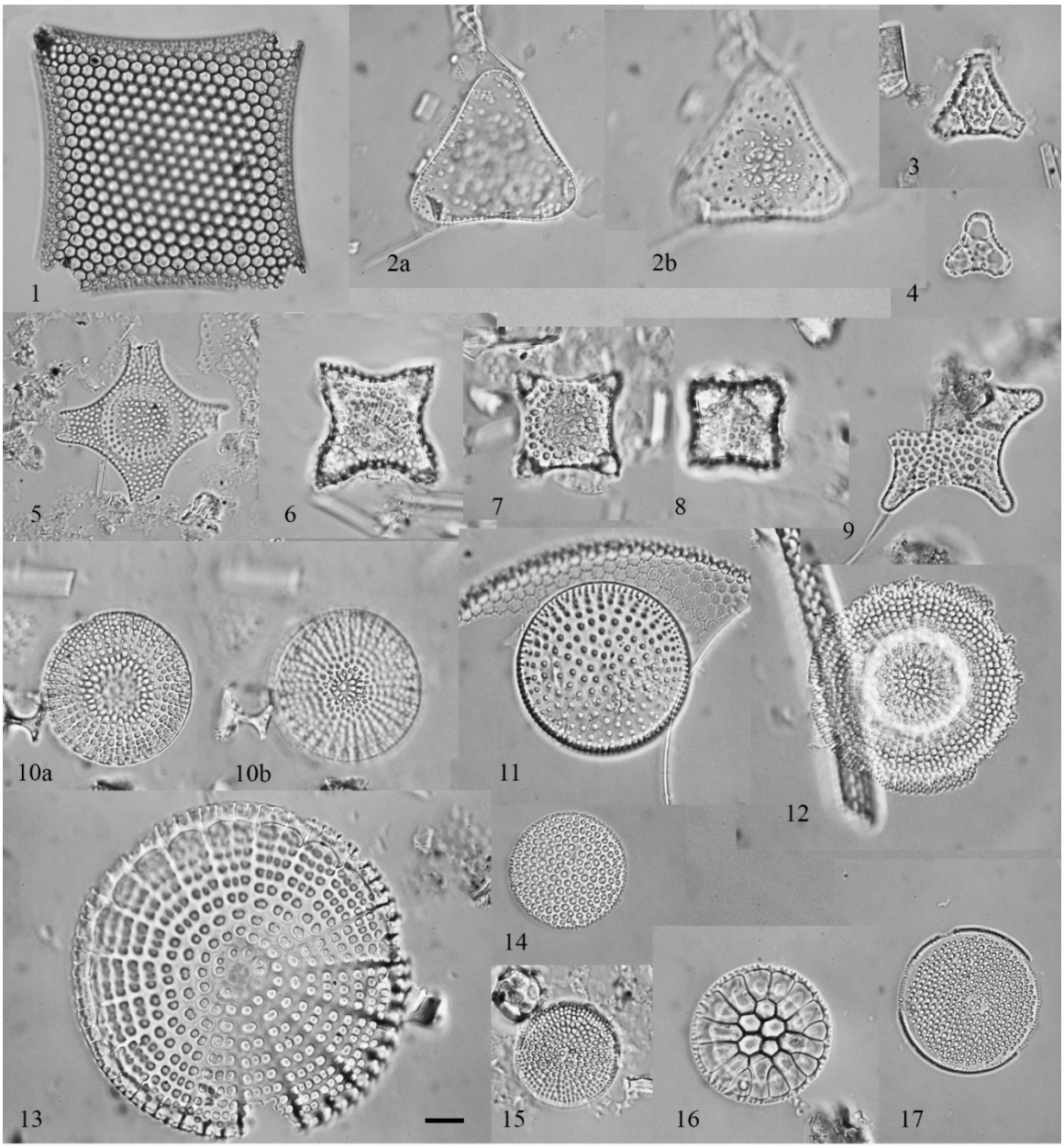


Plate 4. Scale bar equals 10µm. **1.** *Triceratium unguiculatum* Greville; Sample 1678-20, 105-106 cm. **2.** *Triceratium sp. B*; Sample 1176-12CC. **3-4.** *Fenneria kanayae* Fenner; (3) Sample 1678-20CC; (4) Sample 1678-20, 125-126 cm. **5.** *Triceratium sp. C*; Sample 1678-20CC. **6.** *Triceratium quadrangulare* Fenner; Sample 1176-12CC. **7.** *Trinacria excavata var. tetragona* Schmidt; Sample 1678-20CC. **8.** *Triceratium columbi var. quadrata* Reinhold; Sample 1176-12CC. **9.** *Triceratium reticulum* f. *pentagona* Hustedt; Sample 1678-20, 128-129 cm. **10.** *Arachnoidiscus stictodiscoides* Hanna, Hendey & Brigger; Sample 1678-48, 40-41 cm. **11, 14.** *Rocella praenitida* (Fenner) Fenner in Kin & Barron; (11) Sample 1678-20, 134-135 cm; (14) Sample 1678-20, 125-126 cm. **12.** *Cestodiscus robustus* Jousé; Sample 1678-20, 114-115 cm. **13.** *Arachnoidiscus clarus* Brown; Sample 1678-20, 114-115 cm. **15, 17.** *Azpeitzia gombosii* Harwood & Maruyama; (15) Sample 1678-48CC; (17) Sample 1678-20, 134-135 cm. **16.** *Stephanopyxis marginata* Grunow; Sample 1678-20, 114-115 cm.

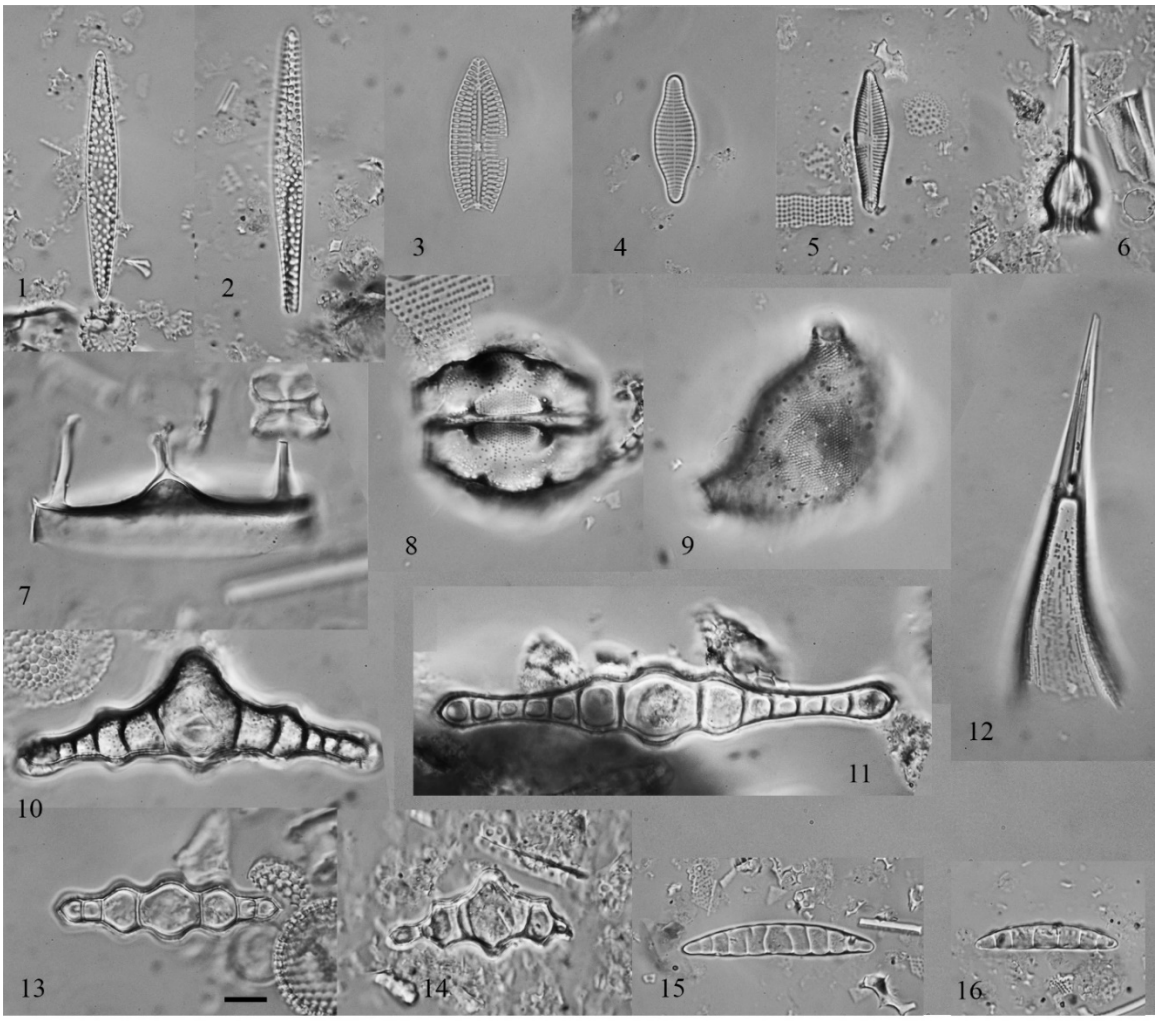


Plate 5. Scale bar equals 10µm. **1-2.** *Rossiella symmetrica* Fenner emend Yanagisawa; (1) Sample 1678-44CC; (2) Sample 1176-12CC. **3.** *Rouxia obesa* Schrader in Schrader & Fenner; Sample 1678-20, 131-132 cm. **4.** *Synedra sp. A*; Sample 1678-20, 121-122 cm. **5.** *Rhaphoneis sp. A*; Sample 1678-48, 40-41 cm. **6.** *Pterotheca aculeifera* Grunow; Sample 1678-44CC. **7.** *Dicladia trinodis* Hanna; Sample 1678-48 45-46 cm. **8.** *Goniothecium odontella* Ehrenberg; Sample 1176-12CC. **9.** *Biddulphia sp. B*; Sample 1678-20, 114-115 cm. **10.** *Pseudorutilaria hannai* Ross & Sims; Sample 1678-43CC. **11, 13.** *Pseudorutilaria clavata* Ross & Sims; (11) Sample 1678-20, 128-129 cm; (13) Sample 1678-20CC. **12.** *Rhizosolenia oligocaenica* Schrader; Sample 1678-20, 121-122 cm. **14.** *Pseudorutilaria hannai var. A* Ross & Sims; Sample 1678-20CC. **15, 16.** *Eunotogramma productum* Grunow; Sample 1176-12CC.

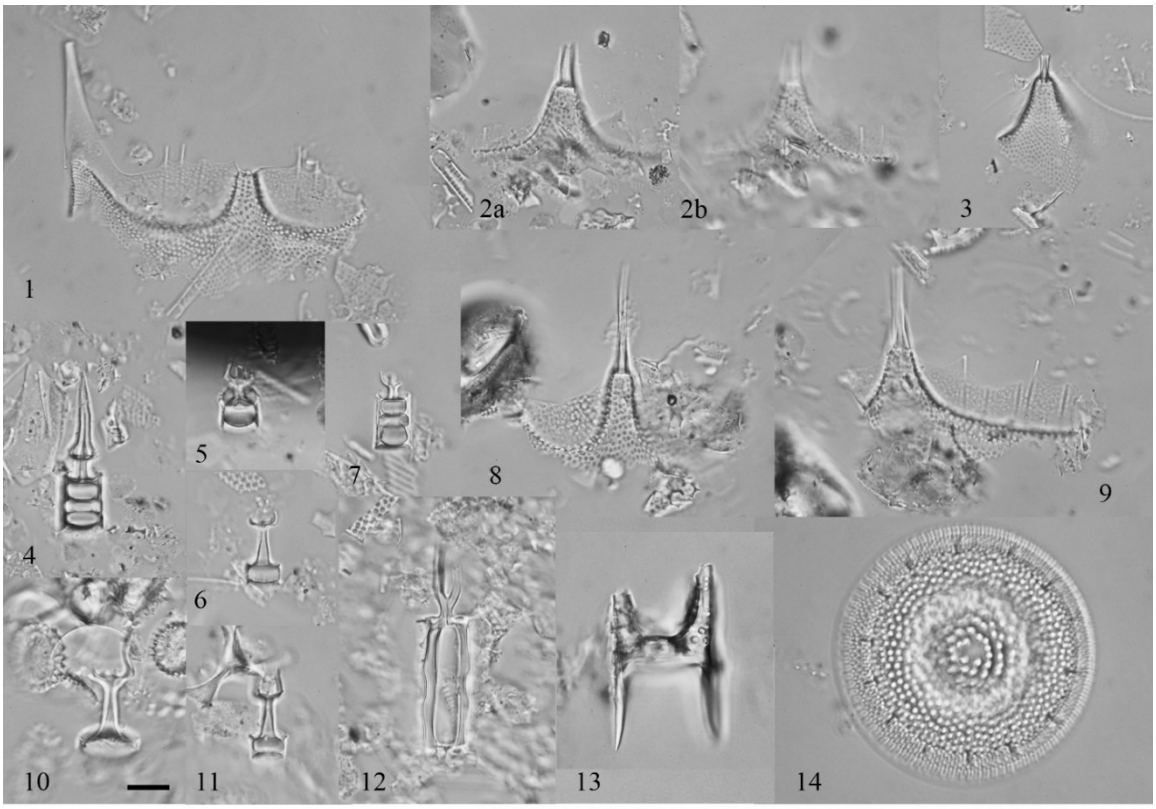


Plate 6. Scale bar equals 10µm. **1-3, 8-9.** Genus and species uncertain #1 Gombos, 1983; (1-2, 8-9) Sample 1176-12CC; (3) Sample 1678-43CC. **4-7, 10-11.** *Cerataulina sp. A*; (4-5) Sample 1176-12CC; (6, 10-11) Sample 1678-44CC; (7) Sample 1678-43CC. **12.** *Chaetoceros sp*.; Sample 1678-20CC. **13.** *Hemiaulus caracteristicus* Hajós; Sample 1678-20, 131-132 cm. **14.** *Coscinodiscus superbus*, Grove?; Sample 1678-20, 117-118 cm

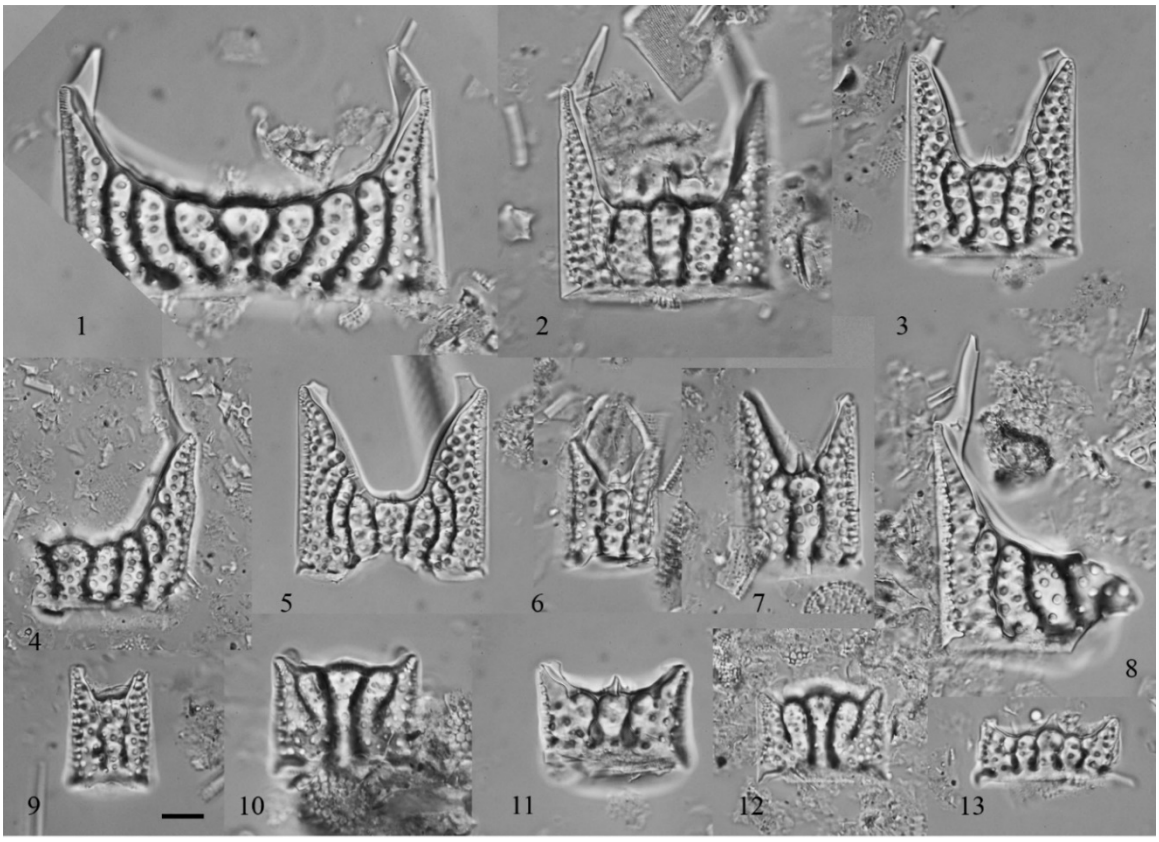


Plate 7. Scale bar equals 10µm. **1-5, 8.** *Hemiaulus reflexispinosus* Ross & Sims; (1) Sample 1678-20, 134-135 cm; (2-4) Sample 1176-12CC; (5) Sample 1678-20, 134-135 cm; (8) Sample 1678-20CC. **6-7.** *Hemiaulus reflexispinosus* transitional form Ross & Sims; Sample 1176-12CC. **9-13.** *Hemiaulus sp.* Gombos & Ciesielski, 1983; (9, 13) Sample 1176-12CC; (10) Sample 1678-20, 125-126 cm; (11) Sample 1678-43CC; (12) Sample 1678-20CC.


Plate 8. Scale bar equals 10µm. **1-8.** *Tubaformis unicornis* Gombos; (1, 4, 8) Sample 1678-20, 125-126 cm; (2) Sample 1678-20, 134-135 cm; (3) Sample 1678-20CC; (5, 7) Sample 1176-12CC; (6) Sample 1678-20, 121-122 cm.

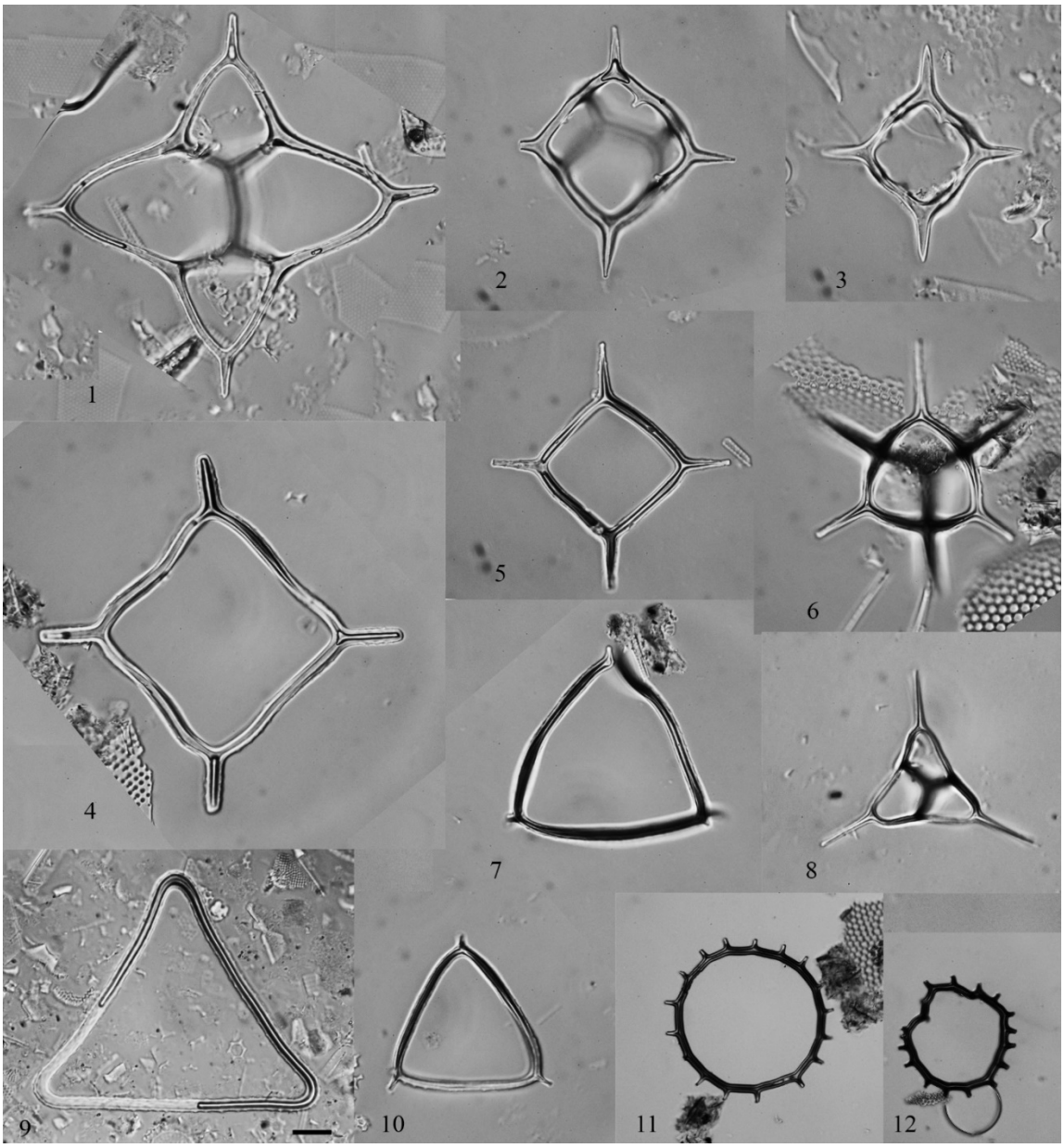


Plate 9. Scale bar equals 10µm. **1.** *Dictyocha aspera aspera*; Sample 1678-43CC. **2.** *Dictyocha fibula*, Sample 1678-20, 131-132 cm. **3.** *Dictyocha sp.*; Sample 1176-12CC. **4-5.** *Mesocena occidentalis*; (4) Sample 1678-20, 131-132 cm; (5) Sample 1678-20, 134-135 cm. **6.** *Dictyocha hexacantha*; Sample 1678-20, 131-132 cm. **7.** *Mesocena sp. A*; Sample 1678-20, 131-132 cm. **8.** *Corbisema flexuosa*; Sample 1678-20, 128-129 cm. **9.** *Mesocena oamareunsis*; Sample 1176-12CC. **10.** *Mesocena apiculata,* Sample 1678-20, 125-126 cm. **11-12.** *Mesocena bispicata*; (11) Sample 1678-20, 134-135 cm; (12) Sample 1678-20, 108-109 cm.

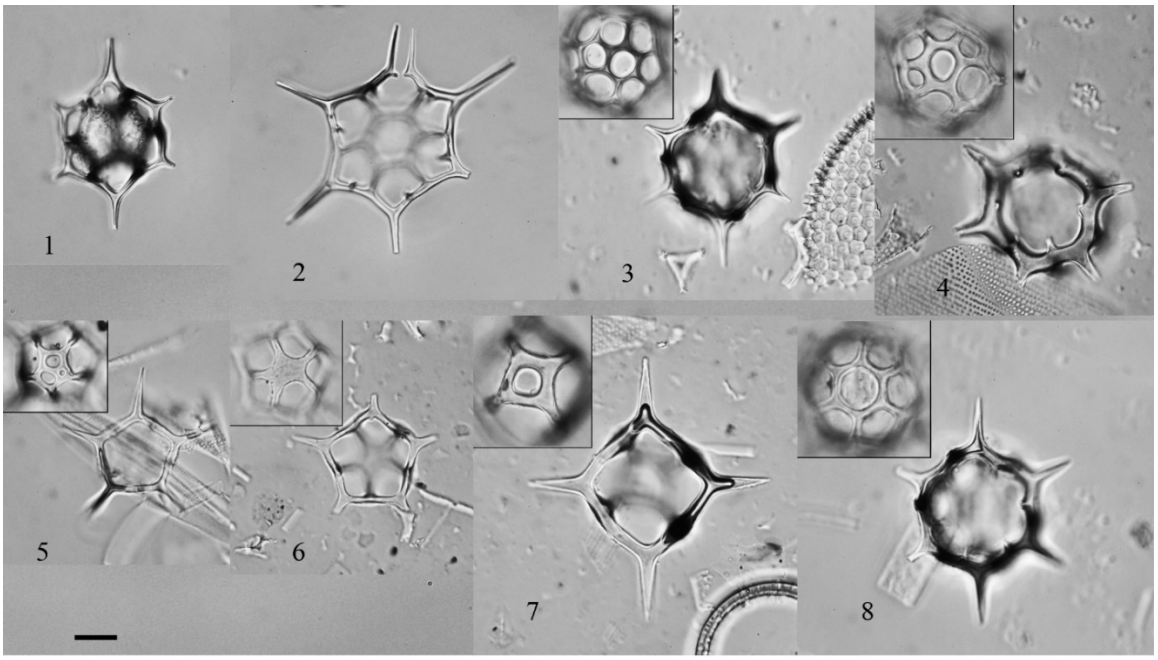


Plate 10. Scale bar equals 10µm. **1.** *Distephanus speculum*; Sample 1678-20, 134-135 cm. **2.** *Distephanus* boliviensis; Sample 1678-20, 131-132 cm. **3-4, 8.** *Cannopilus sphaericus;* (3) Sample 1678-48, 45-46 cm; (4) Sample 1678-48, 45-46 cm; (8) Sample 1678-48CC. **5-6.** *Dictyocha pentagona*; Sample 1678-48, 45-46 cm. **7.** *Distephanus crux crux*; Sample 1678-48, 45-46 cm.